UNIVERSITAT POLITÈCNICA DE VALÈNCIA

Insights into the molecular mechanisms of the N^6-methyladenosine (m^6A) methylation machinery in the regulation of the infection cycle of RNA plant viruses

Luis Fernando Alvarado Marchena

June 2022

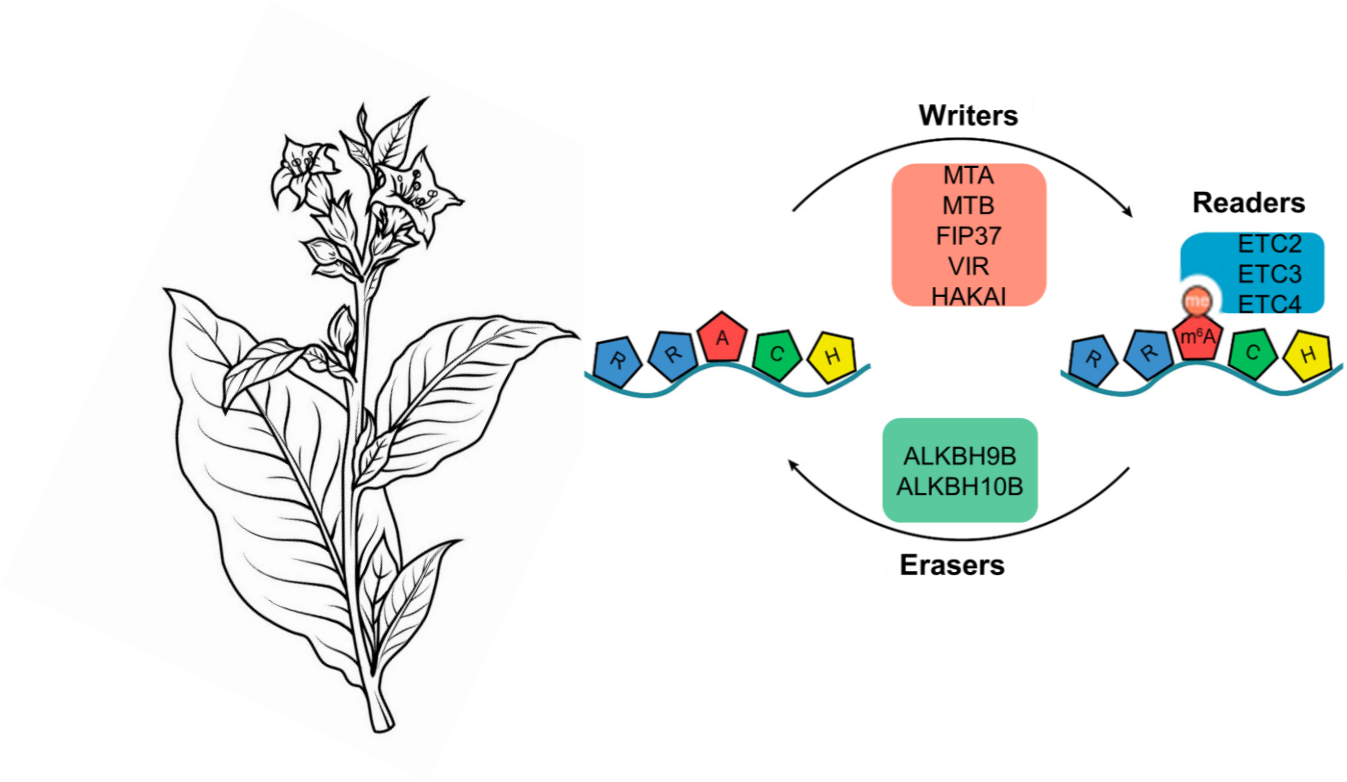

Directors

Prof. Vicente Pallás Benet

Dr. Frederic Aparicio Herrero

Insights into the molecular mechanisms of the N^6-methyladenosine (m^6A) methylation machinery in the regulation of the infection cycle of RNA plant viruses

Luis Fernando Alvarado Marchena

June, 2022

Directors:

Prof. Vicente Pallás Benet

Dr. Frederic Aparicio Herrero

AGRADECIMIENTOS

Mediante la presente deseo agradecer a las siguientes personas e instituciones que de una forma u otra colaboraron en la realización de la presente tesis doctoral:

- Al Prof. Vicente Pallás Benet y al Dr. Frederic Aparicio Herrero por aceptar ser mis tutores y por todos los valiosos consejos que me han brindado, siendo profesores esenciales en mi desarrollo académico y profesional. Fede, gracias por ir más allá de mi tutor, y sacar algún tiempo personal para una cena, almuerzo o cerveza. Fueron momentos **verdaderamente** valiosos que siempre recordaré. Vicente, gracias por siempre estar pendiente de mí, tu doctorando. Además de mis tutores, fueron las dos personas más cercanas a mi durante este complejo tiempo del SARS-CoV-2. Agradezco cada charla, profesional o personal, que tuvieron conmigo.
- A los Doctores Jesus Ángel Sánchez Navarro y Jose Antonio Navarro Bohigues, por todo su tiempo y disposición cuando requerí de su mentoría.
- A los Doctores Mireya Martínez Perez y Joan Márquez Molins por su total disposición y apoyo en el desarrollo de la presente tesis.
- A todo el personal del Laboratorio de Virología Molecular de Plantas (Lab. 2.01) del IBMCP, CSIS-UPV, por abrirme sus puertas para desarrollar la presente tesis doctoral.
- A Lorena Corachán Valencia, por todo el trabajo que realizas dentro del Laboratorio. Gracias por todo tu esfuerzo y compromiso con cada uno de los que trabajamos en el 2.01.
- Al Ministerio de Ciencia, Innovación, Tecnología y Telecomunicaciones (MICITT) de Costa Rica, por la financiación de la presente tesis doctoral; y a la Escuela de

Biología del Tecnológico de Costa Rica (TEC), quien me dio su apoyo para embarcarme en esta travesía profesional, la cual fue mi sueño por muchos años.

- A mis padres Felix Alvarado Alvarado y Guisselle Marchena López, por su apoyo, amor y deseos de ver en mí una gran persona de éxito personal y profesional.
- A mis hermanas Stefanny y Laura, que han estado siempre a mi lado brindándome su apoyo incondicional.
- A mi esposa Anna Laura Mena Brenes, por estar siempre a mi lado y apoyarme en cada una de mis metas personales y profesionales.

Don Vicente Pallás Benet, Doctor en Ciencias Biológicas, Profesor de Investigación del Consejo Superior de Investigaciones Científicas del Instituto de Biología Molecular y Celular de Plantas (Universidad Politécnica de Valencia-Consejo Superior de Investigaciones Científicas) de Valencia.

Don Frederic Aparicio Herrero, Doctor en Biología, Profesor Contratado Doctor (Universidad Politécnica de Valencia) de Valencia.

CERTIFICAN:

Que Luis Fernando Alvarado Marchena, Máster en Biología por la Universidad de Costa Rica e Ingeniero en Biotecnología por el Tecnológico de Costa Rica, ha realizado bajo su dirección el trabajo que con título "*Insights into the molecular mechanisms of the N^6-methyladenosine (m^6A) methylation machinery in the regulation of the infection cycle of RNA plant viruses*" presenta para optar al grado de Doctor en Biotecnología por la Universidad Politécnica de Valencia.

Y para que así conste a los efectos oportunos, firman el presente certificado en Valencia a _____ de _____ de 2022.

Vicente Pallás Benet **Frederic Aparicio Herrero**

Table of contents

Summary

N^6-methyladenosine (m^6A) is a widespread modification on cellular RNAs of different organisms that can impact many cellular processes and pathways. In plants, m^6A-methylation is mainly installed by a methylation complex containing several proteins: MTA, MTB, FIP37, VIR, and HAKAI. This modification is removed by demethylases of the *AlkB* family, and members of the EVOLUTIONARILY CONSERVED C-TERMINAL REGIONS (ECT) family are the best described proteins that recognize and process m^6A-modified RNAs. In *Arabidopsis*, m^6A has been reported to control embryonic stage plant development, vegetative growth and flowering. This modification is also present in the genomic RNAs of viruses and in the transcripts of some DNA viruses. Studies of viral epitransciptomics have revealed an equally important role of m^6A during virus infection; however, there is no global proviral or antiviral role of m^6A-methylation that can be generalized. In plants, there are few studies of the regulatory activity of m^6A during viral infections. The laboratory where this work was carried out has been a pioneer in the study of the effect of m^6A on plant-viruses, using the Alfalfa mosaic virus (AMV) as a model-virus. AMV belongs to the *Bromoviridae* family and, as the rest of the members of this family, its genome consists of three single-stranded RNAs of plus polarity. RNA 1 and RNA 2 encode the replicase subunits (P1 and P2), whereas RNA 3 encodes the movement protein (MP) and serves as a template for the synthesis of subgenomic RNA 4 (sgRNA 4), which encodes the coat protein (CP). At the beginning of this thesis, our laboratory had already reported on: (i) the presence of putative m^6A-motifs in the 3'UTR RNA 3, a critical region for AMV replication, (ii) the first *Arabidopsis* m^6A- demethylase (ALKBH9B), (iii) the functional relevance of ALKBH9B to maintain adequate m^6A/A levels for correct AMV replication, (iv) the ability of AMV-CP to interact with ALKBH9B, possibly to usurp ALKBH9B activity, and (v) the capability of *Arabidopsis* ECT2, ECT3 and ECT5 to interact with m^6A-containing AMV vRNAs. Given the functional relevance of m^6A on the biology of AMV, in this thesis it was decided to deepen the knowledge of the implications of the m^6A regulation mechanism on the viral

infectious cycle of AMV. For this, it was decided: (i) deepen the functional understanding of the m^{6}A- demethylase ALKBH9B, (ii) evaluate the *in vivo* function of the putative two m^{6}A-sites present in the 3'UTR-RNA 3, and (iii) explore a possible involvement of some m^{6}A-methyltransferases in infection caused by AMV.

Regarding the first objective, we mapped functional subdomains in the atALKBH9B m6A-demethylase required for its binding to the viral RNA and to the coat protein of alfalfa mosaic virus. Remarkably, it was observed the presence of intrinsically disordered regions (IDRs) in the N-terminal region, within the internal domain like *AlkB* and in the C-terminal region. About 78% of the RNA binding domain (RBD) identified in ALKBH9B is contained in the C-terminal IDR. In this context, it has been proposed that the capability to specifically target different RNAs in RBPs containing IDRs is due to conformational flexibility as well as the establishment of extended conserved electrostatic interfaces with RNAs. Additionally, due that IDRs are frequently localized in proteins that undergo liquid-liquid phase separation (LLPS), a process that likely contributes to the formation and stability of RNA granules, its possible that the IDRs and the RBD of ALKBH9B could act cooperatively to promote RNA granule formation.

The analysis of the putative DRACH-motifs located in the hpB loop and the lower-stem of hpE in the 3'UTR RNA 3 present hot sites involved in AMV replication *in vivo*. The identity of residues $_{2012}$A, $_{2013}$A and $_{2014}$A in the hpB loop appears to be a key structural requirement for AMV replication and/or accumulation. Regarding hpE, our results determined that the putative m^{6}A-residue $_{1902}$A, as well as the base pairing of the lower-stem of hpE, are also essential requirements for the *in vivo* plus-strand synthesis in AMV. To our knowledge, this is the first evidence in AMV to show that the hpB loop and the lower-stem of hpE are involved in viral replication/accumulation and plus-strand synthesis, respectively.

Finally, regarding the study of the influence of m^{6}A-methyltransferases on the viral infection cycle of AMV, a non-proviral and/or antiviral effect was determined in the m^{6}A-mRNA methyltransferase complex made up of atMTA:atMTB, nor of the putative m^{6}A-rRNA

methyltransferase complex made up of atMETTL5-*like*:atTRMT112-*like* on the biology of AMV.

In summary, this work: (i) elucidates the functional structure of the first plant m^6A-demethylase, ALKBH9B, (ii) reveals the functional importance of putative DRACH-motifs located in the 3'UTR-RNA 3 for viral RNA replication/accumulation in AMV,and (iii) explores the involvement of m^6A-methyltransferases in AMV biology. Therefore, this thesis provides new observations that seek to understand the implications of the m^6A regulation mechanism in the viral infectious cycle of AMV.

Resumen

La N^6-metiladenosina (m^6A) es una modificación generalizada en los ARN celulares de diferentes organismos que puede afectar muchos procesos y vías celulares. En las plantas, la modificación de m^6A ocurre mediante un complejo de metilación que contiene varias proteínas: MTA, MTB, FIP37, VIR y HAKAI. Esta modificación es eliminada por desmetilasas de la familia *AlkB*, mientras que los miembros de la familia ECT (EVOLUTIONARILY CONSERVED C-TERMINAL REGIONS) son las proteínas mejor descritas que reconocen y procesan los ARN modificados con m^6A. En *Arabidopsis*, se ha informado que m^6A controla el desarrollo de plantas en etapa embrionaria, el crecimiento vegetativo y la floración. Esta modificación también está presente en los ARN genómicos de los virus y en las transcripciones de algunos virus ADN. Los estudios de epitransciptómica viral han revelado un papel igualmente importante de m^6A durante la infección por virus; sin embargo, no existe una función proviral o antiviral de la metilación de m^6A que pueda generalizarse. En plantas, hay pocos estudios de la actividad reguladora de m^6A durante infecciones virales. El laboratorio donde se ha llevado a cabo este trabajo ha sido pionero en el estudio del efecto de m^6A en la interacción planta-virus, utilizando como virus modelo el Virus del mosaico de la alfalfa (AMV). AMV pertenece a la familia *Bromoviridae* y, como el resto de los miembros de esta familia, su genoma está formado por tres ARN monocatenarios de polaridad positiva. El ARN 1 y el ARN 2 codifican las subunidades de replicasa (P1 y P2), mientras que el ARN 3 codifica la proteína de movimiento (MP) y sirve como molde para la síntesis del ARN subgenómico 4 (sgARN 4), que codifica la proteína de cubierta (CP). Al comienzo de esta tesis, nuestro laboratorio ya había informado sobre: (i) la presencia de supuestos motivos m^6A en el 3'UTR del RNA 3, una región crítica para la replicación de AMV, (ii) la primera m^6A-desmetilasa de *Arabidopsis* (ALKBH9B), (iii) la relevancia funcional de ALKBH9B para mantener niveles adecuados de m^6A/A para la correcta replicación de AMV, (iv) la capacidad de la CP de AMV para interactuar con ALKBH9B, posiblemente para usurpar la actividad de ALKBH9B, y (v) la capacidad de las

proteínas de *Arabidopsis* ECT2, ECT3 y ECT5 para interactuar con el ARNv de AMV que contienen m^6A. Dada la relevancia funcional de m^6A en la biología de AMV, en esta tesis se decidió profundizar en el conocimiento de las implicaciones del mecanismo de regulación de m^6A en el ciclo infeccioso viral de AMV. Para ello, se decidió: (i) profundizar en la comprensión funcional de la m^6A-desmetilasa ALKBH9B, (ii) evaluar la función *in vivo* de los supuestos dos sitios m^6A presentes en el 3'UTR del RNA 3, y (iii) explorar una posible implicación de algunas m^6A metiltransferasas en la infección causada por AMV.

Con respecto al primer objetivo, mapeamos los subdominios funcionales de atALKBH9B necesarios para su unión al ARN viral y a la CP de AMV. Sorprendentemente, se observó la presencia de regiones intrínsecamente desordenadas (IDRs) en la región N-terminal, dentro del dominio interno similar a *AlkB* y en la región C-terminal. Alrededor del 78% del dominio de unión a ARN (RBD) identificado en ALKBH9B está contenido en el IDR C-terminal. En este contexto, se ha propuesto que la capacidad de las RBP que contienen IDRs a dirigirse específicamente a diferentes ARN se debe a la flexibilidad conformacional, así como al establecimiento de interfaces electrostáticas conservadas extendidas con ARN. Además, debido a que las IDRs se localizan con frecuencia en proteínas que se someten a la separación de fases líquido-líquido (LLPS), un proceso que probablemente contribuye a la formación y estabilidad de los gránulos de ARN, es posible que las IDR y la RBD de ALKBH9B puedan actuar de manera cooperativa para promover la formación de gránulos de ARN.

El análisis de los putativos motivos DRACH localizados en el bucle de hpB y en el tallo inferior de hpE del 3'UTR/ARN 3 de AMV demostró que son sitios críticos involucrados en la replicación *in vivo* de AMV. La identidad de los residuos $_{2012}A$, $_{2013}A$ y $_{2014}A$ en el bucle hpB parece ser un requisito estructural clave para la replicación y/o acumulación de AMV. Con respecto a hpE, nuestros resultados determinaron que el supuesto residuo de m^6A ($_{1902}A$), así como el apareamiento de bases del tallo inferior de hpE, también son requisitos esenciales para la síntesis *in vivo* de ARNs de cadena positiva en AMV. Hasta donde sabemos, esta es la primera evidencia en AMV que muestra que el bucle de hpB y el tallo inferior de hpE están

involucrados en la replicación/acumulación viral y la síntesis de ARNs de cadena positiva, respectivamente.

Finalmente, en cuanto al estudio de la influencia de las m^6A-metiltransferasas en el ciclo de infección viral de AMV, no se determinó un efecto proviral y/o antiviral en el complejo m^6A-ARNm metiltransferasa conformado por atMTA:atMTB, ni en el putativo complejo m^6A-ARNr metiltransferasa conformado por atMETTL5-*like*:atTRMT112-*like* sobre la biología de AMV.

En resumen, este trabajo: (i) aclara la estructura funcional de la primera m^6A-desmetilasa de plantas, ALKBH9B, (ii) revela la importancia funcional de los supuestos motivos DRACH ubicados en 3'UTR del RNA 3 para la replicación/acumulación de ARN viral en AMV, y (iii) explora la participación de las m^6A-metiltransferasas en la biología de AMV. Por lo tanto, esta tesis aporta nuevas observaciones que buscan comprender las implicaciones del mecanismo de regulación de m^6A en el ciclo infeccioso viral de AMV.

Resum

La N^6-metiladenosina (m^6A) és una modificació generalitzada en els ARN cellulars de diferents organismes que pot afectar molts processos i vies cellulars. En les plantes, la modificació de m^6A ocorre mitjançant un complex de metilació que conté diverses proteïnes: MTA, MTB, FIP37, VIR i HAKAI. Aquesta modificació és eliminada per desmetilasas de la família *AlkB*, mentre que els membres de la família ECT (EVOLUTIONARILY CONSERVED C-TERMINAL REGIONS) són les proteïnes més ben descrites que reconeixen i processen els ARN modificats amb m^6A. En *Arabidopsis*, s'ha informat que m^6A controla el desenvolupament de plantes en etapa embrionària, el creixement vegetatiu i la floració. Aquesta modificació també és present en els ARN genòmics dels virus i en les transcripcions d'alguns virus ADN. Els estudis de epitransciptómica viral han revelat un paper igualment important de m^6A durant la infecció per virus; no obstant això, no existeix una funció proviral o antiviral de la metilació de m^6A que puga generalitzarse. En plantes, hi ha pocs estudis de l'activitat reguladora de m^6A durant infeccions virals. El laboratori on s'ha dut a terme aquest treball ha sigut pioner en l'estudi de l'efecte de m^6A en la interacció planta-virus, utilitzant com a virus model el Virus del mosaic de l'alfals (AMV). AMV pertany a la família *Bromoviridae* i, com la resta dels membres d'aquesta família, el seu genoma està format per tres ARN monocatenarios de polaritat positiva. L'ARN 1 i l'ARN 2 codifiquen les subunitats de replicasa (P1 i P2), mentre que l'ARN 3 codifica la proteïna de moviment (MP) i serveix com a motle per a la síntesi de l'ARN subgenómico 4 (sgRNA 4), que codifica la proteïna de coberta (CP). Al començament d'aquesta tesi, el nostre laboratori ja havia informat sobre: (i) la presència de suposats motius m^6A en el 3'UTR del RNA 3, una regió crítica per a la replicació de AMV, (ii) la primera m^6A-desmetilasa de *Arabidopsis* (ALKBH9B), (iii) la rellevància funcional d'ALKBH9B per a mantindre nivells adequats de m^6A/A per a la correcta replicació de AMV, (iv) la capacitat de la CP de AMV per a interactuar amb ALKBH9B, possiblement per a usurpar l'activitat d'ALKBH9B, i (v) la capacitat de les proteïnes de *Arabidopsis* ECT2, ECT3 i ECT5 per a interactuar amb el ARNv

de AMV que contenen m^6A. Donada la rellevància funcional de m^6A en la biologia de AMV, en aquesta tesi es va decidir aprofundir en el coneixement de les implicacions del mecanisme de regulació de m^6A en el cicle infecciós viral de AMV. Per a això, es va decidir: (i) aprofundir en la comprensió funcional de la m^6A-desmetilasa ALKBH9B, (ii) avaluar la funció *in vivo* dels supòsits dos llocs m^6A presents en el 3'UTR del RNA 3, i (iii) explorar una possible implicació d'algunes m^6A metiltransferasas en la infecció causada per AMV.

Respecte al primer objectiu, hem mapatge els subdominis funcionals de atALKBH9B necessaris per a la seua unió a l'ARN viral i a la CP de AMV. Sorprenentment, es va observar la presència de regions intrínsecament desordenades (IDRs) a la regió N-terminal, dins del domini intern similar a AlkB i a la regió C-terminal. Al voltant del 78% del domini d'unió a ARN (RBD) identificat en ALKBH9B està contingut en el IDR C-terminal. En aquest context, s'ha proposat que la capacitat de les RBP que contenen IDRs a dirigirse específicament a diferents ARN es deu a la flexibilitat conformacional, així com a l'establiment d'interfícies electroestàtiques conservades esteses amb ARN. A més, pel fet que les IDRs es localitzen amb freqüència en proteïnes que se sotmeten a la separació de fases líquid-líquid (LLPS), un procés que probablement contribueix a la formació i estabilitat dels gràmuls d'ARN, és possible que les IDR i la RBD d'ALKBH9B puguen actuar de manera cooperativa per a promoure la formació de gràmuls d'ARN.

L'anàlisi dels putatius motius DRACH localitzats en el bucle de hpB i en la tija inferior de hpE del 3'UTR/ARN 3 de AMV va demostrar que són llocs crítics involucrats en la replicació *in vivo* de AMV. La identitat dels residus $_{2012}A$, $_{2013}A$ i $_{2014}A$ en el bucle hpB sembla ser un requisit estructural clau per a la replicació i/o acumulació de AMV. Respecte a hpE, els nostres resultats van determinar que el suposat residu de m^6A ($_{1902}A$), així com l'aparellament de bases de la tija inferior de hpE, també són requisits essencials per a la síntesi *in vivo* de ARNs de cadena positiva en AMV. Fins on sabem, aquesta és la primera evidència en AMV que mostra que el bucle de hpB i la tija inferior de hpE estan involucrats en la replicació/acumulació viral i la síntesi de ARNs de cadena positiva, respectivament.

Finalment, quant a l'estudi de la influència de les m^{6}A-metiltransferasas en el cicle d'infecció viral de AMV, no es va determinar un efecte proviral i/o antiviral en el complex m^{6}A-ARNm metiltransferasa conformat per atMTA:atMTB, ni en el putatiu complex m^{6}A-ARNr metiltransferasa conformat per atMETTL5-*like*:atTRMT112-*like* sobre la biologia de AMV.

En resum, aquest treball: (i) aclareix l'estructura funcional de la primera m^{6}A-desmetilasa de plantes, ALKBH9B, (ii) revela la importància funcional dels suposats motius DRACH situats en 3'UTR del RNA 3 per a la replicació/acumulació d'ARN viral en AMV, i (iii) explora la participació de les m^{6}A-metiltransferasas en la biologia de AMV. Per tant, aquesta tesi aporta noves observacions que busquen comprendre les implicacions del mecanisme de regulació de m^{6}A en el cicle infecciós viral del AMV.

Abbreviations

VIRUSES

In plants:

AMV Alfalfa mosaic virus

BMV Brome mosaic virus

CGMMV Cucumber green mottle mosaic virus

CMV Cucumber mosaic virus

PVA Potato virus A

PVX Potato virus X

PVX Potato virus Y

RBSDV Rice black-streaked dwarf virus

RSV Rice stripe virus

TCV Turnip crinkle virus

TMV Tobacco mosaic virus

TRV Tobacco rattle virus

TuMV Turnip mosaic virus

WYMV Wheat yellow mosaic virus

In Animals:

Ad5 Adenoviral serotype 5

ASLV Avian sarcoma leukosis virus

AV Adenovirus

CHIKV Chikungunya virus

DENV Dengue virus

EBV Epstein-Barr virus

EV71 Enterovirus type 71

HBV Hepatitis B virus

HCMV Human cytomegalovirus

HCV Hepatitis C virus

HIV-1 Human Immunodeficiency virus-1

HMPV Human metapneumovirus

HSV-1 Herpes simplex virus-1

IAV Influenza A virus

KSHV Kaposi's sarcoma-associated herpesvirus

PEDV Porcine epidemic diarrhea virus

PV Poliovirus

RSV Rous sarcoma virus

SARS-CoV-2 Severe acute respiratory syndrome coronavirus 2

SV40 Simian virus 40

VSV Vesicular stomatitis virus

ZIKV Zika virus

OTHERs

A Adenosine

AGO ARGONAUTE

AlkB Alkylation B

ALKBH AlKB homolog

AN ANGUSTIFOLIA

APA alternative polyadenylation

BiFC Bimolecular fluorescence complementation

cDNA Complementary DNA

CLSM Confocal laser-scanning microscopy

CP Coat protein

CPB CP binding

CPSF30 Cleavage and Polyadenylation Specificity Factor 30

DCP1/DCP2 mRNA-decapping enzyme 1 and 2

DDX Nuclear DEAD-box

DNA Deoxyribonucleic acid

Dpa Days post-agroinfiltration

Dpi Days post-inoculation

dsRNA Double strand RNA

ECT EVOLUTIONARILY CONSERVED C-TERMINAL REGION

Edc3, Pat1, DDX6 and EDLS/GE1 decapping coactivators activatorst

eIF3 Eukaryotic initiation factor 3

EMSA Electrophoretic Mobility Shift Assays

eRNA enhancer RNA

FIO1 *Arabidopsis* FIONA1

FIP37 FKBP12 interacting protein 37

FTO Fat mass and obesity associated protein

G3BP Ras-GAP SH3 domain binding protein

GFP Green fluorescence protein

gRNA Genomic RNA

GST Glutathione S-transferase

HA Hemagglutinin

HCPro helper-component protein

His Histidine

hnRNPA2B1 Heterogeneous nuclear RNP A2B1

hr hour

ICR Internal control region

ICTV International Committee on Taxonomy of Viruses

IDR Intrinsically disordered domain

IFN Interferon

iRNA interference RNA

JA jasmonic acid

Kb Kilobase

K_d constant dissociation

LLPS liquid-liquid phase separation

lncRNA long non-coding RNA

Lsm1-7 Deadenylation complex or decapping activators

m6A N^6-methyladenosine

m^7G N^7-Methylguanosine

m-ASP m^6A–assisted polyadenylation

mCherry monomeric red fluorescent proteins

METTL Methyltransferase-like protein

min minutes

miRNA micro RNA

MP Movement protein

mRNA Messenger RNA

MTase methyltransferase

MVB Multivesicular body

ncRNA non-coding RNA

NES nuclear export signal

ng nanograme
nm nanometre
NMD Nonsense-mediated decay
NP Nucleoprotein
nts nucleotides
OD Optical density
ORF Open reading frame
P Polymerase
P1/P2 AMV polymerase subunits
PABP poly(A)-binding protein
PAS Polyadenylation signal
PATL3 Patellin 3
P-bodies or PB Processing body
PsbP subunits of photosystem II
PTC Premature termination codon
PTGS Post-transcriptional gene silencing
RBD RNA-binding domain
RBP RNA-binding protein
RDR RNA dependent RNA polymerase
RNA pol RNA polymerase
RNA Ribonucleic acid
RNAi RNA interference
RNase Ribonuclease
RNP Ribonucleoprotein
ROS reactive oxygen species
RRM RNA recognition motifs
rRNA Ribosomal RNA
RT Reverse transcription
SA salicylic acid
SAM S-adenosyl-L-methionine
SAM shoot apical meristem
SG Stress granule
sgRNA Subgenomic RNA
SGS3 SUPRESSOR OF GENE SILENCING 3
siRNA Small interfering RNA
snRNAs small nuclear RNA
ssDNA Single-stranded DNA
ssRNA(+/-) Positive or negative-sense single-stranded RNA
tasiRNA trans-acting siRNA
TLS tRNA-like structure
TRAF TUMOR NECROSIS FACTOR RECEPTOR ASSOCIATED FACTOR
tRNA Transference RNA
TSN TUDOR STAPHYLOCOCCAL
UBP1 oligouridylate-binding protein 1
UPF Up-frameshift proteins
UTR Untranslated region
VAR VARICOSE
VIR VIRILIZER
VOZ VASCULAR PLANT ONE-ZINC FINGER
VPg viral genome-linked protein
VRC Viral replication complexes/factories
vRNA Viral RNA
WT Wild-type
WTAP WILMS' TUMOR-ASSOCIATED PROTEIN
XRN 5'-3' exoribonuclease
YTH YT521-B homology

General introduction

1. Viruses concept

Viruses (from the Latin, meaning "venom") have been documented since the beginning of our history (Taylor, 2014). However, their discovery and investigation as infectious agents did not begin until the end of the 19th century, when Martinus Beijerinck and Dmitri Iwanowski, using the postulates of Koch (1882), independently described an unusual agent that caused mosaic disease in tobacco (later named Tobacco mosaic virus -TMV-) (Iwanowski, 1892; Beijerinck, 1898).

Viruses are obligate biotrophic parasites that need to infect living cells and use host components to make copies of themselves. The viral genome can be composed of segmented or non-segmented DNA or RNA molecules of positive or negative polarities and with single or double strand and linear or circular (DNA viruses) structures. This genetic code is encapsulated by coat or capsid proteins; in addition, some viruses have a second layer of proteins, while others acquire a lipoprotein membrane from the host cell, forming an envelope (Hull, 2013).

The International Committee for the Taxonomy of Viruses (ICTV, http://www.ictvonline.org/) is responsible for setting the names of all viruses and establishing their classification, based on the general hierarchical scheme used for all living organisms: Order, Family, Subfamily, Genus and Species (Moreno et al., 2016). According to the tenth ICTV report, plant viruses comprise 118 genera and 1,516 species. In general, plant viruses have a very small genome, 2.5-19 Kb, with most of them between 4 and 6 Kb. The genetic material accounts for between 5 and 40% of the total weight of the virion. Most of these viruses have positive-sense single-stranded RNA genomes ((+)ssRNA), while only a few comprise negative-sense single-stranded RNA genomes ((-)ssRNA). In addition, these genomes harbor at least 3 genes: 1 (or more) involved in the replication of the genetic material, 1 (or more) associated with the cell-cell movement and 1 (or more) that code for the capsid proteins. Additionally, they may contain genes that have regulatory functions or

that are required for transmission between plants in association with a vector or for invasion of certain host species (Culver and Padmanabhan, 2007; Pallas and García, 2011; Moreno et al., 2016).

Plant viruses make up almost 50% of emerging and re-emerging diseases worldwide, damaging both natural vegetation and cultivated plants (Bos, 1981; Jones, 2009). Its economic consequences for global agriculture are estimated at more than $30 billion annually (Jones and Naidu, 2019). This means that viral diseases represent a global threat to food security, which has been worsening in recent years due to (i) agricultural globalization and international trade, as a result of rapid population growth, which favor the spread of viruses and their vectors in new geographic regions with unexpected consequences for food production and natural ecosystems, and (ii) variable environmental conditions generated by climate change, which make epidemics more difficult to manage (Jones, 2014, 2016). Understanding the biology of the virus, as well as the mechanisms of virus-host interaction, is essential to combat its negative impact.

2. Alfalfa Mosaic Virus

2.1.Origin, geographical distribution and economic impact

Alfalfa mosaic virus (AMV) is the only member of the *Alfamovirus* genus in the *Bromoviridae* family (Bujarski et al., 2019). It was identified in the state of Washington, United States in 1931 (Weimer, 1931), and it is considered the most important viral pathogen in alfalfa (*Medicago sativa*) (Avgelis and Katis, 1989; Al-Saleh and Amer, 2013). It has a wide host range (more than 250 species of plants belonging to 48 families), and it is distributed worldwide (Moury and Verdin, 2012; Kenyon et al., 2014).

Data from 2020 indicate that Spain is the main exporter of alfalfa in Europe, and the second worldwide after the United States. In fact, in the last campaign, the total production exceeded 1.3 million tons and 83% of it was destined for international trade, with the United Arab

Emirates and China being the main importers. The quality of the alfalfa has been a decisive factor in the success of the internationalization of this product (Sereno, 2020).

Control of AMV in the field is considered crucial to maintain the quality of the alfalfa crop because: (i) it has very high infection rates (between 53 and 76%), (ii) it reduces forage production between 14.8 and 22.8%, and (iii) decreases between 15 and 18.1%, the fresh and dry weight, respectively, of the harvest (Bailiss and Ollennu, 1986; Yardımcı et al., 2006). Also, the economic importance of AMV control in other crops of agricultural interest has been reported, such as: faba beans (*Vicia faba*), lentils (*Lens culinaris*) and chickpeas (*Cicer arietinum*), where reductions in shoot dry weight of 41, 74 and 50% respectively, as well as a decrease in seed yield of 45, 87 and 98%, respectively, have been reported (Latham et al., 2004).

2.2.Viral transmission and symptomatology

AMV is transmitted mechanically, by grafting, and in the nonpersistent manner by several aphid species, including species that frequently colonize alfalfa crops: *Aphis craccivora*, *Acyrthosiphon pisum* and *Therioaphis trifolii*; and species that typically infect vegetable crops: *Aphis fabae* and *Myzus persicae* (Escriu et al., 2011; Moreno and Fereres, 2012). Moreover, AMV can be transmitted through pollen and seeds (Pathipanowat et al., 1995). The impact of these type of transmission in commercial production is unknown (Hill and Whitham, 2014).

Symptoms of an infected plant are highly dependent on: (i) virus strain, (ii) host variety, (iii) plant growth stage, and (iv) environmental conditions. However, The most widespread symptom that gives its name to AMV is the presence of yellow mottling or mosaics (Figure 1 A, B and C), sometimes accompanied by wrinkling of the leaves, dwarfism, malformations and in the most extreme cases, necrosis of the fruits (Figure 1 D) (Smith, 1991; Goldberg, 2012). In alfalfa, a reduced growth of roots and aerial parts of infected plants has been reported, caused by the reduction in the degree of nodulation and, therefore, in its ability to fix atmospheric nitrogen. Consequently, the partial loss of nitrogen fixation produces a lower

amount of crude protein decreasing the nutritional quality and increasing the susceptibility to extreme weather conditions such as frost and the infection by other pathogens (Escriu et al., 2011). Finally, AMV isolates can be classified into two phylogenetic subgroups (Parrella et al., 2000). This separation did not correlate with differences in host range or symptoms (necrotic or non-necrotic) induced in tomato but rather it reflected variations in the amino acid sequence of their CP, which might be related to structural properties of virus particles.

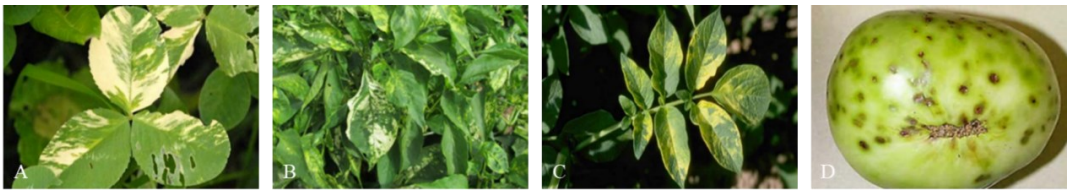

Figure 1. Symptoms associated with AMV. Yellow mosaics in alfalfa (A), pepper (B) and potato (C), and necrosis in tomato fruit (C). Adapted from Goldberg (2012).

2.3.Genome organization and life cycle

The AMV genome consists of three single-stranded RNA molecules (RNA1 to RNA3) of positive polarity. RNA1 (3.6 Kb) encodes the protein 1 (P1), which contains an N-terminal methyltransferase-like domain and C-terminal helicase-like domain; RNA2 (2.6 Kb) encodes the protein 2 (P2), which contains a polymerase-like domain; and RNA3 (2.1 Kb) is bicistronic and encodes the movement protein (MP) and the coat protein (CP), although the latter is expressed from a subgenomic RNA (sgRNA4; 0.88 Kb). Each RNA contain untranslated regions (UTRs) at their 5' and 3' terminus and are capped (m^7G) at the 5' end but lack of poly(A)-tail at the 3' (Figure 2) (Bol, 2008). Also, the viral RNAs (vRNAs) are separately encapsidated into bacilliform particles, which present a constant diameter of 18 nm and a length that varies from 30 to 57 nm, depending on the encapsidated molecule (Makkouk et al., 2012).

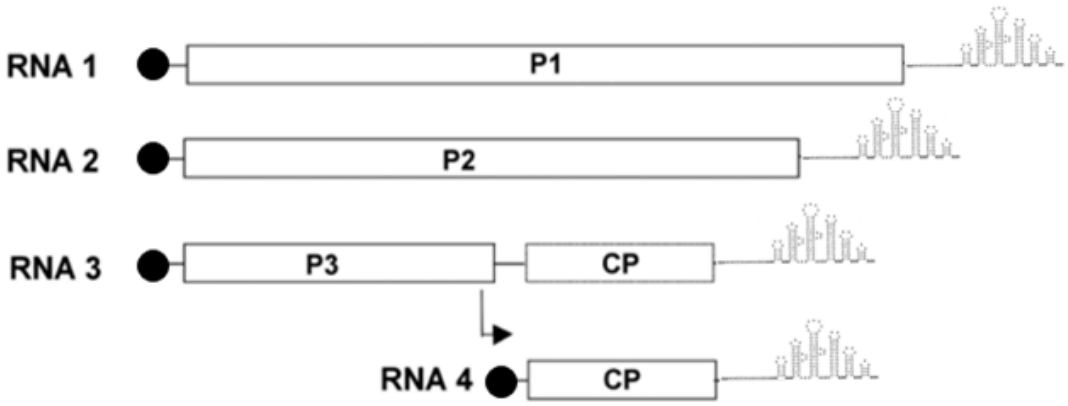

Figure 2. AMV genome organization. Schematic representation of the AMV RNAs and the encode proteins. The m^7G structure in the 5'UTR is represented by spheres and the stem-loop structure at the 3'UTR is displayed. Adapted from Bol, (2003).

Similar to ilarviruses, the 3'UTRs of AMV gRNAs have a high homology (>80%), and can form two mutually exclusive conformers that are believed to act as a molecular switch from translation to replication (Figure 3) (Koper-Zwarthoff et al., 1979; Aparicio et al., 2003; Chen and Olsthoorn, 2010; Pallas et al., 2013). On one hand, the 3′UTRs are folded into a linear array of several hairpin structures (hpA to hpE) flanked by AUGC-motif, which represent specific CP binding (CPB) sites (Reusken and Bol, 1996). The CP RNA-binding motif is a sequence rich in basic residues located in the N-terminal part, in which the arginine at position 17 is critical for this interaction (Ansel-McKinney et al., 1996). This RNA-protein interaction is critical in AMV and Ilarvirus to initiation of the infection in a phenomena-denominated "*genome activation*" (Bol, 1999; Jaspars, 2014). On other hand, the 3'UTR of AMV RNAs can adopt an alternative tertiary conformation resembling a tRNA-like structure (TLS) by base pairing between the UCCU and AGGG sequences of hpD and hpA, respectively (Figure 3). The TLS conformer promotes the synthesis of negative polarity vRNAs. Furthermore, hpE is the primary element recognized by the AMV RNA-dependent RNA polymerase (RdRp) (Olsthoorn et al., 1999). Therefore, according to the switch model, 3'UTR-TLS conformer favors negative vRNA synthesis, whereas 3'UTR-CPB conformation favors protein translation (Olsthoorn et al., 1999; Chen and Olsthoorn, 2010).

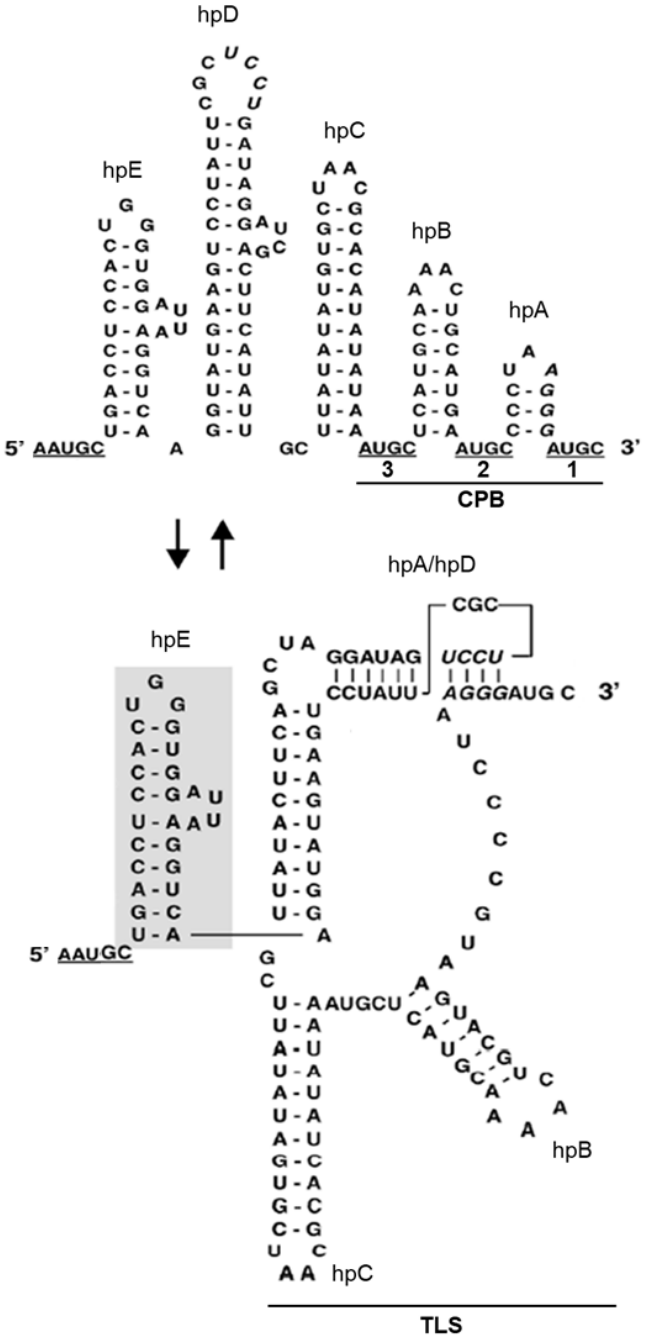

Figure 3. Schematic representation of the last 145 nucleotides of the AMV 3'UTR RNA 3. Molecular switch between CPB (A) and TLS conformer (B). AUGC-sequence motifs of the CPB confirmer are underlined. Adapted from Bol, (2003).

2.3.1. Replication, translation and encapsidation

Following host entry and subsequent disassembly of AMV virions, some CP molecules bound to the 3'UTR of the vRNAs stabilizing the CPB conformation (Figure 3). CP primarily enhances translation of RNAs 1 and 2 possibly because it (i) mimics the role of binding of the poly(A)-binding protein (PABP) to the poly(A)-tail of cellular messengers RNAs, (ii) can interact with eIF4G as well as other host translation initiation factors, and (iii) blocks TLS formation to prevent a collision between translating ribosomes and viral replicase (Bol, 2003). Then, the P1 protein (RNA 1) recruits the plus-strand vRNAs from the translation machinery and the P2 protein (RNA 2) into vesicles derived from the tonoplast (also called multivesicular bodies: MVB), forming replication complexes, which are transported posteriorly to the tonoplast (Ibrahim et al., 2012). Synthesis of negative-strand vRNAs comprises that conserved hpE to function as minus-strand promoter and the TLS conformer guides the replicase to the 3′-terminal initiation site on the RNA template (Olsthoorn and Bol, 2002; Chen and Olsthoorn, 2010). The formation of the TLS structure requires removing the CP (Figure 3) and this dissociation has been proposed to be caused by the proteolytic cleavage of the CP N-terminus, product of the union of the replicase complex with hpE, or by the insertion of the CP-vRNAs complex into the MVB (Bol, 2005). Although AMV CP is not necessary for the synthesis of positive or negative vRNAs (Houwing and Jaspars, 1986; Bol, 2003) it plays a fundamental role during viral replication: protecting positive-sense vRNAs from degradation and thus, promoting their accumulation (Bol, 2005). The synthesis of positive-sense vRNAs would require the binding of P1 to the internal control region type 2 (ICR2 motif) identified in a stem-loop structure within the 5'UTR that resembles the eukaryotic promoter recognized by host RNA polymerase II (Marsh et al., 1989). The ICR2 motif as well as the stem-loop structure where it is located, are important in maintaining the activity of the plus-strand promoter (Van der Vossen and Bol, 1996). Finally, regarding the assembly of the virion, the entire molecular mechanism of this process is unknown (Bol, 2005, 2008).

2.3.2. Cell-to-cell and systemic movement

Cell-to-cell movement of plant viruses occurs via plasmodesmata and involves one or more virus-encoded MPs. Two main mechanisms of cell-to-cell movement have been characterized in plant viruses: (i) altering the size exclusion limit of plasmodesmata and cell-to-cell transport of a complex of vRNA and MP, together with the complexes of viral replication by a mechanism that does not involve CP; (ii) the formation of tubular structures that traverse plasmodesmata and guide the transport of virions to a neighboring cell (Sánchez-Navarro et al., 2006; Heinlein, 2015; Navarro et al., 2019).

In AMV, the mechanism used for cell-cell transport through the plasmodesma is unclear. Some studies indicate that both MP and CP are necessary for cell-to-cell movement, with the interaction between the C-terminal region of MP and CP being critical for the process (Sánchez-Navarro and Bol, 2001). It has also been observed that the elimination of C-terminal residues in the CP interferes with the formation of viral particles (Tenllado and Bol, 2000), but not with cell-to-cell movement which suggests that AMV could move as an RNA-protein complex involving MP and CP (Sánchez-Navarro and Bol, 2001). Furthermore, transient expression studies have suggested that cell-cell transport might be guided by MP tubule formation (Zheng et al., 1997); and that, in some cases, the plasmodesmata of infected cells may be full of virions (Kasteel et al., 1997); suggesting that virions can also be transported from one cell to another.

On the other hand, it is relevant to indicate that the AMV MP belonging to the 30K superfamily can be replaced by MPs of *Cucumo*-, *Tobamo*-, *Ilar*-, *Bromo*- and *Comovirus*, all belonging to the same superfamily, without affecting cell-cell movement (Sánchez-Navarro et al., 2006). Furthermore, it has been shown that in order to facilitate intra- and inter-cellular movement, viruses also use host proteins: plasmodesmata and cell wall-associated proteins, cytoskeleton, protein kinases, calcium sensors, and putative transcriptional coactivators that could alter viral movement (Pallas and García, 2011). For example, it has been determined that the overexpression in *Arabidopsis* of atPATL3 and/or

atPATL6, proteins containing a Sec14 domain, interfered with the plasmodesmata targeting of AMV MP and correlated with reduced infection foci size. Interestingly, Sec14 domains are implicated in membrane trafficking, cytoskeleton dynamics, lipid metabolism and lipid-mediated regulatory functions (Peiro et al., 2014).

Finally, for systemic invasion of plants, viruses need to reach the vascular system. For this, it is necessary to overcome various cellular barriers that surround the sieve elements of the phloem: vascular bundle, parenchyma and companion cells (Navarro et al., 2019). AMV has been reported to achieve long-distance transmission as viral particles (Seo et al., 2016); however, the molecular mechanism involved in this process is still unknown.

2.4.Interaction of AMV CP with host proteins

AMV CP is a multifunctional protein that in addition to virion formation is involved in the regulation of replication and translation of vRNAs and in cell-to-cell and systemic movement of the virus (Bol, 2003). Furthermore, as found for other viral proteins, AMV CP interacts with host factors to elicit the transcriptional reprogramming of diverse cellular pathways. Currently, it is well stablished that to initiate translation, AMV CP interacts with eIF4G and eIFiso4G, subunits of the initiation factors eIF4F and eIFiso4F, respectively (Krab et al., 2005). In addition, the CP has been shown to interact with the *Arabidopsis* protein PsbP, a nucleus-encoded subunit of the photosystem II oxygen-generating complex. Binding of CP sequesters PsbP in the cytosol preventing its transport to chloroplasts. PsbP would have an antiviral function since PsbP overexpression markedly reduced AMV accumulation (Balasubramaniam et al., 2014). More recently it was shown in our laboratory that the AMV CP interacts with the *Arabidopsis* protein ALKBH9B, an m^6A-demethylase that recognizes AMV vRNAs and decreases the relative abundance of m^6A to promote viral accumulation (Martínez-Pérez et al., 2017).

Early electron microscopy studies showed that AMV CP accumulates in the cytoplasm, nucleus and the nucleolus of infected cells (Van Pelt-Heerschap et al., 1988). Later, a mutational analysis identified two domains implicated in the nucleocytoplasmic localization

of CP: a lysine-rich N-terminal nucleolar localization signal (NoLS) required to enter the nucleus and accumulate in the nucleolus, and a leucine-rich C-terminal domain that could function as a nuclear export signal (NES) (Herranz et al., 2012). Additionally, AMV replication was found to be favored at low CP levels, and strongly inhibited at high CP levels (Guogas et al., 2005), and it was suggested that AMV could use the nucleus or nucleolus as a temporary CP storage site to reduce excess CP in the cytoplasm (Herranz et al., 2012). On the other hand, the CP was found to interact with an *Arabidopsis* helix-loop-helix (bHLH) family transcription factor (ILR3) and the formation of the CP-ILR3 complex negatively affects the activity of the protein NEET (Aparicio and Pallás, 2017). AtILR3 is implicated in modulating multiple stress responses (Samira et al., 2018) whereas that NEET is involved in plant development, senescence, iron metabolism, and reactive oxygen species (ROS) homeostasis (Nechushtai et al., 2012). Thus, CP-ILR3 interaction induced the activation of the signaling defenses dependent on ROS, salicylic acid (SA) and jasmonic acid (JA) leading to a state of plant hormonal balance, where the infection remains at a level that does not affect plant viability (Aparicio and Pallás, 2017). The accumulation of the CP in the nucleus could function not only as a merely CP storage site, but also modulating or recruiting other host nuclear or nucleolar factors either promoting infection or acting as antiviral factors.

3. RNA granules

Cells are continually subject to fluctuating environments. To respond, adapt and/or survive, cells rapidly and dynamically reprogram their transcriptomic, metabolomic, proteomic and degradomic profiles (Kollist et al., 2019). RNA metabolism is essential for growth, development, and responses to stress (Chantarachot and Bailey-Serres, 2018). These processes require the assembly of RNA-ribonucleoprotein (RNP) complexes, which may be located in the nucleus: nuclear specks, nuclear stress bodies, and plant photobodies; nucleolus: Cajal bodies; as well as in the cytoplasm: processing bodies (PB, also called: P-bodies), stress granules (SGs) or the small interfering RNA (siRNA) bodies (Anderson and Kedersha, 2008; Campos-Melo et al., 2021). These membrane-less biomolecular

condensates, commonly called RNA granules, are formed as a result of phase separation and/or condensation of their molecular components (Banani et al., 2017).

SGs and P-bodies are the main RNA granules involved in post-transcriptional regulation and translational control. They are made up of translationally inactive mRNAs and different RNPs, in particular with components of translation initiation (SGs) and components of mRNA degradation machinery (P-bodies) (Ivanov et al., 2019). While P-bodies are constitutively present in cells, SGs only become detectable under stress conditions (increased number of translationally inactive mRNAs) (Youn et al., 2019). Although SGs and P-bodies are considered to be distinct RNA granules, these complexes are physically, compositionally, and functionally associated (Chantarachot and Bailey-Serres, 2018; Maruri-López et al., 2021).

Different marker proteins for each type of granule have been identified, as well as proteins that are shared by both granules. In mammals, the SGs associated RNPs are: cytoplasmic polyadenylation element binding protein, Histone deacetylase 6, Tudor domain-containing protein 3 or Ras-GAP SH3 domain binding protein (G3BP) (Anderson and Kedersha, 2008). In plants, some identified SGs-forming RNPs are: the G3BP homologue (Krapp et al., 2017), and ANGUSTIFOLIA (AN) (Bhasin and Hülskamp, 2017) (Figure 4). On the other hand, P-bodies are mainly composed of RNPs involved in translational repression and/or mRNA decay pathway: the enzymes DCP1/DCP2, 5'-3' exoribonuclease 1 (XRN1), Lsm1-7 deadenylation complex, decapping coactivators (Edc3, Pat1, DDX6 and the scaffolding proteins HEDLS/GE1) (Luo et al., 2018). In *Arabidopsis*, the presence of DCP1-2 and 5, and VARICOSE (VAR) in P-body formation has also been reported (Figure 4) (Xu et al., 2020). Also, it has been reported that P-bodies participate in the degradation of mRNA through the pathway known as nonsense mediated decay (NMD). The NMD complex composed by RNA helicase up-frameshift proteins 1-3 (UPF1-3) direct mRNAs with premature termination codons (PTC) to P-bodies for degradation (Figure 4) (He and Jacobson, 2015). Finally, proteins associated with both granules have been reported, among these the following stand

out: the TUDOR STAPHYLOCOCCAL NUCLEASE PROTEINS (TSN1-2) and the Vascular Plant One-Zinc Finger protein (VOZ) (Figure 4) (Bhasin and Hülskamp, 2017).

Another fundamental mechanism in the regulation of gene expression is the post-transcriptional gene silencing (PTGS) mediated by interference RNAs (Martínez De Alba et al., 2015). siRNA bodies are biomolecular condensates associated with trans-acting siRNA (tasiRNA) synthesis and amplification of the RNA silencing signal. Many plant viruses interfere with the functions of siRNA bodies to suppress their contribution to siRNA production (Mäkinen et al., 2017). ARGONAUTE 7 (AGO7), SUPPRESSOR OF GENE SILENCING 3 (SGS3) and the RNA-DEPENDENT RNA POLYMERASE 6 (RDR6) are essential RNPs for the proper functioning of siRNA bodies (Figure 4) (Kumakura et al., 2009; Jouannet et al., 2012).

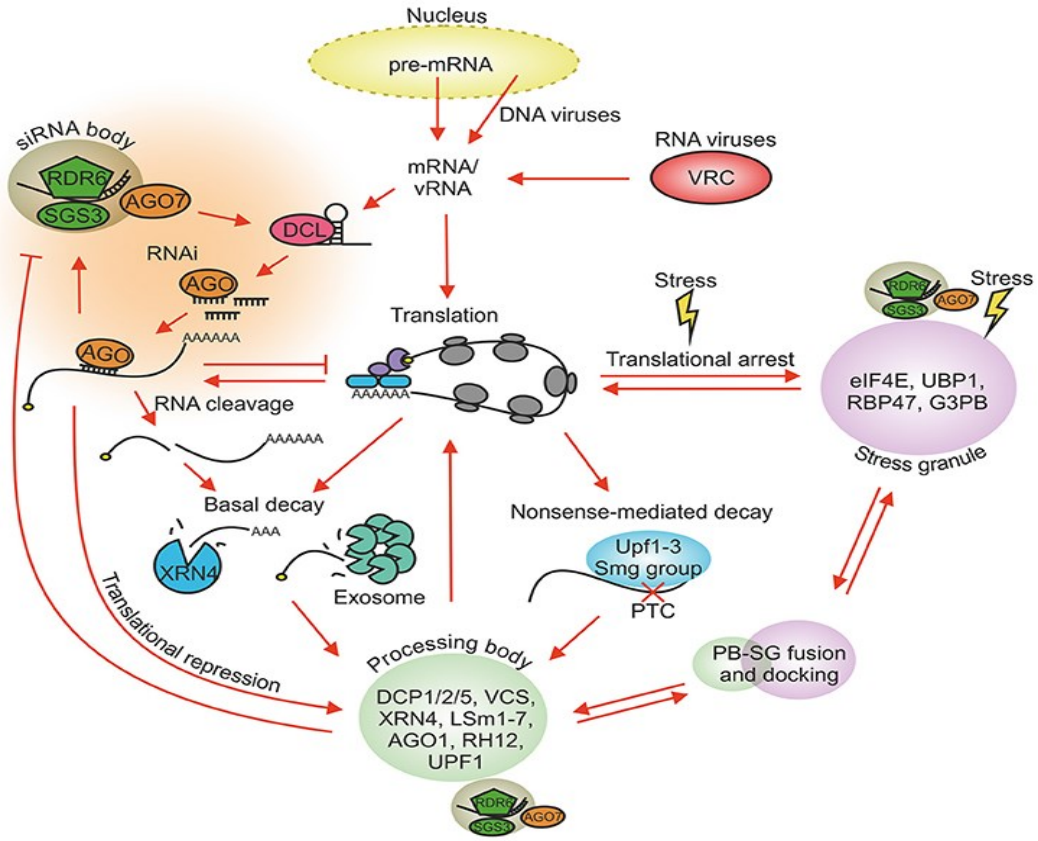

Figure 4. Regulatory mechanisms of RNA metabolism in plant cells. Ribosomes recruit host mRNAs for translation. Viruses have developed molecular strategies to utilize the host's translational machinery. Cellular stress generated by translationally inactive mRNAs increases the rate of SGs formation, as well as the number and size of P-bodies. Translationally blocked pre-initiation complexes condense into SGs during stress conditions. Translationally repressed RNAs can be passed from P-bodies back into translation. The P-bodies and SGs merge and exchange components. While decay mechanisms target aberrant RNAs (without m^7G-cap or poly(A) tail), RNA silencing and NMD machineries can target host mRNAs and vRNAs for degradation. During stress, siRNA bodies can associate with SGs and P-bodies. Only major components are mentioned. PB, P bodies; SG, stress granule; NMD, nonsense-mediated decay; PTC, premature termination codon; VRC, virus replication complex. Source: Mäkinen et al., (2017).

Finally, an emerging topic in research associated with RNA granules is the role that RNA modifications and their effects play in the assembly of these biomolecular condensates (Hofmann et al., 2021). More than 50% of the mRNAs associated with RNA granules show modifications of the N^6-methyladenosine (m^6A) type (Anders et al., 2018). The emerging hypothesis resulting from these investigations suggests that the assembly of these biomolecular condensates is largely driven by the liquid-liquid phase separation (LLPS) of

proteins associated with the m^6A machinery, specifically those belonging to the YTH family (YTHDF) (Ries et al., 2019; Fu and Zhuang, 2020). Additionally, in our laboratory it was demonstrated, through subcellular localization studies, that the AMV CP interacting protein ALKBH9B co-localizes with siRNA bodies and associates with P-bodies (Martínez-Pérez et al., 2017).

3.1.Cytoplasmic RNA granules and viral infections

While the host environment and cellular machinery provide the necessary tools for viral replication, these machineries are not readily available. In fact, viruses must counteract various defense mechanisms to achieve infection. In this context, RNA granules are important components in host cell antiviral defense (Zhang et al., 2019b).

As indicated in the previous section, SGs contain many translation initiation factors, while P-bodies are enriched with proteins involved in RNA degradation. Given the inverse relationship between the increase in RNA granules and the persistence of translation, viruses must modulate these biomolecular condensates to achieve replication. For robust and productive infection to occur, many mammal infecting viruses disrupt RNA granule formation and/or coopt proteins from RNA granules as a function of viral replication (Reineke and Lloyd, 2013). For example, during poliovirus (PV) infection, viral proteinase 3C cleaves G3BP (SGs protein) as well as Pan3, Xrn1, and DCP1 (P-body proteins), preventing the formation of RNA granules (White et al., 2007; Dougherty et al., 2011). During Dengue virus (DENV) infection it has been shown that the DENV-2 3'UTR recruits SGs proteins (G3BP, USP10 and Caprin1) necessary for its replication (Ward et al., 2011). Chikungunya virus (CHIKV) protein nsP3 interacts with G3BP, blocking the assembly of SGs and sequestering translation-associated components from the host (Fros et al., 2012). Similarly, nonstructural protein 1 of influenza A virus (IAV) prevents the formation of SGs by favoring the translation of viral mRNAs (Khaperskyy et al., 2012).

In plants, the role of RNA granules in regulatory networks, including their involvement in viral infections, is an emerging field for which little is known (Hafrén et al., 2015). However,

the few studies that exist to date have revealed essential roles for plant development and immune response (Dong et al., 2016; Meteignier et al., 2016; Bhullar et al., 2017). For example, in tobacco plants, P-bodies have been found to play a role in reprogramming mature cells and restarting the cell division cycle (Bhullar et al., 2017); while in *Nicotiana benthamiana*, responses of dominant R genes that encode nucleotide-binding and leucine-rich repeat (NB-LRR) proteins, induce a dramatic increase in P-body biogenesis (Meteignier et al., 2016). On the other hand, viruses have been found to interact with these biomolecular condensates and act either proviral, to enable and support viral infection and facilitate viral movement, or antiviral, protecting or clearing hosts from viral infections (Xu et al., 2020). In this context, it has been reported that during an infection caused by Potato virus A (PVA), the *Arabidopsis* acidic ribosomal protein P0 is co-purified with the viral genome-linked protein (VPg) as well as with the viral RdRp. Colocalization studies have also revealed that SGs and the nuclear component eIF(iso)4E also colocalize with viral granules formed by VPg and P0 whereas that P0 overexpression favors viral translation of PVA. In this context, it has been proposed that P0 and eIF(iso)4E enhance the infection process through the protection of vRNAs against degradation (Hafrén et al., 2013). In another study, the helper-component (HCPro) of PVA also induces the formation of RNA granules that, in addition to P0 and eIF(iso)4, may contain UBP1 (oligouridylate-binding protein 1) and/or VAR; components of SGs and P-bodies, respectively. When HCPro colocalizes with VAR they stimulate translation; whereas when colocalizing with UBP1 this process is inhibited, indicating that PVA translation and potyviral RNA granules are interrelated (Hafrén et al., 2015). On other hand, it was recently shown that mRNA decay is involved in degradation of turnip mosaic virus (TuMV) vRNAs. In response, TuMV suppresses the DCP1-DCP2 complex (P-body proteins) through direct interaction of viral genome-linked protein (VPg) with DCP2 (Li and Wang, 2018). TuMV-like effects have been reported in tobacco rattle virus (TRV) and TMV where mRNA degradation process has an antiviral effect (Ma et al., 2015; Conti et al., 2017). Furthermore, NMD pathway also functions in cellular stress responses. In this sense, an increase in the infection of potato virus X (PVX) and turnip wrinkle virus (TCV) infection were enhanced in plants expressing a negative dominant

mutant of the UPF1 protein (Garcia et al., 2014). These authors suggested that the genomic vRNAs used as templates for synthesis of sgRNAs contain stop codons followed by atypically long 3'UTRs making these vRNAs targets of the NMD pathway (Garcia et al., 2014). Additionally, studies conducted in our laboratory showed that AMV CP interacts with ALKBH9B, which can bind vRNAs and remove the m^6A-modification from single-stranded RNA *in vitro*. Furthermore, the accumulation of vRNAs is reduced and the systemic movement of AMV is totally blocked in *alkbh9b* plants (Martínez-Pérez et al., 2017, 2021).

4. RNA modifications: N^6-methyladenosine (m^6A)

RNAs perform vital functions in biological systems, not only as structural components (ribosomal RNA: rRNA), translators (transfer RNA: tRNA), and messengers (mRNA), but also as regulators of various biological processes (for example: siRNAs and enhancers RNA: eRNAs) (Kumar and Mohapatra, 2021). The functions of all these RNAs are regulated through chemical modifications (Boccaletto et al., 2018). In this context, around 170 post-transcriptional modifications have been described (Saletore et al., 2012), which can alter (i) the nucleotide charge and their matching properties, (ii) the RNA folding, and (iii) act as a regulatory element for recognition of RNA-protein interaction (Zhang et al., 2020). Consequently, these modifications (also known as "*epitranscriptomics*") play a central role in RNA metabolism, regulating gene expression patterns and thereby modulating the biological behavior of cells (Frye et al., 2016; Wang et al., 2020).

m^6A is the most abundant internal modification in cellular RNA, including mRNAs, which has made it the most well-known and studied RNA modification (Boccaletto et al., 2018; Covelo-Molares et al., 2018; Arribas-Hernández and Brodersen, 2020; Zhou et al., 2020). It was discovered by analyzing different eukaryotic mRNAs (Adams y Cory, 1975), and shortly after, in RNAs of viral origin (Kane y Beemon, 1985; Krug *et al.,* 1976). Currently, it has been described in practically all types of eukaryotic organisms, such as yeasts (Bodi *et al.,* 2010), insects (Hongay y Orr-Weaver, 2011), mammals (Xu *et al*., 2017; Yoon *et al.*, 2017)

and plants (Růžička *et al.*, 2017; Zhong *et al.,* 2008). In addition, it has been determined that m^6A is a selective modification that occurs in the sequence context: DRACH (D=A/G/U, R=A/G, H=A/C/U) (Arribas-Hernández et al., 2021). The existence of a predominant consensus motif throughout the entire eukaryotic phylogenetic line implies that the adenosine methyltransferase complex was originated in ancestral states of eukaryotic phylogeny (Balacco y Soller, 2019).

Mammals have a rate of m^6A modification of 0.1 to 0.4%, which is equivalent to an average of one m^6A site per 2000 ribonucleotides (Dominissini et al., 2012). In *Saccharomyces cerevisiae* a slightly higher rate of 0.7 to 0.9% has been reported (Bodi et al., 2010). On the other hand, in *Arabidopsis* a m^6A consensus rate of 0.5 to 0.7% per 1000 nucleotides or 0.7 to 1.0 sites per actively expressed transcript was agreed (Luo et al., 2014), while it has been suggested between 1 and 15 m^6A-sites per RNA molecule in various viruses (Zhong et al., 2008; Luo and Tong, 2014; Luo et al., 2014; Zhao et al., 2016). Interestingly, most genes highly enriched with m^6A in eukaryotes are involved in response to environmental variations (Dominissini et al., 2012), growth and development (Meyer et al., 2012), as well as in plant photosynthetic pathways (Luo et al., 2014). In addition, it is important to highlight that: (i) this modification is very dynamic, (ii) the m^6A level varies according to the stage of development (Dominissini et al., 2012; Meyer et al., 2012), and (iii) m^6A is not evenly distributed over mRNAs. On this point, it is well known that m^6A is mainly located in: long exons, near stop codons, as well as in the 5'- and 3'-UTR regions (Bodi *et al*., 2012; Haussmann *et al*., 2016; Ke *et al*., 2015; Meyer *et al.*, 2012; Wan *et al.,* 2015).

Despite recent progress in understanding the biological roles of m^6A methylation, most of these studies have focused on human and other mammalian systems (Yue et al., 2019). In plants, further studies of m^6A at the molecular level are necessary to understand the role that this modification plays in plant development, response to abiotic stress, and antiviral defense (Arribas-Hernández and Brodersen, 2020).

4.1. The main components of the m^{6}A modification system: Writers, Erasers, and Readers

The m^{6}A regulatory machinery is post-transcriptionally assembled by a conserved set of proteins at the DRACH consensus motif. Different proteins involved in the addition, removal and identification of m^{6}A have been identified, which are classified into three groups called *"writers"*, *"erasers"* and *"readers"*, respectively. In mammals, m^{6}A is produced by a methyltransferase (MTase) complex comprising: METHYLTRANSFERASE-LIKE 3 (METTL3) (Bokar et al., 1994), WILMS' TUMOR 1-ASSOCIATING PROTEIN (WTAP) (Agarwala et al., 2012), and the METHYLTRANSFERASE-LIKE 14 (METTL14) (Liu et al., 2014). The m^{6}A-tag is removed by the action of FAT MASS AND OBESITY-ASSOCIATED PROTEIN FTO (Jia et al., 2011) and the α-KETOGLUTARATE-DEPENDENT DIOXYGENASE ALKB5 HOMOLOG 5 (ALKBH5) (Zheng et al., 2013). On the other hand, proteins that recognize the m^{6}A-tag play a regulatory role. The main readers identified so far are YTH (YT512-B Homology) domain-containing proteins: YTHDC1/YTHDC2 (Zhang et al., 2010; Bailey et al., 2017; Hsu et al., 2017; Roundtree et al., 2017) and YTHDF1/YTHDF2/YTHDF3 (Dominissini et al., 2012; Wang et al., 2014; Zhou et al., 2015). These proteins are capable of specifically recognize the methyl group of m^{6}A through a hydrophobic binding domain called the "aromatic box", composed of three aromatic residues (Imai et al., 1998; Luo and Tong, 2014; Theler et al., 2014). The eukaryotic initiation factor 3 (eIF3) (Meyer et al., 2015) and the HNRNPA2B1 protein (Agarwala et al., 2012) have also been reported as m^{6}A-readers.

How the writer and eraser proteins selectively add and/or remove the m^{6}A-tag is almost entirely unknown. It is for this reason that the discovery and functional studies of these proteins is a key factor in understanding the regulatory mechanism of m^{6}A (Zheng et al., 2020a).

The following sections describe the best characterized m^{6}A writer, eraser and reader proteins in *Arabidopsis*, as well as their putative functions related to this mechanism.

4.1.1. Writers

In *Arabidopsis*, the catalytic core is formed by two proteins of the MTA-70 family, METHYLTRANSFERASE A (MTA, AT4G10760) - homolog of METTL3 - (Zhong et al., 2008) and METHYLTRANSFERASE B (MTB, AT4G09980) - homolog of METTl14 - (Růžička et al., 2017). Furthermore, several additional factors have been identified to participate in m^6A deposition (Arribas-Hernández and Brodersen, 2020). These are: FKBP12 interacting protein 37 (FIP37, AT3G54170) - homolog of WTAP - (Zhong et al., 2008; Shen et al., 2016), VIRILIZER (VIR, AT3G05680) - homolog of human KIAA1429 - (Schwartz et al., 2014; Růžička et al., 2017) and the putative ubiquitin E3 ligase (HAKAI, AT5G01160) - homolog of human CBLL1 - (Figure 5). Additionally, MTase activity from other proteins has been reported (Oerum et al., 2021). The human METHYLTRANSFERASE-LIKE 5 (METTL5) bound to the known activator tRNA MTase SUBUNIT 11–2 (TRMT112) and the monomeric human protein ZCCHC4 were identified as the responsible enzymes for m^6A modification of 18S and 28S rRNAs, respectively (Van Tran et al., 2018; Ma et al., 2019; Ren et al., 2019; Pinto et al., 2020; Oerum et al., 2021). It has also been reported that structured RNAs containing the UAC<u>A</u>GAGAA consensus sequence can be methylated by METHYLTRANSFERASE-LIKE 16 (METTL16), which also appears to bind to U6 small nuclear RNAs (snRNAs), pre-RNAs, mature mRNAs, and other non-coding RNAs (ncRNAs) and long non-coding RNAs (lncRNAs) (Pendleton et al., 2017; Shima et al., 2017; Warda et al., 2017; Mendel et al., 2018).

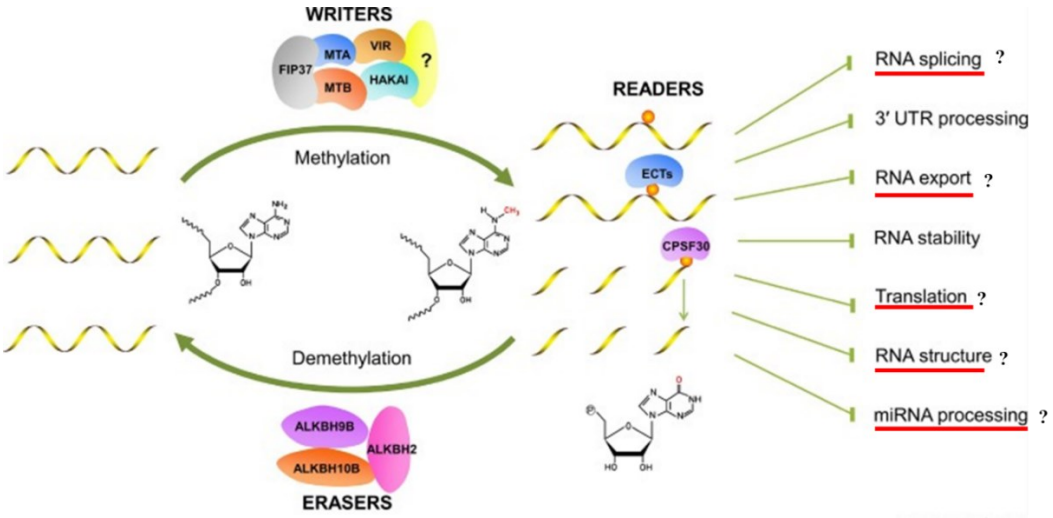

Figure 5. Major components of the m^{6}A methylome in plants. Writers and erasers add or remove the m^{6}A-tag from the RNA. Readers interact with the modified RNA and regulate: RNA structure and 3'UTR processing. So far, the m^{6}A regulatory role on RNA splicing, alternative polyadenylation, RNA export, RNA stability, translation, RNA structure and microRNAs only been shown in mammals. Adapted from Zheng et al., (2020b).

So far, other MTases, orthologs of mammalian METLL5 and ZCCHC4 have not yet been found in plants. On the other hand, it was recently shown that *Arabidopsis* FIONA1 (FIO1, AT2G21070) is the homolog of human METLL16 (Pendleton et al., 2017) and also installs m^{6}A in U6 snRNA and a small subset of poly(A) RNA (Wang et al., 2022).

4.1.2. Erasers

To date, the m^{6}A-erasers described are homologues of the Alkylation B (AlkB) protein of *Escherichia coli* (Samson and Cairns, 1977). The AlkB protein family is part of the superfamily of the 2-oxoglutarate (2OG) and Fe(II)-dependent oxygenases (Aravind and Koonin, 2001). In general, these proteins catalyze the oxidative detoxification of alkylated bases, in DNA, RNA, and proteins (Fedeles et al., 2015). It should be noted that the discovery of the m^{6}A-demethylase activity of some members of the AlkB protein family made it possible to address the study of this modification, now being considered a reversible mark and, therefore, subject to possible dynamic regulation (Zheng et al., 2013).

The *Arabidopsis* genome encodes 14 homologs of AlkB family of eraser proteins: ALKBH1A-D, ALKBH2, ALKBH6, ALKBH8A-B, ALKBH9A-C, and ALKBH10A-B

(Mielecki et al., 2012; Kawai et al., 2014), of which, ALKBH9B (AT2G17970) and ALKBH10B (AT4G02940), have been shown to present m^6A-demethylase (Duan et al., 2017; Martínez-Pérez et al., 2017). ALKBH9B, the first eraser reported in *Arabidopsis*, removes m^6A-modification from ssRNA *in vitro*. It also has a positive effect on the infection caused by AMV, aspect that suggests that the methylation status plays an important role in the regulation of viral infection in *Arabidopsis* (Martínez-Pérez et al., 2017). On the other hand, the RNA-demethylation mediated by ALKBH10B affects the mRNA stability of key flowering time regulators (Duan et al., 2017). Moreover, in *Solanum lycopersicum* it was found that the SlALKBH2 protein has m^6A-eraser activity *in vitro* and *in vivo*, and that activity modules the stability of the mRNA of key regulators in fruit maturation (Zhou et al., 2019) (Figure 5).

Finally, it is important to highlight that a conserved AlkB domain has been identified in ssRNA genomes of some plant viruses belonging to the *Flexi*-, *Caria*-, *Tricho*- and *Potexvirus* families (Aravind and Koonin, 2001; Bratlie and Drabløs, 2005; van den Born et al., 2008). Functional characterization analyzes have shown that these viral AlkB domains can repair deleterious damage caused by methylation in their genome, suggesting that this domain may be biologically relevant in preserving the viability of the viral genome (van den Born et al., 2008; Rubio-Costa, 2021).

4.1.2. Readers

It is known that the m^6A-modification is specifically recognized by proteins containing YT521-B homology domains (YTH), which form a hydrophobic methyl-binding pocket (Bai, 2022). These YTH-family members are highly conserved in humans, *Drosophila*, yeast, and *Arabidopsis*; and are divided into two phylogenetic groups: YTHDF and YTHDC (Li et al., 2014; Meyer and Jaffrey, 2017). In *Arabidopsis* the YTHDF phylogenetic-group can be divided into 11 YTHDF proteins called: EVOLUTIONARILY CONSERVED C-TERMINAL REGION 1 to 11 (ECT1-11) (Bai, 2022). Meanwhile, the YTHDC phylogenetic-group presents one classical YTHDC1-type protein (AT4G11970) and one

YTHDC-like protein, unusual because it also contains additional folded domains: CLEAVAGE AND POLYADENYLATION SPECIFICITY FACTOR 30 (CPSF30) and the 30-kD subunit involved in pre-mRNA clavage and 3'end formation (Thomas et al., 2012; Bruggeman et al., 2014; Pontier et al., 2019). These YTHDC-like protein was called CPSF30. Also, *Arabidopsis* genome encodes two distinct transcripts of CPSF30; the shorter transcript encodes a 28-kDa protein (CPSF30S) and the longer transcript encodes a 70-kDa protein (CPSF30L), that contains an additional YTH domain in the C terminus (Hou et al., 2021).

To date, only ECT2, ECT3 and ECT4 have been described as *Arabidopsis* m^6A-readers, which perform redundant functions in the m^6A-dependent control of developmental timing and leaf morphogenesis (Arribas-Hernández et al., 2018). In addition, multiple studies have described stochastic defects in the control of the number of trichomes in plants with ETC2 loss-function (Arribas-Hernández et al., 2018; Scutenaire et al., 2018; Wei et al., 2018), a process in which ECT3 has an equivalent but not completely redundant function (Arribas-Hernández et al., 2018). Moreover, sequence homology analysis revealed that residues involved in RNA and m^6A binding of human YTHDF proteins are highly conserved in ECT1, ECT2, ECT3 and ECT4, including the three tryptophan residues that make up the m^6A binding aromatic cage (Arribas-Hernández et al., 2018). Besides, mutational analyzes demonstrated the criticality of these tryptophan residues for: (i) maintaining the integrity of the aromatic cage in ECT2 and thus, binding to m^6A-RNAs (Scutenaire et al., 2018), and (ii) for ECT2 and ECT3 to function *in vivo* (Arribas-Hernández et al., 2018). Finally, it has been shown that ECT1 has a predominant nuclear localization (Ok et al., 2005), while ECT2, ECT3 and ECT4 are cytoplasmic (Arribas-Hernández et al., 2018). However, some studies propose that ETC2 may also localize to the nucleus (Scutenaire et al., 2018; Wei et al., 2018).

On the other hand, studies carried out in our laboratory showed that the triple mutant *ect2/ect3/ect5* of Arabidopsis favors the systemic infection of AMV and Cucumber mosaic virus -CMV- (members of the *Bromoviridae* family). Additionally, Arabidopsis *ect2* mutant plants defective in m^6A recognition, were found to lose wild-type antiviral activity suggesting

that, at least for ECT2, ECT/m^{6}A binding is necessary to modulate virus biology (Martínez-Pérez, 2020).

Finally, it has been reported that FIP37 and CPSF30L participate in a 3'UTR/m^{6}A-mediated alternative polyadenylation (APA) pathway that protects the integrity of the transcriptome in *Arabidopsis* (Pontier et al., 2019; Hou et al., 2021). This aspect will be discussed in section 4.2.2.

4.2. Roles of m^{6}A

4.2.1. Effects of m^{6}A on RNA

In mammals, m^{6}A has a central role in the regulation of RNA metabolism: splicing (Haussmann et al., 2016; Lence et al., 2016; Xiao et al., 2016), stability (Wang et al., 2014; Mishima and Tomari, 2016; Huang and Yin, 2018), export (Roundtree et al., 2017; Edens et al., 2019), 3'UTR processing (Bartosovic et al., 2017; Wei et al., 2018), translation (Zhou et al., 2015; Shi et al., 2017), and miRNA processing (Alarcón et al., 2015; Bhat et al., 2019). In contrast, our understanding of the regulatory role of m^{6}A-modification in plants is limited as it acts as an mRNA-stabilizer (Shen et al., 2016; Hofmann, 2017; Wei et al., 2018) and assists in 3'UTR processing at specific genomic loci (Pontier et al., 2019). Roles of m^{6}A in plant's RNA export, RNA splicing, and translation remain unexplored (Figure 5) (Zheng et al., 2020a).

It should be noted that the current research on the effect of the m^{6}A-modification has been focused primarily on genetic interference. Until now, it has not been possible to develop a strategy capable of accurately predicting the effect of m^{6}A at the level of the entire transcriptome. Current strategies allow to identify one or few effects on the RNA, caused by the m^{6}A-modification.

4.2.1.1. mRNA Stability

Although the m^{6}A-modification has been shown to stabilize mRNA, no consensus has yet been reached on this issue. Shen et al., (2016) determined that loss of function of atFIP37

results in m^{6}A-reduction in mRNAs related to shoot apical meristem (SAM) proliferation: WUSCHEL (WUS) and SHOOTMERISTEMLESS (STM). This decreasing improved the stability of these mRNAs, and consequently increased the amount of WUS and STM proteins, causing an excessive proliferation of SAM (Shen et al., 2016). Contrary, Duan et al., (2017) showed that *alkbh10b* mutants exhibited an m^{6}A-increase in key genes regulating flowering. This loss of function of ALKBH10B reduced the stability of the involved transcripts, accelerating their degradation, and causing a delayed flowering phenotype (Hofmann, 2017). On the other hand, it was also determined that the m^{6}A-writer ECT2 binding sites are strongly enriched in the 3'UTR of mRNAs and that loss of ECT2 function accelerates the degradation of three ECT2-binding transcripts related to trichome morphogenesis, affecting the branching of trichomes (Wei et al., 2018).

4.2.1.2. 3'UTR Processing

In mammals, m^{6}A modulates the alternative polyA (APA) usage site during 3'UTR processing (Ke et al., 2015; Bartosovic et al., 2017). In this context, it has been reported that VIRMA associates with the mCFI polyadenylation complex in an RNA-dependent manner when m^{6}A is close to the proximal APA site within the 3'UTR and/or close to the stop codon region (Liu et al., 2018). Accordingly, Molinie et al., (2016) found that methylated transcripts tend to couple to the APA-proximal site, and therefore have shortened 3'UTRs while unmethylated transcript isoforms tend to use APA-distal sites. A similar situation has been reported in plants through a recently discovered pathway called m^{6}A–assisted polyadenylation (m-ASP). Targets of this pathway are rearranged gene pairs, GENE1/GENE2, - such as the pair AT4G30570/580 or AT1G71330/340 - that present duplicated or translocated paralog/pseudogene at GENE2 position. This suggests that gene rearrangements at target loci could be responsible for the observed termination/polyadenylation defects. m^{6}A can assist in the polyadenylation of the GENE1, thereby limiting mis-splicing to form chimeric mRNA. For this, its necessary assistance of FIP37 and CPSF30L. In this context, this pathway ensures transcriptome integrity at rearranged genomic loci in plants (Pontier et al., 2019).

4.2.2. m^{6}A on plant growth, development and response to stress

In plants, previous studies have shown that loss of function of key components for the m^{6}A-machinery can lead to abnormal growth and/or development (Zhong et al., 2008; Shen et al., 2016; Duan et al., 2017; Růžička et al., 2017; Chen et al., 2018; Zhang et al., 2019a; Zhou et al., 2019). In this sense, studies on the phenotype of *Arabidopsis* lines defective in the expression of MTA (Zhong et al., 2008; Bodi et al., 2012), MTB (Růžička et al., 2017), FIP37 (Vespa et al., 2004), VIR (Růžička et al., 2017) and HAKAI (Růžička et al., 2017) have shown that the decrease in m^{6}A-modification results in: embryo lethality, growth retardation, abnormal organ development, loss of apical dominance, defective branching of trichomes, defective gravitropic responses, and aberrant development of lateral roots and vasculature. On the other hand, loss-function of m^{6}A-erasers results in leaf dysplasia and a late flowering phenotype in *alkbh10b* mutants (Hofmann, 2017); and reductions in the fresh weight of the aerial part of *Arabidopsis alkbh9b* plants (Martínez-Pérez, 2016). Additionally, several studies on m^{6}A-readers have demonstrated the role of the YTH-domain proteins, ECT2, ECT3 and ECT4, in the regulation of *Arabidopsis* leaf and epidermal hair development (see the section "4.1.2. Readers"). The role of m^{6}A in regulating the growth and development of other plants has also begun to be elucidated. In rice, the MTases OsFIP and OsMTA2 have also been reported to be essential for sporogenesis (Zhang et al., 2019a) and, in tomato, together with DNA 5-methylcytosine, m^{6}A regulates fruit ripening (Zhou et al., 2019).

Current evidence also suggests that m^{6}A could be involved in the regulation of the response to various abiotic and biotic stresses (Yue et al., 2019). Two fundamental pieces of evidence support this hypothesis: (i) *Arabidopsis* and rice modulate the expression of ECT-proteins by various abiotic stress factors (heat, cold, drought, osmotic and saline stress and hypoxia), and by infection by nematodes, bacteria, fungi and viruses (Li et al., 2014; Hu et al., 2019; Miao et al., 2020), and because, (ii) some m^{6}A-readers are relocated to stress cytoplasmic granules after heat or osmotic stress (Arribas-Hernández et al., 2018; Scutenaire et al., 2018).

With regard to salt stress, a recent study by Hu et al., (2021) revealed a crucial role for the m^{6}A writer-machinery in tolerance to this abiotic stress. Loss-of-function mutants of: MTA, MTB, VIR and HAKAI, showed salt-sensitive phenotypes in an m^{6}A-dependent manner. In addition, a methylome analysis in *Arabidopsis vir* plants, which exhibited the most salt-hypersensitive phenotypes, demonstrated a transcriptome-wide loss of the m^{6}A-modification in the 3'UTR. Finally, VIR-mediated m^{6}A methylation was shown to modulate reactive oxygen species homeostasis by downregulating the mRNA stability of several negative regulators of salt stress, including the NAC transcription factor (ATAF1), GIGANTEA (GI), and the and glutathione S-transferase U17 (GSTU17); by influencing the length of the 3′-UTR via alternative polyadenylation.

The role of m^{6}A in response to viral infections will be analyzed in the following sections.

5. Role of m^{6}A in mammal infecting viruses

In addition to the roles of m^{6}A in cellular RNA metabolism, this modification is implicated in viral infections (Yue et al., 2022). Early studies conducted in the 1970s identified m^{6}A-modifications in viral mRNAs of Simian virus 40 (SV40) (Lavi and Shatkin, 1975), adenovirus (AV) (Hashimoto and Green, 1976), Influenza A viruses (IAV) (Krug et al., 1976), Herpes simplex virus-1 (HSV-1) (Moss et al., 1977), Avian sarcoma leukosis virus (ASLV) (Dimock and Stoltzfus, 1977) and Rous sarcoma virus (RSV) (Beemon and Keith, 1977). However, due to the lack of technology available at the time, investigations were limited to descriptive reports such as chromatographic analysis of radiolabeled viral RNAs (Yue et al., 2022). In subsequent decades, with the advancement of new technologies, it was possible to detect m^{6}A in viral RNA genomes and mRNAs (Baquero-Perez et al., 2021). In addition, attempts have been made to elucidate the function of m^{6}A in viral systems, mainly employing manipulation of the m^{6}A-machinery (depletion or overexpression of writers, erasers, and readers), and the subsequent mapping of the m^{6}A-sites along the RNAs using some of the available methodologies (Linder and Jaffrey, 2019a).

To date, the presence of m^6A has been reported in members of the families: *Flaviviridae, Orthomyxoviridae, Paramyxoviridae, Retroviridae, Togaviridae, Picornaviridae, Polyomaviridae, Hepadnaviridae, Adenoviridae, Rhabdoviridae, Herpesviridae* and *Coronaviridae*. In addition, it has been described that m^6A plays an essential role in the biology of these viruses (review, Baquero-Perez et al., 2021). Depending on the virus, m^6A modification pathway can exert a pro- or anti-viral effects (Table 1) (Williams et al., 2019).

Table 1. Proviral (+), antiviral (-), or non-significant (NS) effects on animal virus replication, after altering the host m^6A-machinery. Adapted from Baquero-Perez et al., (2021).

Virus	**Depletion**						
RNA genome	**METTL3**	**METTL14**	**FTO**	**ALKBH5**	**YTHDF1**	**YTHDF2**	**YTHDF3**
HIV-1	-	-	+	+	+	+/-	+
HCV	+	+	-	NS	+	+	+
ZIKV	+	+	-	-	+	+	+
CHIKV					+	-	+
PEDV	+	+	-		+	+	NS
IAV	-						
RSV	-	-	+	+	-	-	-
SARS-CoV-2	+	+		-	NS	+	NS
EV71	-		+		+	+	+
HMPV			+	+			
VSV	+/-	NS	-	-	NS	NS	-
DNA genome	-						
SV40	-						
KSHV	+/-		+		-/NS	+/-	-/NS
EBV	+	+/-		-/NS	+	+/NS	+
Ad5	-	-	NS	NS	NS	NS	NS
HBV	+	+	-	-		+	+
HCMV	-	-	NS	+	-	-	-
	Overexpression						
RNA genome	**METTL3**	**METTL14**	**FTO**	**ALKBH5**	**YTHDF1**	**YTHDF2**	**YTHDF3**
HIV-1					+/-	+/-	+/-
ZIKV					-	-	-
CHIKV					-	+	NS
PEDV							
IAV					NS	+	NS
RSV	+	+	-	-	+	+	+
SARS-CoV-2							
EV71						+	+
HMPV	+	+			+	+	+
VSV	+			+			
DNA genome	-			-			
SV40						+	NS
KSHV						-	

Human immunodeficiency virus 1 (HIV-1): (Kennedy et al., 2016; Lichinchi et al., 2016a; Tirumuru et al., 2016; Jurczyszak et al., 2020); **Hepatitis C virus (HCV):** (Gokhale et al., 2016); **Zika virus (ZIKV):** (Lichinchi et al., 2016b); **Chikungunya virus (CHIKV):** (Kim et al., 2020); **Porcine epidemic diarrhea virus (PEDV):** (Chen et al., 2020); **IAV:** (Courtney et al., 2017; Winkler et al., 2018); **RSV:** (Xue et al., 2019); **Severe acute respiratory syndrome coronavirus 2 (SARS-CoV-2):** (Liu et al., 2021); **Enterovirus 71 (EV71):** (Hao et al., 2019); **Human metapneumovirus (HMPV):** (Lu et al., 2020); **Vesicular stomatitis virus (VSV):** (Liu et al., 2019; Zhang et al., 2019c; Qiu et al., 2021); **SV40:** (Tsai et al., 2018); **Kaposi's sarcoma-associated herpesvirus (KSHV):** (Ye et al., 2017; Hesser et al., 2018; Tan et al., 2018; Baquero-Perez et al., 2019); **Epstein–barr virus (EBV):** (Lang et al., 2019; Xia et al., 2021); **Adenoviral serotype 5 (Ad5):** (Price et al., 2020); **Hepatitis B virus (HBV):** (Imam et al., 2018); **Human cytomegalovirus (HCMV):** (Rubio et al., 2018; Winkler et al., 2018).

In addition to affect the infection process by regulating m^6A deposition on vRNA, this modification can also modulate the immune response to infection trough different mechanisms such as degradation of foreign RNAs and altering cellular expression and/or stability of mRNAs associated with proteins involved in signaling immune responses (Williams et al., 2019).

Thus, vRNAs can be detected as foreign by pattern recognition receptors (PRR, including: Toll-like receptors -TLRs- and Retinoic acid-inducible gene I (RIG-I)-like receptor) (McFadden et al., 2017). These receptors recognize vRNAs motifs that have specific characteristics, such as dsRNA-regions or naked 5'-triphosphate ends driving signaling programs that ultimately induce cytokines such as interferon (IFN) that leads to an antiviral response. It has been reported that chemically modified transcripts with m^6A reduce the magnitude of these PRR responses.(Karikó et al., 2005; Durbin et al., 2016). This would suggest that the presence of m^6A in viral genomes could be a strategy to evade the innate immune response (Williams et al., 2019). Additionally, tight control of antiviral protein expression is a critical factor in promoting effective immunity and preventing cellular toxicity. In this context, it has been reported that mRNAs that encode signaling molecules involved in antiviral responses such as TUMOR NECROSIS FACTOR RECEPTOR ASSOCIATED FACTOR 3 and 6 (TRAF3 and TRAF6) are m^6A-marked in the 3'UTR (Zheng et al., 2017; Rubio et al., 2018; Winkler et al., 2018). After a viral infection, the protein DDX46 (nuclear DEAD-box (DDX) helicases family member) recruits ALKBH5

and demethylates TRAF3 and TRAF3 transcripts. Consequently, mRNAs are retained in the nucleus, suppressing translation as well as innate antiviral immunity (Zheng et al., 2017).

6. m^{6}A in plant viral infections

Unlike animal viruses, there are few reports on m^{6}A-methylation in plant viruses. However, recent evidence indicates that m^{6}A plays a dual role during viral infection of plants (Martínez-Pérez et al., 2017, 2021; Yue et al., 2022).Diverse studies suggest that m^{6}A could modulate viral infection. In this sense, it has been shown that the m^{6}A-level is reduced after TMV infection in *Nicotiana tabacum* plants (Li et al., 2018). In watermelon, global m^{6}A levels are reduced in response to cucumber green mottle mosaic virus (CGMMV) infection implying that a global hypomethylation of m^{6}A likely activates watermelon defense responses early in CGMMV infection (He et al., 2021). Furthermore, infected plants showed and increased expression of a potential demethylase (orthologue of human ALKBH5) whereas expression of the putative MTases were repressed (Li et al., 2018). In *Solanum tuberosum* plants exposed to PVY infection presented drastic changes in mRNA methylation (Glushkevich et al., 2022). In rice, it was found that m^{6}A-levels increased in response to infection by rice black-streaked dwarf virus (RBSDV) and rice stripe virus (RSV), and that m^{6}A-methylation is mainly associated with genes that are not actively expressed in virus-infected rice plants (Zhang et al., 2021b). m^{6}A transcriptome of two varieties of wheat, with different resistance to wheat yellow mosaic virus (WYMV) revealed that many genes related to plant defense responses and plant-pathogen interaction were significantly changed in both m^{6}A and mRNA levels (Zhang et al., 2021c). Furthermore, the presence of m^{6}A in the genomes of two members of the *Bromoviridae* family, AMV and CMV, has been previously reported in our laboratory. In AMV, loss of function of the m^{6}A-eraser ALKBH9B in *Arabidopsis* correlates with an increase in the m^{6}A levels of the AMV vRNAs. Furthermore, early stages of viral infection and systemic movement are affected in *alkbh9b* plants most probably due to a blockage of the viral upload into the phloem (Martínez-Pérez et al., 2017, 2021).

In the case of CMV, despite containing m^6A in its genome, neither the abundance of m^6A in the viral genome nor virus infection was changed in *alkbh9b* plants relative to wild-type plants suggesting that the modification of m^6A could negatively affect the infection of some plant viruses. One possibility to this different response would be related to the fact that AMV CP, but not CMV CP, has the ability to interact with ALKBH9B *in vivo*. The CP of AMV is a multifunctional protein that interacts with a variety of host factors and is indispensable for replication and translation. Thus, it may be possible that the interaction between ALKBH9B and the CP is essential to usurp ALKBH9B activity to the advantage of the virus (Martínez-Pérez et al., 2017).

Furthermore, the m^6A-modification could act as an antiviral immune response studies carried out in our lab determined that the lack of the *Arabidopsis* m^6A-readers ECT2, ECT3 and ECT5 generate an increase in viral titer in systemic infections, indicating that these proteins negatively regulate AMV infection. This effect was observed to a greater extent when infecting double mutants *ect2/ect3* and *ect2/ect5*, and triple mutants *ect2/ect3/ect4* and *ect2/ect3/ect5* (Martínez-Pérez, 2020). The necessity of mutating at least two of these genes to perceive a pronounced effect is presumably due to their previously reported partial functional redundancy (Arribas-Hernández et al., 2018, 2021; Arribas-Hernández and Brodersen, 2020). Furthermore, it was suggested that *Arabidopsis* ECT2 plays the most relevant role among the ECTs evaluated in AMV infection, since: (i) double mutants lacking ECT2 presented the highest systemic viral titers, while (ii) atECT2^{W464A}, a mutant that cannot recognize m^6A, was unable to interact with vRNAs, and, consistently, unable to complement the ect2/ect3 double mutant susceptibility phenotype. Interestingly, CMV infection levels were also increased when ECT2 and ECT3 or ECT5 were absent, suggesting that the m^6A mechanism would likely not be exclusive to AMV, but rather influence other viral pathogens (Martínez-Pérez, 2020).

Finally, several plant viruses have been found to contain homologues or domains of the AlkB protein (Yue et al., 2022). Interestingly, most of these viruses are members of the *Flexiviridae* family and infect woody or perennial plants, where they have to establish infections that

persist for years (Bratlie and Drabløs, 2005; van den Born et al., 2008; Gokhale et al., 2016; Rubio-Costa, 2021). Sequence analysis showed that this putative AlkB domain is functionally conserved, and associated with repair of DNA or RNA molecules, and with protecting the viral genome from damage caused by methylation during infection (van den Born et al., 2008). In this sense, Yue et al., (2022) suggests that plant viruses recruited the plant AlkB transcript to avoid being altered by host m^6A-methylation, meanwhile viruses that lack the AlkB domain have likely evolved other strategies that confer resistance to m^6A. It would be the case of AMV, that would recruit ALKBH9B through its binding to the CP to benefit viral infection (Martínez-Pérez et al., 2017).

Motivation and objectives

Recent research has identified the m^6A-modification as an important mechanism for regulating mRNA biology (Zheng et al., 2013; Wang et al., 2014, 2015; Xu et al., 2014; Zhao et al., 2014; Liu et al., 2015). The components of this regulatory system (writers, erasers and readers) have been described in mammals, yeasts (Fu et al., 2014), and more recently in plants (Růžička et al., 2017), where they play a fundamental regulatory role in their development (Zhong et al., 2008; Bodi et al., 2012; Shen et al., 2016). It has also been shown that the m^6A-machinery can modify the RNA genomes of several viruses, indicating that m^6A is a conserved marker that regulates viral infection (Gokhale et al., 2016; Lichinchi et al., 2016a). However, most of these studies have focused on animal viruses (Dang et al., 2019; Williams et al., 2019; Arribas-Hernández and Brodersen, 2020), while research on plant viruses is very limited (Martínez-Pérez et al., 2017; Li et al., 2018; Arribas-Hernández and Brodersen, 2020).

The laboratory of Dr. Vicente Pallás has been a pioneer in the study of the effect of m^6A on plant-viruses, using as model the Alfalfa mosaic virus. During the last years, the laboratory has reported: (i) the first *Arabidopsis* protein with *in vitro* m^6A-eraser capability (ALKBH9B), (ii) the presence of putative m^6A-motifs in critical genomic regions for AMV replication [including the 3'UTR of RNA 3] (iii) the functional relevance of ALKBH9B to maintain adequate m^6A/A levels in vRNAs for correct AMV replication, (iv) the ability of AMV-CP to interact with ALKBH9B, possibly to usurp ALKBH9B activity, and (v) the capability of *Arabidopsis* ECT2, ECT3 and ECT5 readers to interact with m^6A-containing AMV vRNAs (Martínez-Pérez, 2016, 2020; Martínez-Pérez et al., 2017, 2021; Rodríguez Úbeda, 2020).

In this context, the objective of this doctoral thesis is ***to deepen the knowledge of the m^6A regulation mechanisms on the infectious cycle of AMV***. To address this global objective, the following three partial objectives were defined:

- **Objective 1.** Develop a functional mapping of ALKBH9B to identify the putative domains involved in the interaction with the vRNA and the AMV-CP.

- **Objective 2.** Analyze *in vivo* the function of the possible m^6A methylation motifs present in the 3'UTR RNA3 of AMV.

- **Objective 3.** To carry on a preliminary analysis to identify putative *Arabidopsis* m^6A-methyltransferases implicated in the AMV infection cycle.

Chapter I

Mapping of Functional Subdomains in the *at*ALKBH9B m^{6}A-Demethylase Required for Its Binding to the Viral RNA and to the Coat Protein of Alfalfa Mosaic Virus

Chapter published:

Alvarado-Marchena, L.; Marquez-Molins, J.; Martinez-Perez, M.; Aparicio, F.; Pallás, V. (2021). Mapping of Functional Subdomains in the *at*ALKBH9B m^{6}A-Demethylase Required for Its Binding to the Viral RNA and to the Coat Protein of Alfalfa Mosaic Virus. Front. Plant Sci. 12, 1–12, doi:10.3389/fpls.2021.701683.

ANTECEDENTS

The m^6A pathway has been widely described as a viral regulatory mechanism in animals. We previously reported that the AMV CP interacts with the *Arabidopsis* m^6A-demethylase ALKBH9B regulating m^6A abundance on vRNAs and systemic invasion of floral stems (Martínez-Pérez et al., 2017). This regulation seems to be specific of ALKBH9B since ALKBH9A and ALKBH9C were observed not to be involved in the AMV cycle (Martínez-Pérez et al., 2021). Given the functional relevance of atALKBH9B in AMV biology, in this thesis we decided to characterize in deep the AMV RNA/CP-ALKBH9B interactions.

However, before delving into these aspects, we evaluate in more detail the spatio-temporal distribution of AMV infection in *Arabidopsis* plants and evaluate the possible loss of stability of AMV virions as a probable cause of the absence of the virus in systemic tissue. For this, we compared the viral titers in different non-inoculated tissues (roots, rosette leaves, and floral stems). After total RNA extraction, vRNAs load in these tissues was evaluated by northern blot at 11 and 15 dpi (Figure A1). Although the lower susceptibility of *atalkbh9b* plants to AMV was evident in all cases, it was especially notable in roots and floral stems, in which we practically observed a block of the viral infection. Considering that to invade upper sink leaves and roots, viruses enter the phloem of the inoculated leaves (Hipper et al., 2013; Navarro et al., 2019), our results suggest that AMV phloem loading in *atalkbh9b* plants is restricted.

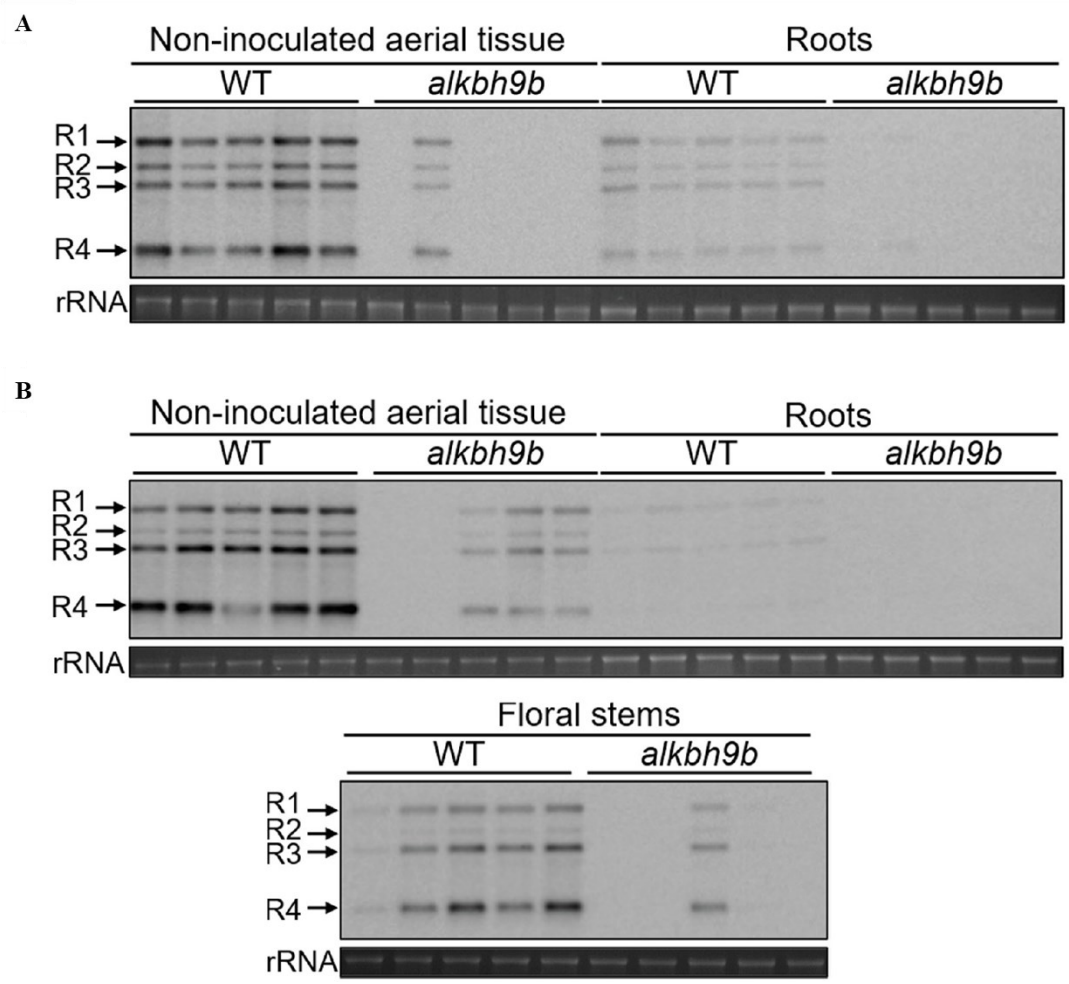

Figure A1. AMV systemic infection of diverse tissues is severely impaired in *alkbh9b* plants. Representative northern blots of different tissues (indicated on top of each panel) from five wild-type and *atalkbh9b* plants at 11 **(A)** and 15 **(B)** dpi. Five biological replicates of each tissue are shown. Positions of the vRNAs are indicated on the left. Ethidium bromide staining of ribosomal RNAs (rRNA) was used as RNA loading control.

These observations show that AMV systemic infection is generally impaired by the absence of ALKBH9B and vRNA is unable to reach floral stems and roots. More remarkably, these new findings suggest that ALKBH9B is involved, somehow, in the viral upload to the phloem in Arabidopsis, and thus, when this protein is not present, AMV very rarely invades the vascular tissues. In contrast to cell-to-cell movement, AMV needs to form viral particles to move systemically (Sánchez-Navarro et al., 2006). The diminished systemic invasion observed in Arabidopsis *alkbh9b* plants could be caused by compromised stability of the

AMV particles. To check this hypothesis, we evaluated the stability of viral particles obtained from wild-type and *atalkbh9b* plants. It would be expected that encapsulated vRNAs were hardly processed by RNases. Hence, WT- and *alkbh9b*-infected leaves were homogenized with PIPES buffer and, after different times of incubation at 37°C, vRNAs levels were evaluated by northern blot assays (Figure A2). While ribosomal RNAs were completely degraded after 30 min of incubation, vRNAs from both WT and mutant plants remained intact to the same extent. Therefore, the absence of ALKBH9B activity does not affect the stability of AMV viral particles.

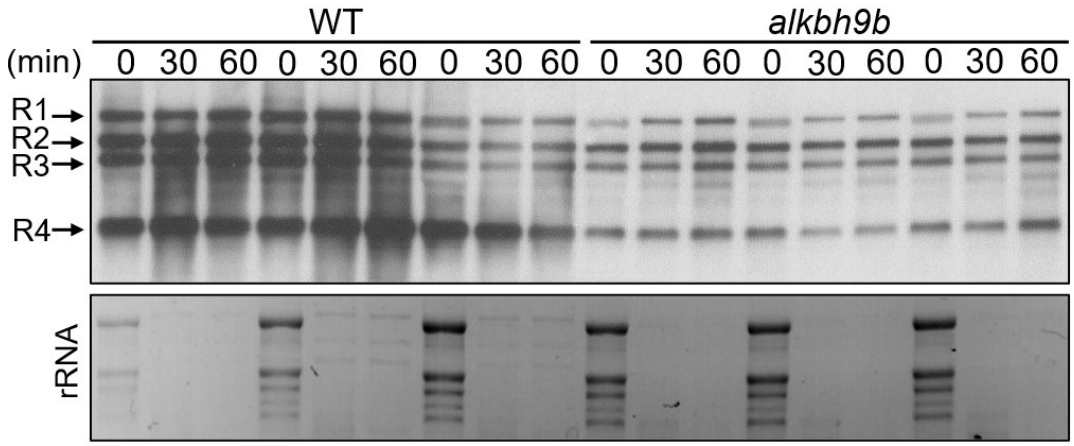

Figure A2. Northern blot analysis to determine AMV virion stability. Upper panel shows accumulation levels of vRNAs extracted from virions purified from three WT and *alkbh9b* plants at 0, 30 and 60 min after the RNase sensitivity assay treatment (see main text). Positions of the AMV RNAs are indicated on the left. Lower panel shows ethidium bromide staining of total RNAs from the same samples.

Thus, we define ALKBH9B as a new possible factor involved in long-distance transport via phloem and we contribute to expanding the knowledge of m^6A-dependent modulation of plant viral infections. We then decided to characterize in more detail this plant demethylase.

Abstract

N6-methyladenosine (m^6A) modification is a dynamically regulated RNA modification that impacts many cellular processes and pathways. This epitranscriptomic methylation relies on the participation of RNA methyltransferases (referred to as "*writers*") and demethylases (referred to as "*erasers*"), respectively. We previously demonstrated that the *Arabidopsis thaliana* protein atALKBH9B showed m^6A-demethylase activity and interacted with the coat protein (CP) of alfalfa mosaic virus (AMV), causing a profound impact on the viral infection cycle. To dissect the functional activity of atALKBH9B in AMV infection, we performed a protein-mapping analysis to identify the putative domains required for regulating this process. In this context, the mutational analysis of the protein revealed that the residues between 427 and 467 positions are critical for *in vitro* binding to the AMV RNA. The atALKBH9B amino acid sequence showed intrinsically disordered regions (IDRs) located at the N-terminal part delimiting the internal AlkB-*like* domain and at the C-terminal part. We identified an RNA binding domain containing an RGxxxRGG motif that overlaps with the C-terminal IDR. Moreover, bimolecular fluorescent experiments allowed us to determine that residues located between 387 and 427 are critical for the interaction with the AMV CP, which should be critical for modulating the viral infection process. Finally, we observed that atALKBH9B deletions of either N-terminal 20 residues or the C-terminal's last 40 amino acids impede their accumulation in siRNA bodies. The involvement of the regions responsible for RNA and viral CP binding and those required for its localization in stress granules in the viral cycle is discussed.

Keywords: N^6-methyladenosine, RNA covalent modifications, RNA-binding proteins, plant viruses, alfamovirus, RNA demethylases, epitranscriptomics, ALKBH

Introduction

The addition of a methyl group to the N^6 position of adenosine (m^6A) is the most abundant internal modification in eukaryote mRNAs (Boccaletto et al., 2018; Covelo-Molares et al., 2018; Arribas-Hernández and Brodersen, 2020; Zhou et al., 2020). It regulates many steps of RNA metabolism, including splicing (Zhao et al., 2014), stability (Wang et al., 2014), translation (Meyer et al., 2015), nuclear-export (Zheng et al., 2013), RNA structures (Bayoumi et al., 2020), and protein/RNA interactions (Liu et al., 2015). Also, it modulates the epigenetic effects of some non-coding RNAs (ncRNA) (Meyer and Jaffrey, 2017). Since the 1970s, m^6A modification has been known to tag not only cellular RNAs but also RNAs of multiple viruses (Wei and Moss, 1975; Furuichi et al., 1976; Krug et al., 1976; Dimock and Stoltzfus, 1977), although its functional relevance has remained elusive mainly due to the lack of efficient methods of m^6A detection and subsequent analysis. Recent studies have demonstrated the crucial roles of m^6A in the virus–host interactions; however, most of these studies have focused on animal viruses (Dang et al., 2019; Williams et al., 2019; Arribas-Hernández and Brodersen, 2020), whereas it remains very limited in plant viruses (Martínez-Pérez et al., 2017; Li et al., 2018; Arribas-Hernández and Brodersen, 2020).

In mammals, m^6A methylation is catalyzed co-transcriptionally by a multicomponent m^6A methyltransferase complex (MTC, also known as "writer") (Liu et al., 2014; Ping et al., 2014). The core component of MTC is a ~200 kDa heterodimer comprised of METTL3 and METTL14 (Huang et al., 2020). Other regulatory subunits of MTC have also been identified, including WTAP and its cofactors KIAA1429 (VIRMA), ZC3H13, and RBM15/RBM15B, which play roles in anchoring MTC to nuclear speckles and U-rich regions adjacent to m^6A sites in mRNAs. Two main RNA demethylases, "erasers," belonging to Fe(II)/2-oxoglutarate (2OG) dioxygenase superfamily, named AlkB homology 5 (ALKBH5) and FTO, have been described to remove m^6A marks (Aik et al., 2014; Xu et al., 2014). The third component of the m^6A modification machinery consists of "reader" proteins that recognize this modification and modulate the activity and half-life of diverse RNAs. Thus, several YTH domain family members, YTHDF1, YTHDF2, YTHDF3, YTHDC1, and YTHDC2, mediate

many of the phenotypic effects of this epitranscriptomic modification (Luo and Tong, 2014; Xiao et al., 2016).

By homology with mammals, functional orthologous genes of the m^{6}A machinery have been discovered in *Arabidopsis* (Arribas-Hernández and Brodersen, 2020). MTA, MTB, FIP37, VIRILIZER, orthologs of METTL3, METTL14, WTAP, and KIAA1429 (human protein), respectively, have been identified as member proteins of the m^{6}A *writer* complex (Zhong et al., 2008; Bodi et al., 2012; Shen et al., 2016; Růžička et al., 2017). In the *Arabidopsis* genome, 14 "readers" of the YTH family have been identified (ECT1-11; Evolutionarily Conserved C-Terminal Region 1–11, At4g11970 and the Cleavage and Polyadenylation Specificity Factor 30). The *Arabidopsis* genome encodes 14 homologs of Alk B family of "eraser" proteins (*at*ALKBH1A-D, *at*ALKBH2, *at*ALKBH6, *at*ALKBH8A-B, *at*ALKBH9A-C, and *at*ALKBH10A-B) (Mielecki et al., 2012; Kawai et al., 2014), of which, *at*ALKBH9B and *at*ALKBH10B, have been shown to present m^{6}A demethylase activity *in vitro* and m^{6}A-related functions *in vivo* (Duan et al., 2017; Martínez-Pérez et al., 2017). Recently the potential *eraser at*ALKBH6 has been shown to play important roles in seed germination, seedling growth, and survival of *Arabidopsis* under abiotic stresses (Huong et al., 2020). Interestingly, *at*ALKBH9B is the only m^{6}A demethylase that is located exclusively in the cytoplasm (Mielecki et al., 2012), forming granules that colocalize with SGS3 (a component of siRNA bodies) and in some cases, associates with DCP1 (P bodies) (Ingelfinger et al., 2002; Martínez de Alba et al., 2015; Martínez-Pérez et al., 2017).

Arabidopsis genome has been described to encode more than 200 putative RNA-binding proteins (RBP) (Lorković and Barta, 2002; Abbasi et al., 2011; Ambrosone et al., 2012). RBPs are key factors in post-transcriptional gene regulation, protein synthesis, viral replication, cellular defense, and developmental regulation (Terribilini et al., 2006; Glisovic et al., 2008; Pallas and Gómez, 2013; Prall et al., 2019). RBPs are often modular and contain one or more conserved RNA-binding domains (RBD) (Lee et al., 2012; Re et al., 2014). RNA recognition motifs (RRM) and the K homology (KH) domain are the most abundant structural motifs in eukaryotes (Lorković and Barta, 2002; Chen and Varani, 2013). Other RBDs

include the glycine-rich motif (GRM), the double-stranded RNA binding domain (dsRBD), DEAD- Box-, PUF, SAM-, ZnF-domains (Lunde et al., 2007; Re et al., 2014; Lee and Kang, 2016), and the RGG/RG motif (Thandapani et al., 2013). However, the majority of residues predicted to be in the protein-RNA interface are not part of a characterized RBDs (Terribilini et al., 2006). In many cases, intrinsically disordered regions (IDRs) have been identified in proteins that do not display characterized RNA-binding sites (Calabretta and Richard, 2015; Varadi et al., 2015). Among other roles, IDRs participate in protein-protein and protein-RNA interactions and are enriched in "disorder-promoting amino acids" such as G, P, or R (Gsponer and Madan Babu, 2009). In this context, IDRs can encompass diverse functional motives such as RNA binding motifs or low-complexity (LC) domains (Castello et al., 2012). These proteins often go through binding induced-folding. Thus, as a consequence of their structural felxibility, the RNA-protein interactions can experiment conformational changes in the protein structure, the RNA or both (Frankel, 1999). Additionally, proteins containing IDRs promote liquid-liquid phase separation in the assembly and degradation of RNA granules such as stress granules or P-bodies (Spector, 2006; Lin et al., 2015). Similar to what was observed in mammals, some *Arabidopsis* m^6A *readers*, such as ECT2, ECT3, and ECT4 present IDRs and can form cytoplasmic granules (Scutenaire et al., 2018; Arribas-Hernández et al., 2020). Moreover, ECT2 was found to undergo a gel-like phase transition *in vitro* (Arribas-Hernández et al., 2018).

Alfalfa mosaic virus (AMV) belongs to the *Bromoviridae* family and, like the rest of the members of this family, its genome consists of three single-stranded RNAs of plus polarity (Bujarski et al., 2019). RNA1 and RNA2 encode the replicase subunits (P1 and P2), whereas RNA3 encodes the movement protein (MP) and serves as a template for the synthesis of subgenomic RNA4 (sgRNA4), which encodes the coat protein (CP) (Bol, 2005; Pallas et al., 2013). We previously demonstrated that *at*ALKBH9B is a key factor in AMV infection since the suppression of the *at*ALKBH9B m^6A demethylation activity reduces viral accumulation. Moreover, it was shown that the CP of this virus interacts with *at*ALKBH9B, pointing to a direct subversion of an endogenous regulatory pathway by the virus (Martínez-Pérez et al.,

2017). Due to the functional relevance of *at*ALKBH9B, the first m^6A demethylase described in plants, we carried out a functional mapping of the protein to identify putative domains implicated in the diverse interactions of this m^6A-demethylase with both the viral RNA and the coat protein.

Materials and Methods

Protein Expression and Purification in Bacteria

Full-length *at*ALKBH9B ORF and deletion mutants were subcloned into pGEX-KG (GE Healthcare Life Sciences) to generate a construct with 9B merged to the C-terminal part of the GST. GST and GST:*at*ALKBH9B fusion proteins were expressed in BL21 (DE3) *E. coli* cells and purified with glutathione Sepharose 4B beads (GE Healthcare Life Sciences) according to the manufacturer's recommendations. All protein purification procedures were performed at 4°C.

Nucleic Acid-Binding Assay by Northwestern Blot and EMSA

Dilutions of GST or GST:*at*ALKBH9B purified proteins were electrophoresed in 12% SDS/PAGE and transferred to nitrocellulose membranes. Membranes were incubated overnight at 4°C in Renaturing Buffer (10 mM Tris·HCl pH 7.5, 1 mM EDTA, 0.1 M NaCl, 0.05% Triton X-100, 1X Blocking Reagent, Roche). After this, membranes were incubated with 20 mL of the same buffer containing 50 ng/μL of the AMV sgRNA 4 labeled with digoxigenin for 3 h at 25°C. For the EMSA assay, 5 ng of 3′UTR of AMV RNA 3 transcripts were heated for 5 min at 85°C and cooled at room temperature for 15 min. Different amounts of purified GST:*at*ALKBH9B fusion proteins were added and incubated for 30 min at 4°C in a 10-μl final volume of Union Buffer (100 mM Tris-HCl pH 8.0, 1 M NaCl, 8 units of RiboLock RNase inhibitor, Thermo Fisher Scientific). Following incubations, the samples were separated through 1.2% agarose. RNAs were transferred to positively charged nylon membranes (Roche). RNAs were visualized on blots using DIG-labeled riboprobes corresponding to the 3'UTR of AMV RNA 3. Synthesis of the digoxigenin-labeled

riboprobes, hybridization and digoxigenin-detection procedures were carried out as described in (Pallás et al., 1998).

Bimolecular Fluorescence Complementation and Subcellular Localization Study

$^{N-C}$YFP:*at*ALKBH9B (wild-type and deletion mutants); GFP:*at*ALKBH9B and mCherry:SGS3 fusion proteins were cloned using the Gateway System (Invitrogen) according to the manufacturer's recommendations. Plasmid expressing the CP_{AMV} merged to the N, or C-terminal part of the YFP ($^{N-C}$YFP:CP_{AMV}), was previously described in Aparicio et al. (2006). All binary vectors were transformed into *Agrobacterium tumefaciens* C58 cells. Pairs of cultures carrying specific fusion proteins were mixed at an optical density of 0.5 each in infiltration solution (10 mM MES, pH 5.5, and 10 mM $MgCl_2$) and co-infiltrated into *N. benthamiana* leaves. Laser-scanning confocal images were taken 48 h after agroinfiltration. Excitation and emission wavelengths were 488 and 508 nm for GFP, 514 and 527 nm for YFP, and 545 and 572 nm for mCherry. Expression of fusion proteins was corroborated by western blot analysis using anti-^{Nt}GFP or anti-^{Ct}GFP (Roche) antibodies were conducted following the recommendations of the manufacturer.

Results

In vitro Mapping of *the* RNA-Binding Domain of *at*ALKBH9B

In a previous study, we demonstrated that *at*ALKBH9B interacts with the viral RNA, although the kinetic parameters of this interaction, as well as the identification of the RBD, were not analyzed (Martínez-Pérez et al., 2017). To estimate the capacity of the wild-type *at*ALKBH9B to bind the viral RNA, we first conducted Electrophoretic Mobility Shift Assays (EMSA) by incubating a constant amount (5 ng) of an RNA transcript, corresponding to the 3′ untranslated region of AMV-RNA3 (3′UTR-RNA3), with increasing concentrations of the glutathione S-transferase fusion protein (GST:*at*ALKBH9B$_{wt}$) (Figure 1). We chose this part of the RNA3/4 molecule because it is the same as the one that specifically binds CP, allowing us to directly compare it with this specific interaction. The decrease in the

chemiluminescent signal intensity corresponding to free RNA was evident at quantities exceeding 400 ng of GST:*at*ALBKH9B$_{wt}$ (lane 7, Figure 1A), suggesting the formation of a protein–RNA complex. At this point, it is important to note that the non-radioactive EMSA described here (see section "Material and Methods") requires the transfer to a nylon membrane step to detect both free RNA and the corresponding ribonucleoprotein (RNP) complex. When a large amount of molecules binds to the RNA, as in a non-sequence specific interaction, the transfer of the RNP complex to the nylon membrane and its posterior detection is difficult or even impossible (Marcos et al., 1999; Herranz and Pallás, 2004; Salavert et al., 2020). In any case, the disappearance of the free RNA band is evidence of complex formation (Carey, 1991) and was therefore quantified by film densitometry to calculate the apparent constant dissociation (Kd) of the RNA– GST:*at*ALBKH9Bwt interaction from the linear regression of the mean values from at least three technical replicates (Marcos et al., 1999). The K_d value of GST:*at*ALKBH9B$_{wt}$ was estimated to be 0.30 μM (Figure 1B).

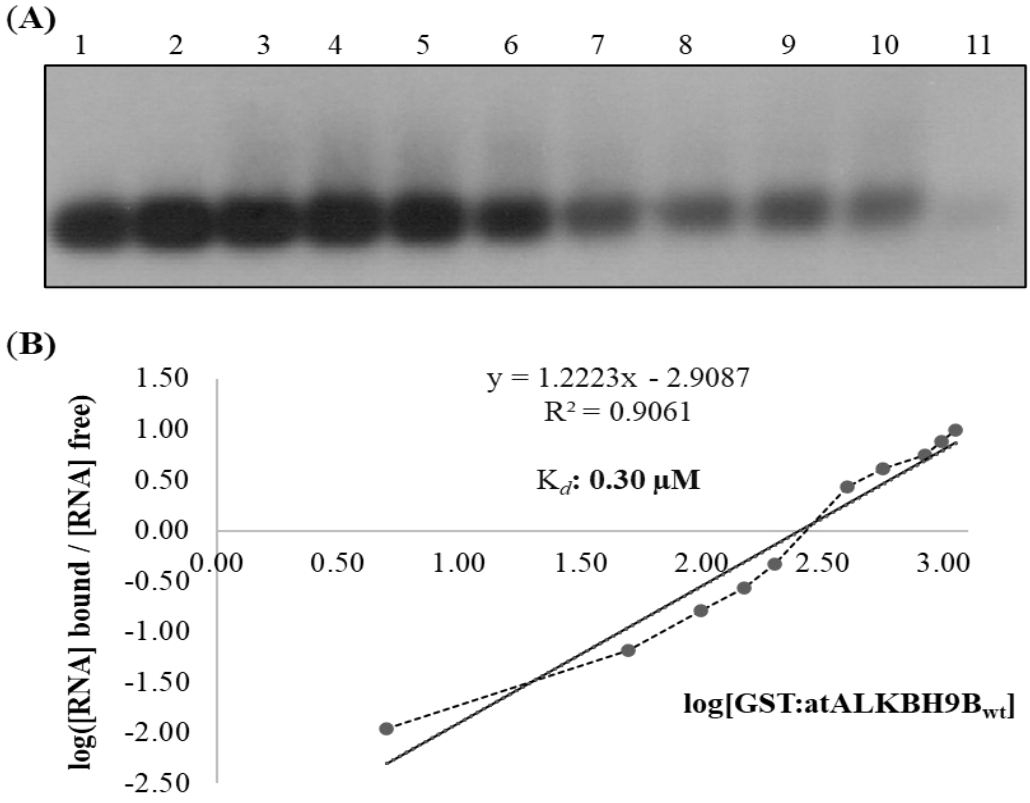

Figure 1. Analysis of RNA-protein complexes formed between purified GST:*at*ALKBH9B$_{wt}$ protein and the 3′UTR transcript of AMV-RNA3/4. (A) EMSA after incubation of 5 ng of 3′UTR transcript with no protein (lane 1) or with 5, 50, 100, 150, 200, 400, 560, 840, 980, and 1120 ng of GST:*at*ALKBH9B$_{wt}$ (lanes 2–11) corresponding to 0.01, 0.06, 0.12, 0.18, 0.24, 0.48, 0.67, 1.00, 1.17, and 1.22 µM, respectively. (B) Hill transformation. The thin line is the best fit determined by least-squares analysis, with the corresponding *r* coefficient and equation given in the insert. The slope of the best-fit equation determines a Hill coefficient of 1.35, indicating no or mild cooperativity, and the *y*-intercepted point gives the value of the K_d, which was 0.30 µM.

In order to determine the region of *at*ALKBH9B$_{wt}$ with RNA-binding activity, we first designed GST:*at*ALKBH9B deletion mutants lacking 160 amino acids at either the N- or C-terminal part (Δ160Nt and Δ160Ct, respectively), or 187 amino acids in the internal region of the protein (Δ187 Int) (Supplementary Figure 1A). Northwestern blot assays using AMV-sgRNA4 labeled with digoxigenin showed a complete loss of RNA-binding capacity of GST:*at*ALKBH9B$_{\Delta 187Int}$ and GST:*at*ALKBH9B$_{\Delta 160Ct}$ proteins (Supplementary Figure 1B). Thus, we designed new GST:*at*ALKBH9B deletion mutants affecting the internal and/or C-

terminal regions: GST:Δ258Nt; GST:Δ258Nt/Δ80Ct; GST:Δ258Nt/Δ40Ct; GST:Δ258Nt/Δ20Ct and GST:Δ387Nt (Figure 2A). Northwestern blot assays showed that only mutant Δ258Nt/Δ80Ct does not bind RNA, indicating that residues between positions 427 and 467 are critical for RNA-protein interaction (Figure 2B). To confirm this observation, we evaluated the RNA-binding activity of a mutant lacking residues from 427 and 467 (GST:ΔRBD) and one comprising only the *at*ALKBH9B 427–467 residues (GST:RBD) (Figure 2A). As shown in Figure 2B, only GST:RBD retained the RNA-binding capacity.

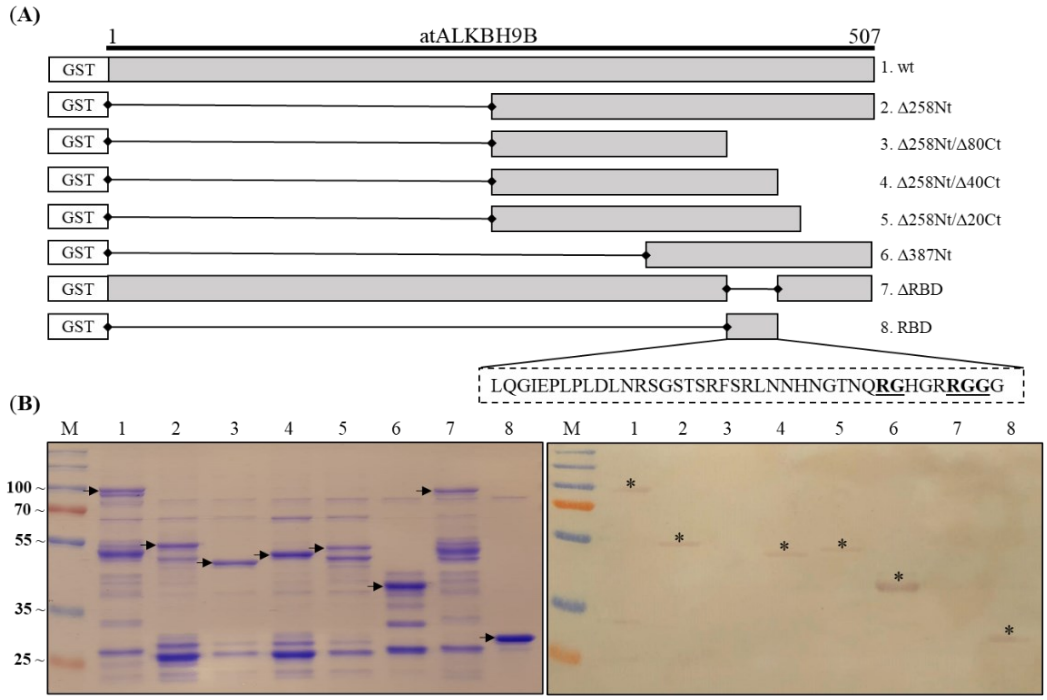

Figure 2. Analysis of the RNA-binding activity of purified GST:*at*ALKBH9B proteins by Northwestern blot assay. (A) GST fusion proteins containing Internal or C-terminal deletions of *at*ALKBH9B were produced in a prokaryotic system. (B) Duplicated membranes with GST:*at*ALKBH9B$_{wt}$ (lane 1) or its mutant variants (lanes 2–8), as depicted in (A), were resolved by 12% SDS–PAGE and, after transferring to nitrocellulose, incubated with 5 µg of AMV-sgRNA 4 labeled with digoxigenin. The left panel shows a Coomassie blue-stained gel, and the right panel shows results from Northwestern blot analysis. Positions of full-length GST:*at*ALKBH9B proteins are indicated by arrows. Asterisks indicate GST:*at*ALKBH9B fusion proteins which interact with the AMV-sgRNA4. The positions of molecular mass markers (in kDa) are shown on the left side.

To validate the northwestern blot assays, EMSAs were performed with GST:*at*ALKBH9B$_{wt}$, GST:Δ160Nt, GST:Δ258Nt; GST:Δ258Nt/Δ80Ct; GST:Δ258Nt/Δ40Ct and GST:Δ258Nt/Δ20Ct by incubating the viral RNA with different protein concentrations. As expected, EMSA showed a decrease in chemiluminescent signal intensity corresponding to the free viral RNA in mutants containing the RBD (Supplementary Figures 2A,B), whereas those lacking the predicted RBD did not reveal RNA binding (GST:Δ258Nt/Δ80Ct). Additionally, we studied the affinity and specificity of the *at*ALKBH9B RBD-RNA interaction by analyzing the shift in electrophoretic mobility of the 3'UTR-RNA3 (AMV) in the presence of GST:RBD fusion protein. As shown in Figure 3, increasing concentrations of GST:RBD diminished the amount of free RNA that becomes undetectable at 450 ng of the protein. A Hill transformation was used to analyze our data (Figure 3B). The K_d value of the RBD fused to GST was 0.64 μM, indicating slightly less RNA-binding than the full-length protein (GST:*at*ALKBH9B$_{wt}$). From the linear regression adjustment, a Hill coefficient c of 2.4 was obtained; this value above 1 (c = 1 indicates no cooperativity) would be taken as an indication of positive cooperativity.

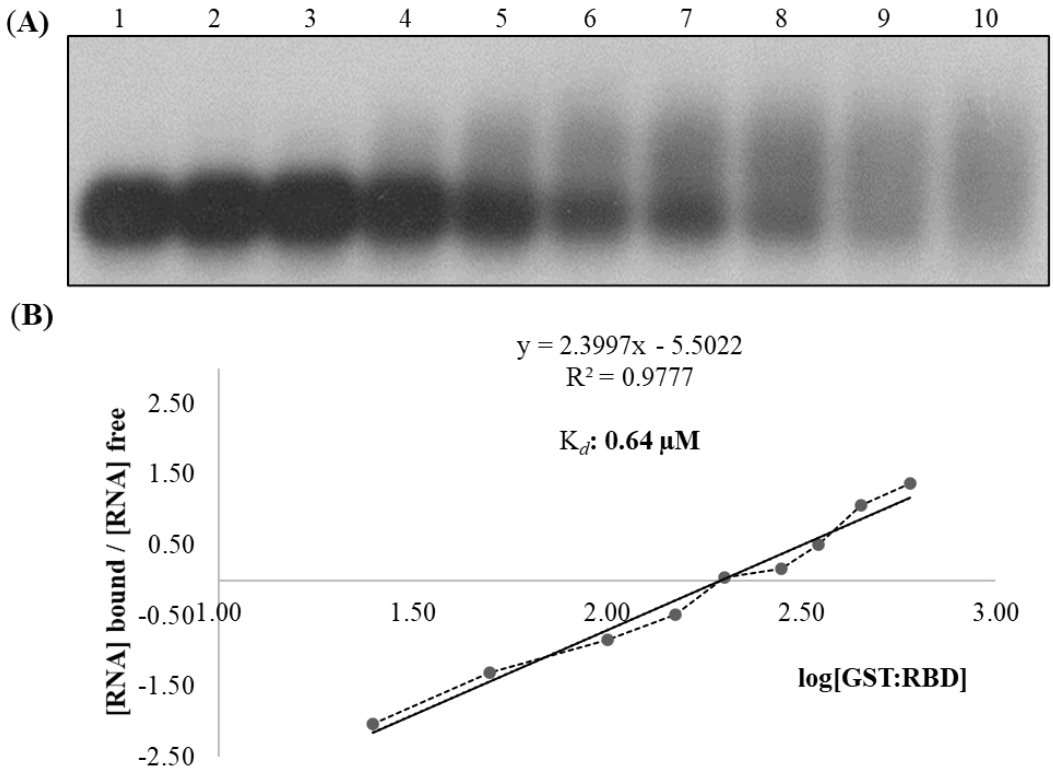

Figure 3. Analysis of RNA–protein complexes formed between purified GST:RBD of *at*ALKBH9B protein and the 3'UTR transcript of AMV-RNA3/4. (A) EMSA after incubation of 5 ng of 3'UTR transcript with no protein (lane 1) or with 25, 50, 100, 150, 200, 280, 350, 450 and 600 ng of GST:RBD of 9B (lanes 2–10) corresponding to 0.08, 0.16, 0.33, 0.49, 0.65, 0.91, 1.14, 1.47, and 1.96 µM, respectively. (B) Hill transformation. The thin line is the best fit determined by least-squares analysis, with the corresponding *r* coefficient and equation given in the insert. The slope of the best-fit equation determines a Hill coefficient of 2.4, and the *y* intercepted point gives the value of the apparent constant dissociation (K_d), which was 0.64 µM.

Subsequently, we used PSI-BLAST (Altschul et al., 1997) to compare *at*ALKBH9B RBD with other RNA binding proteins (RBP) from the databank, but the alignment of sequences did not reveal any significant similarities. Nonetheless, a high percentage of IDRs has been reported in viral, prokaryotic, and eukaryotic RBPs (Varadi et al., 2015). Therefore, we evaluated whether *at*ALKBH9B presented these IDRs, using PrDOS[1] (Ishida and Kinoshita, 2007). The results showed that 45.4% of all amino acids of *at*ALKBH9B form IDRs through

both N- and C-terminal regions, including most RBD (aa 427–467) (Figure 4). Remarkably, this RBD is enriched in G and R residues (20% and 15%, respectively), which are also common in the aforementioned IDRs. It is worth noting the presence of a RGxxxRGG motif and two extras RG residues that have been described in several RBPs showing characteristic disorder regions (Thandapani et al., 2013).

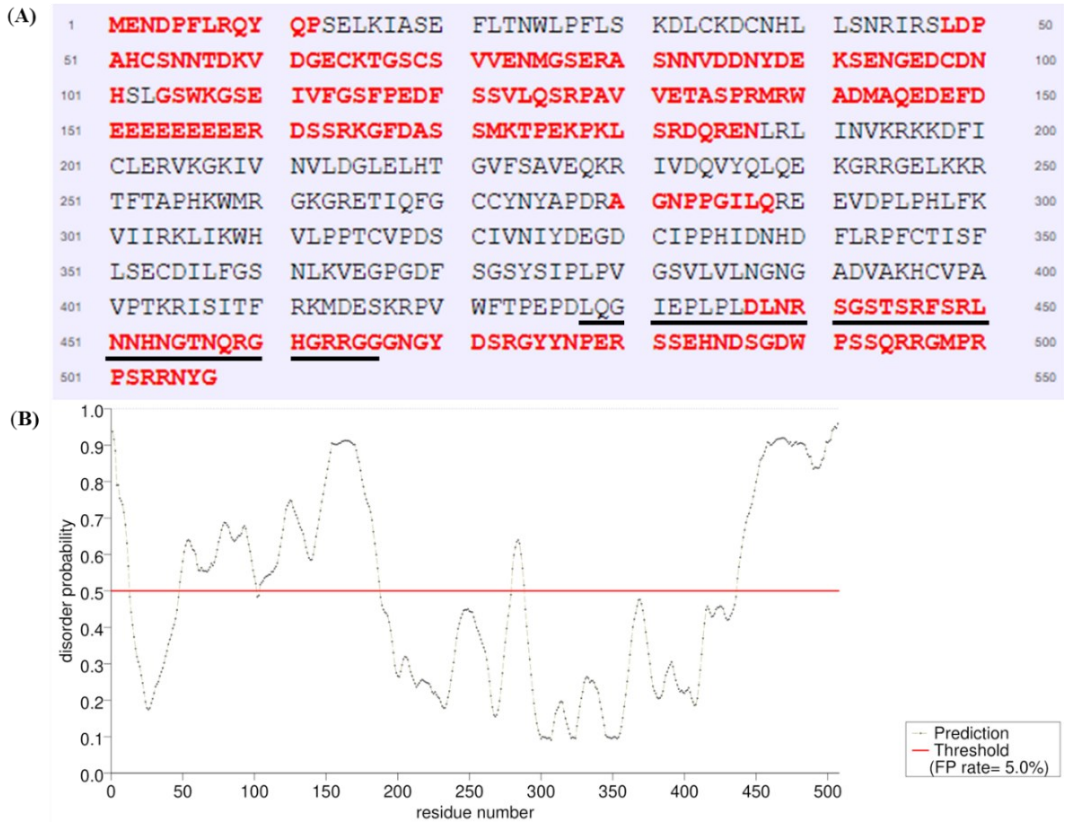

Figure 4. Prediction of natively disordered regions of *at*ALKBH9B using PrDOS. (A) *at*ALKBH9B amino acid sequence with disordered residues in red. The RBD located between positions 427–467 is underlined (black line). RGxxxRGG motif is underlined in green and the two extras RGs are in orange. (B) Disorder profile plot. Prediction false positive rate: 5%.

Taken together, these results indicate that *at*ALKBH9B efficiently cooperatively binds viral RNA through an RBD that has the characteristics of the IDRs present in other viral and eukaryotic RBPs.

In vivo Mapping of *at*ALKBH9B Binding Domain to AMV CP

We previously showed that the demethylase activity of *at*ALKBH9B affected the infectivity of AMV but not of cucumber mosaic virus (CMV), correlating with the ability of *at*ALKBH9B to interact (or not) with their coat proteins (Martínez-Pérez et al., 2017). Since this interaction is, thus, critical for the proviral function of *at*ALKBH9B, we decided to delineate the domain of *at*ALKBH9B involved in the host-protein/viral-protein interaction using the Bimolecular Fluorescent Complementation (BiFC). For this purpose, we first designed three mutants corresponding to the N-terminal, central and C-terminal regions, fused to the N- and C-terminal parts of the YFP (Figure 5A, left panel [I]). These constructs were co-infiltrated with the corresponding $^{N–C}$YFP:CP proteins in *Nicotiana benthamiana* leaves, and fluorescence was examined by confocal laser scanning microscopy (CLSM) after 48h. Leaves co-infiltrated with ^{C}YFP-9B$_{wt}$ plus ^{N}YFP-CP, ^{C}YFP-9B$_{\Delta 160Nt}$ plus ^{N}YFP-CP, and ^{C}YFP:9B$_{\Delta 187Int}$ plus ^{N}YFP-CP rendered a strong YFP fluorescence signal in the cells, whereas no reconstituted YFP fluorescence was detected in leaves co-infiltrated with the pair ^{C}YFP-9B$_{\Delta 160Ct}$ plus ^{N}YFP:CP (Figure 5B and Supplementary Figure 3, upper panels).

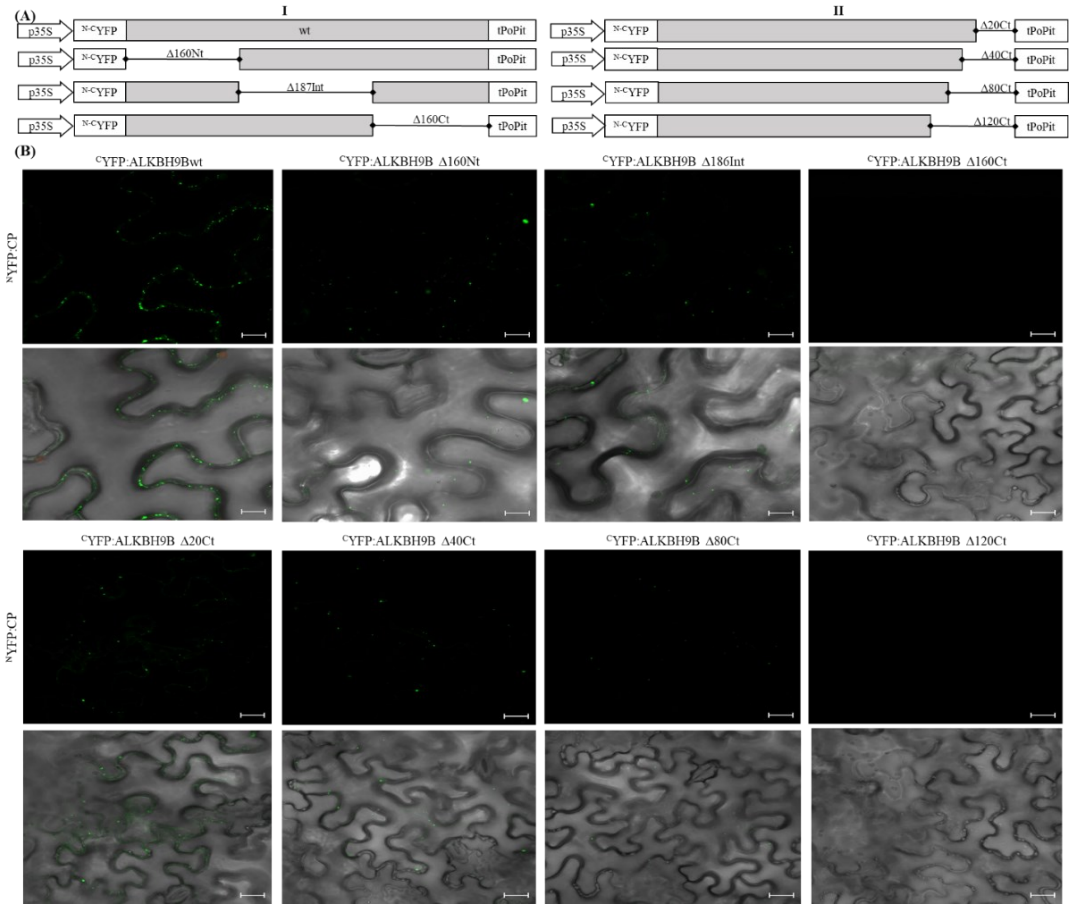

Figure 5. *In vivo* BiCF visualization of the interaction between $^{N–C}$YFP:*at*ALKBH9B fusion proteins and $^{N–C}$YFP:CP of AMV in *N. benthamiana*. **(A)** Schematic representation of the $^{N–C}$YFP:*at*ALKBH9B fusion proteins. **(B)** BiFC images of epidermal cells co-infiltrated with ^{C}YFP:*at*ALKBH9B proteins combined with the ^{N}YFP:CP, previously described in Aparicio et al. (2006). Scale bar = 20 μm.

To further delimit the domain involved in *at*ALKBH9B/AMV-CP interaction, we designed new $^{N–C}$YFP:fusion mutants by deleting residues located at the C-terminal region of *at*ALKBH9B (Figure 5A, right panel [II]). Leaves co-infiltrated with ^{C}YFP-*at*ALKBH9B$_{\Delta 20Ct}$ plus ^{N}YFP:CP, ^{C}YFP:*at*ALKBH9B$_{\Delta 40Ct}$ plus ^{N}YFP:CP and ^{C}YFP:*at*ALKBH9B$_{\Delta 80Ct}$ plus ^{N}YFP:CP produced a reconstituted YFP fluorescence signal in the cells, whereas no YFP fluorescence was detected in leaves co-infiltrated with the pair ^{C}YFP:*at*ALKBH9B$_{\Delta 120Ct}$ plus ^{N}YFP:CP (Figure 5B and Supplementary Figure 3, lower panels). Finally, western blot assays using anti ^{c}YFP and ^{N}YFP antibodies confirmed that all *at*ALKBH9B mutated versions fused to the ^{c}YFP and the ^{N}YFP:CP accumulated at detectable

levels in the co-infiltrated tissues (Supplementary Figure 4). Overall, our results suggest that amino acids located between positions 387 and 427 of *at*ALKBH9B are critical for the interaction with the AMV-CP.

The Subcellular Localization of *at*ALKBH9B Depends on the Correct Folding of the Protein

*at*ALKBH9B is the only protein of the 14 homologs of *E. coli* AlkB that is exclusively localized in the cytoplasm (Mielecki et al., 2012). Our previous studies determined that *at*ALKBH9B can specifically colocalize with SGS3 protein (a component of siRNA bodies), forming biomolecular-condensates associated with stress granules (Martínez-Pérez et al., 2017). To identify the region of the protein involved in this subcellular localization, we performed localization experiments in *N. benthamiana* leaves by expressing a series of deletion mutants of *at*ALKBH9B fused to the GFP (Figure 6A).

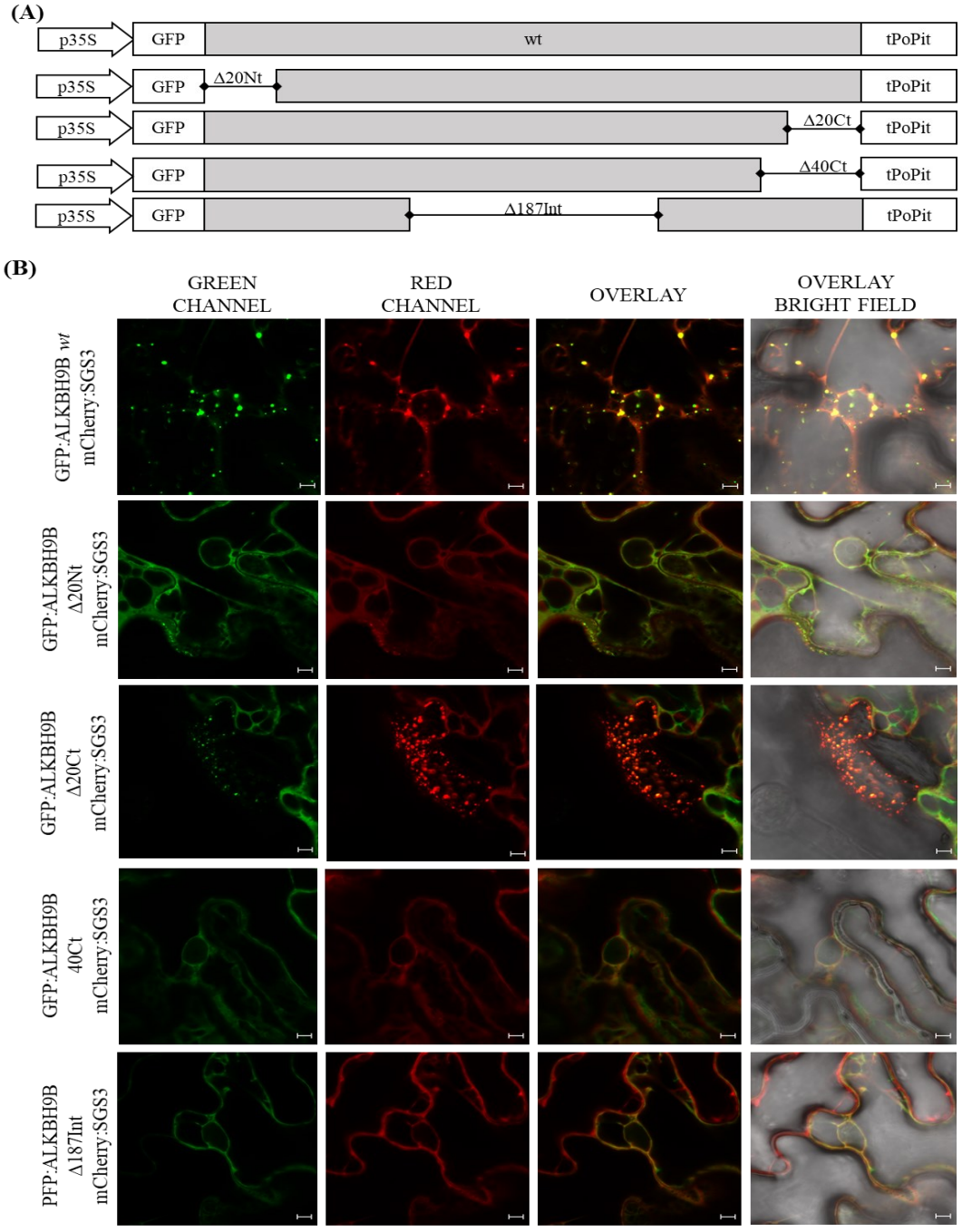

Figure 6. Subcellular localization of *at*ALKBH9B proteins fused with GFP in infiltrated leaves **(A)** Schematic representation of the different GFP:*at*ALKBH9B fusion proteins used. **(B)** CLSM images of *N. benthamiana* leaf epidermal cells co-infiltrated with agrobacterium expressing constructs indicated in **(A)** plus the SGS3 protein fused to the mCherry fluorescent protein (mCherry:SGS3). Scale bar = 20 µm.

Thus GFP:*at*ALKBH9B mutants were transiently co-expressed by agroinfiltration with mCherry:SGS3. As expected, full length *at*ALKBH9B co-localized with SGS3 (Figure 6B, upper panels) whereas that only *at*ALKBH9B with a deletion of the C-terminal 20 residues (Figure 6B panel GFP:*at*ALKBH9B$_{\Delta 20Ct}$) accumulated in cytoplasmic granules colocalizing with SGS3. In contrast, deletion of the N-terminal 20, C-terminal 40 or internal 186 residues (Figure 6A; GFP:*at*ALKBH9B$_{\Delta 20Nt}$, GFP:*at*ALKBH9B$_{\Delta 40Ct}$ and GFP:*at*ALKBH9B$_{\Delta 186Int}$) resulted in proteins showing a diffuse pattern throughout the cytoplasm (Figure 6B). These results indicated that different regions of the *at*ALKBH9B sequence are involved in its subcellular localization, which could be explained assuming that the proper three-dimensional folding of the protein might be a critical requirement to form the cytoplasmic granules and consequently to colocalize with siRNA bodies.

Discussion

m^{6}A RNA methylation in plants has emerged as an important cellular process of gene regulation in development (Wan et al., 2015; Růžička et al., 2017), response to abiotic stress (Li et al., 2014), and antiviral defense (Martínez-Pérez et al., 2017). Recently, *at*ALKBH9B, *at*ALKBH10B, and *at*ALKBH6 were described as m^{6}A *erasers* involved in AMV infection, flowering time in *Arabidopsis*, and growth and abiotic stress responses, respectively (Duan et al., 2017; Martínez-Pérez et al., 2017; Huong et al., 2020).

To dissect the functional activity of *at*ALKBH9B in plant-virus infection, a protein-mapping analysis was carried out to identify putative domains required to regulate this process. In this context, by mutagenesis and northwestern analysis, we analyzed the ALKBH9B RNA binding activity and delimited the region between residues 427 and 467 as critical for binding *in vitro* sgRNA4 (AMV). Moreover, EMSA analysis led us to determine that the K_d of the binding of the RBD alone (0.64 μM, Figure 3) was slightly higher than the one obtained with the full-length protein (0.30 μM, Figure 1), evidencing that other domains of the protein favor the binding to the viral RNA. Nonetheless, the RBD K_d value obtained is

within the range reported for other plant viruses RBPs, such as Nla from Tobacco etch virus -TVE- (1.1–1.3 μM) (Daròs and Carrington, 1997), Turnip crinkle virus CP (0.5 μM) (Skuzeski and Morris, 1995), p7 MP of Carnation mottle virus (0.7 μM) (Marcos et al., 1999), AMV CP (0.5 μM) (Baer et al., 1994), or the MP of prunus necrotic ringspot virus (Herranz and Pallás, 2004). Additionally, Huong et al. (2020) showed the RNA-binding capabilities of *at*ALKBH6, although their biochemical parameters were not determined.

Visual inspection and computational analysis of the *at*ALKBH9B sequence revealed no obvious structured RBD that could justify the RNA-binding properties described above. However, recently Varadi et al. (2015) demonstrated the prevalence of IDRs in RNA binding proteins and domains. Among other functions, IDRs are implicated in protein–protein and RNA–protein interactions (Castello et al., 2012). In fact, IDRs are a type of domain that is frequently found in proteins that undergo liquid–liquid phase separation (LLPS), a process that likely contributes to the formation and stability of RNA granules (Alberti et al., 2019). This has been demonstrated in YTHDF1, YTHDF2, and YTHDF3, m^6A-binding proteins, which undergo LLPS in the presence of polymethylated mRNAs. The resulting mRNA-YTHDF complexes form P-bodies and stress granules (Ries et al., 2019). Additionally, IDRs have been found to encompass diverse functional motives, e.g., well-established RNA binding activity such as RGG/RG and YGG motives, or low-complexity (LC) domains (Castello et al., 2012; Alberti et al., 2019). Both the conformational flexibility and the establishment of extended conserved electrostatic interfaces with RNAs have been proposed to provide the capability of the IDRs to specifically target different RNAs (Varadi et al., 2015). Furthermore, many proteins localized in RNA granules contain IDRs encompassing prion-like LC domains required for RNA granules assembly (Gilks et al., 2004; Reijns et al., 2008). The *at*ALKBH9B RBD identified here is enriched with G and R (20% and 15%, respectively) and presents an RGxxxRGG motif between positions 469 and 465 (Figure 1A) or a Tri-RG motif present in proteins implicated in various cellular processes like RNA biogenesis, DNA damage signaling, and mRNA translation (Thandapani et al., 2013). Interestingly, we found that 45.4% of *at*ALKBH9B amino acid sequence forms IDRs,

located at the N-terminal part, delimiting the internal AlkB-*like* domain located between positions 216 and 411 and at the C-terminal part. In fact, around 77.5% of the RBD is contained in the C-terminal disordered region (Figure 4). Furthermore, the C-terminal IDR of *at*ALKBH9B exhibits two additional RG residues at positions 473–474 and 466–497, respectively (Figure 4).

Our results can be explained considering that the RGxxxRGG motif between positions 459 and 466 plays a critical role in the protein–RNA interface. This interaction might induce the formation of a flexible structure permitting additional contacts through RG residues at positions 473–474 and 496–497 and YG residues at 506–507, enhancing the binding affinity and specificity of the interaction. For example, the splicing factor Tra2-β1 presents IDRs in the N- and C-terminal regions of the RRM. In the interface protein–RNA, this region adopts a folded structure, forming extensive contacts (Cléry et al., 2011). On the other hand, we previously reported that *at*ALKBH9B is exclusively cytoplasmic, forming discrete granules which colocalize with siRNA bodies, and some are associated with P bodies (Martínez-Pérez et al., 2017). Here we show that deletion of the first N-terminal 20 residues or the C-terminal last 40 amino acids impedes its accumulation in siRNA bodies rendering a diffuse cytoplasmic pattern (Figure 6B). Interestingly, the deleted *at*ALKBH9B N- and C-terminal parts are predicted to form IDRs, and the C-terminal is rich in Y and S residues, which would participate in the RNA granules formation. In this sense, mutation of LC domains in hnRNPA2 and FUS reduced the efficiency of their recruitment in hydrogel polymers *in vitro* (Xiang et al., 2015) and stress granules (SG) in cells (Kato et al., 2012), respectively. Moreover, phosphorylation of the SG-nucleating protein G3BP within its IDR (Ser 149) impaired its ability to induce the formation of SGs (Kedersha et al., 2016).

Finally, we found that amino acids located between positions 387 and 427 of *at*ALKBH9B are critical for CP–AMV interaction (Figure 5 and Supplementary Figure 3). Interestingly, this region is located next to the RNA-binding site, but it is not part of the C-terminal IDR (Figure 4). Considering that *at*ALKBH9B binds RNA to remove m^6A-modification (Martínez-Pérez et al., 2017), and the CP is a multifunctional protein indispensable for the

viral replication and translation (Bol, 2005; Guogas et al., 2005; Herranz et al., 2012), it may be possible that the CP binds *at*ALKBH9B in order to modulate the vRNA binding and the m^6A demethylase activity in benefit of the virus.

Conclusions

In this work, we have mapped the *at*ALKBH9B regions responsible for RNA and viral CP binding and those required for its localization in stress granules. CP-binding and RNA binding are located at the protein C-terminal, the former partly overlapping the AlkB-*like* domain, whereas the RBD is partially embedded in the predicted IDR located at the C-terminal (Figure 7). Thus, as found in other proteins (Protter and Parker, 2016), *at*ALKBH9B IDRs and the RBD could act cooperatively to promote the formation of RNA granules. This follows the role of both IDRs and folded domains in mediating RNA binding and oligomerization by acting together with RNAs to produce and maintain these granules (Jonas and Izaurralde, 2013; Protter and Parker, 2016). Therefore, although our results reinforce the existence of this cooperativity in RNA granules formation, the mechanisms underlying IDR-folded domain cooperativity and their potential regulation need further examination.

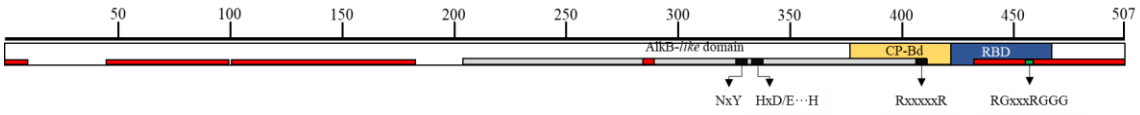

Figure 7. *at*ALKBH9B multi-domain structure. Predicted IDRs, between positions 1–12, 48–101, 104–187, 280–288, and 437–507, are shown in red. AlkB-*like* domain, located at 216–411, is shown in gray. Black boxes in the AlkB-*like* domain delimit the 2-OG stabilizing motif (NxY: 324–326), motif involved in binding to iron -Fe II- (HxD/E···H: 335–340) and the substrate specificity motif (RxxxxxR: 335–411) [Alignment between the *at*ALKBH9B and *hs*ALKBH5 proteins, using the BLAST tool]. The AMV CP binding domain (CP-bd: 387–427) and RNA binding domain (RBD: 427–507) are shown in yellow and blue. Regarding the functional mapping of atALKBH9B motif between positions 459 and 466 within the RBD characterized here is shown in green.

Supplementary Material

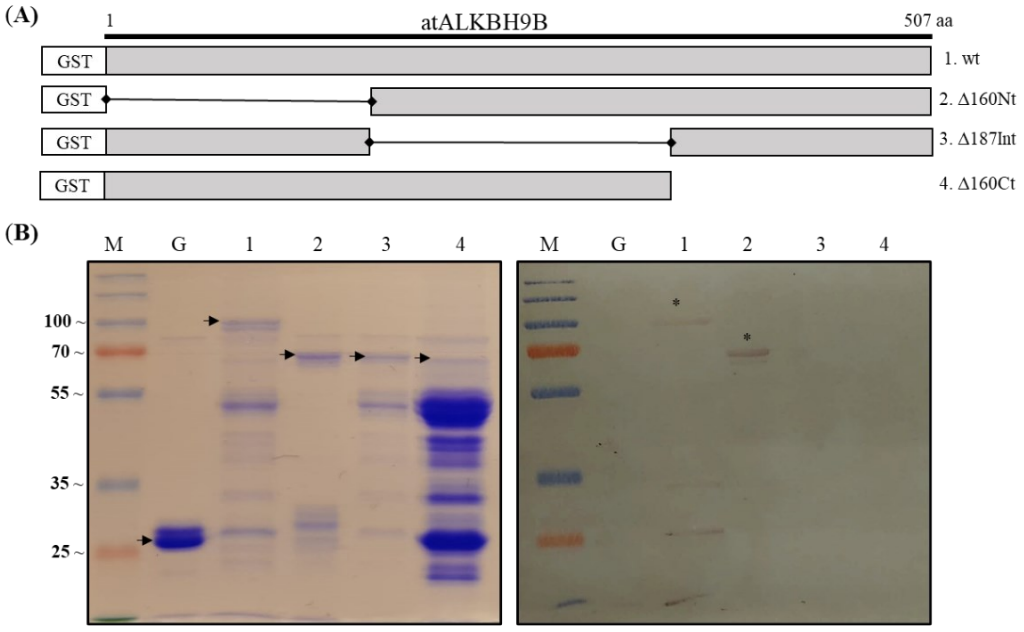

Supplementary Figure 1. Analysis of the RNA-binding activity of purified GST:*at*ALKBH9B fusion proteins by Northwestern blot assay. (A) GST fusion proteins containing N-terminal, Internal or C-terminal deletions of *at*ALKBH9B were produced in a prokaryotic system. (B) Duplicate membranes with GST (lane G), GST:*at*ALKBH9B$_{wt}$ (lane 1) or its mutant variants (lane 2-5), as described in (A), were resolved by 12% SDS–PAGE and, after transfer to nitrocellulose, incubated with 5 µg of AMV-agRNA4 labeled with digoxigenin. The left panel shows a Coomassie blue-stained gel and the right panel shows results from Northwestern blot analysis. Positions of full-length GST and GST:*at*ALKNH9B proteins are indicated by arrows. Asterisks indicate GST:*at*ALKBH9B proteins which interact with the AMV-sgRNA4 labeled with digoxigenin. The positions of molecular mass markers (in kDa) are shown on the left.

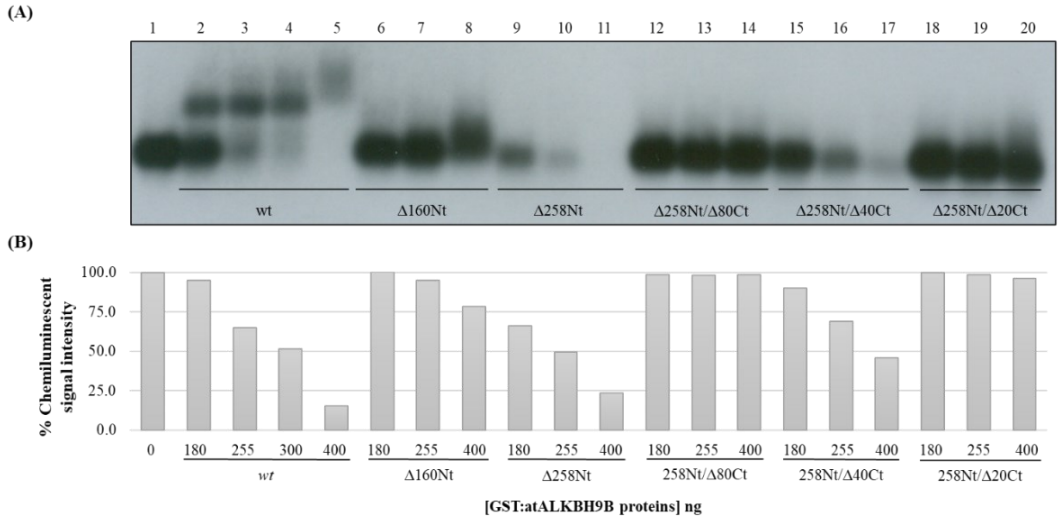

Supplementary Figure 2. Analysis of RNA–protein complexes formed between purified GST:*at*ALKBH9B fusion proteins and the 3'UTR transcript of AMV-RNA3. (A) EMSA after incubation of 5 ng of 3'UTR transcript with no protein (lane 1), 180, 255, 300, 400 ng of GST:*at*ALKBH9B$_{wt}$ (lanes 2 to 5), and 180, 255, 400 ng of GST:9B Δ160Nt (lane 6 to 8), Δ258Nt (lane 9 to 11), Δ258Nt/Δ80Ct (lane 12 to 14), Δ258Nt/Δ40Ct (lane 15 to 17) and Δ258Nt/Δ20Ct (lane 18 to 20). (B) Percentage of chemiluminescent signal intensity obtained from three technical replicates of EMSA that corresponds to the amount of free RNA in presence of GST:*at*ALKBH9B fusion proteins showning in (A).

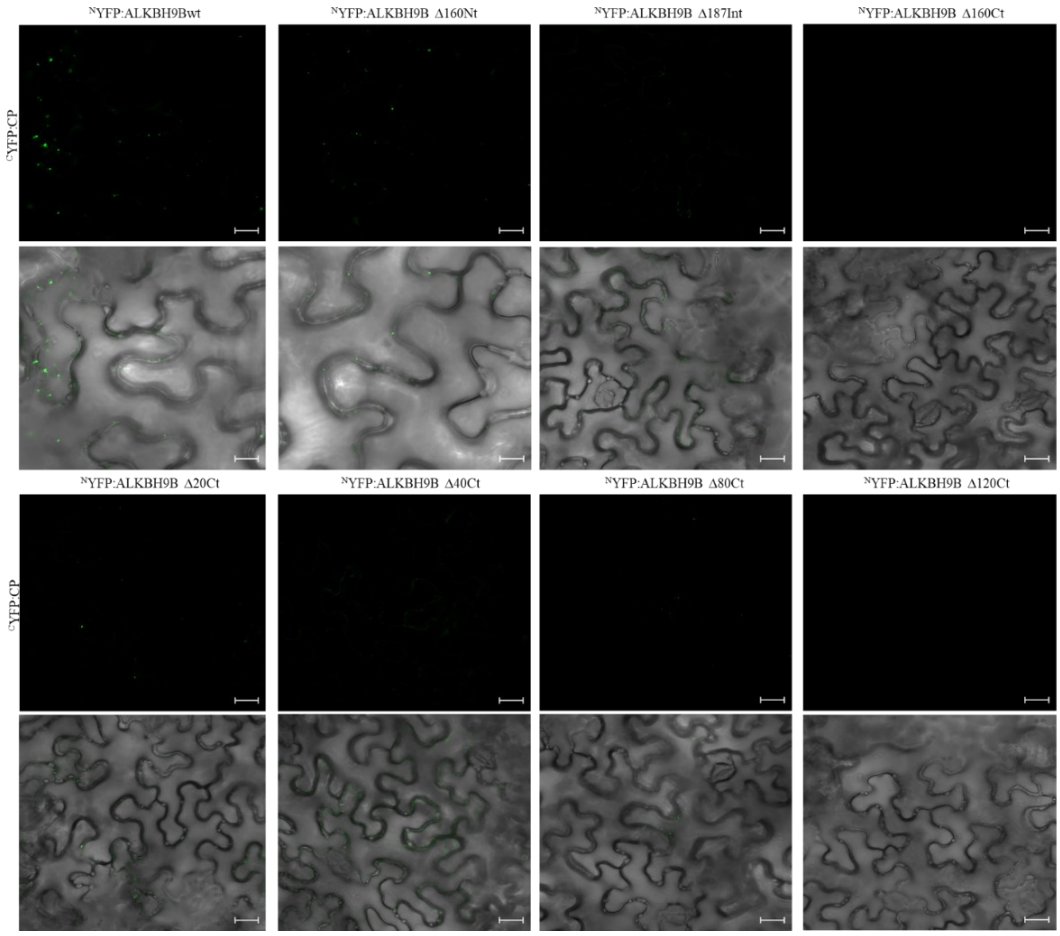

Supplementary Figure 3. BiFC images of epidermal cells co-infiltrated with ^{N}YFP:*at*ALKBH9Bs (indicated in Fig. 5 A, panel left and right, respectively) plus ^{C}YFP:CP fusion proteins. Scale bars, 20 μm.

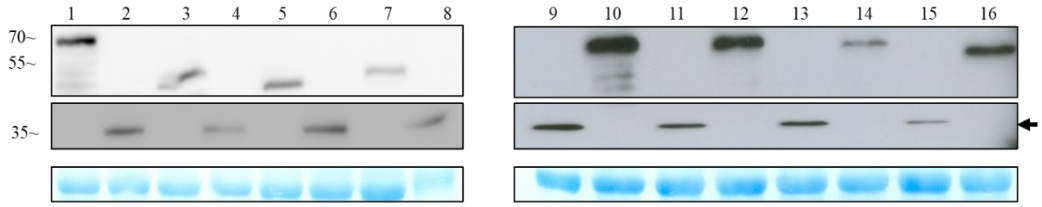

Supplementary Figure 4. Western blot assays to confirm protein expression of co-infiltrated constructs of ^{C}YFP:*at*ALKBH9B's plus ^{N}YFP:CP. Numbers 1, 3, 5, 7, 10, 12, 14 and 16 on top panel correspond to the indicated fusion proteins in Fig. 5 A (panel left and right, respectively) using anti-^{C}YFP antibody. Arrow in the lower panel correspond to the CP protein detected using anti-^{N}YFP antibody. The positions of molecular mass markers (in kDa) are shown on the left.

References

Abbasi, N., Park, Y.-I., and Choi, S.-B. (2011). Pumilio Puf domain RNA-binding proteins in Arabidopsis. Plant Signal. Behav. 6, 364–368. doi:10.4161/psb.6.3.14380.

Aik, W., Scotti, J.S., Choi, H., Gong, L., Demetriades, M., Schofield, C.J., et al. (2014). Structure of human RNA N6-methyladenine demethylase ALKBH5 provides insights into its mechanisms of nucleic acid recognition and demethylation. Nucleic Acids Res. 42, 4741–4754. doi:10.1093/nar/gku085.

Alberti, S., Gladfelter, A., and Mittag, T. (2019). Considerations and Challenges in Studying Liquid-Liquid Phase Separation and Biomolecular Condensates. Cell 176, 419–434. doi:10.1016/j.cell.2018.12.035.

Altschul, S.F., Madden, T.L., Schäffer, A.A., Zhang, J., Zhang, Z., Miller, W., et al. (1997). Gapped BLAST and PSI-BLAST: A new generation of protein database search programs. Nucleic Acids Res. 25, 3389–3402. doi:10.1093/nar/25.17.3389.

Ambrosone, A., Costa, A., Leone, A., and Grillo, S. (2012). Beyond transcription: RNA-binding proteins as emerging regulators of plant response to environmental constraints. Plant Sci. 182, 12–18. doi:10.1016/j.plantsci.2011.02.004.

Aparicio, F., Sánchez-Navarro, J.A., and Pallás, V. (2006). *In vitro* and *in vivo* mapping of the Prunus necrotic ringspot virus coat protein C-terminal dimerization domain by bimolecular fluorescence complementation. J. Gen. Virol. 87, 1745–1750. doi:10.1099/vir.0.81696-0.

Arribas-Hernández, L., Bressendorff, S., Hansen, M.H., Poulsen, C., Erdmann, S., and Brodersen, P. (2018). An m6A-YTH module controls developmental timing and morphogenesis in Arabidopsis. Plant Cell 30, 952–967. doi:10.1105/tpc.17.00833.

Arribas-Hernández, L., and Brodersen, P. (2020). Occurrence and functions of m6A and other covalent modifications in plant mRNA. Plant Physiol. 182, 79–96. doi:10.1104/pp.19.01156.

Arribas-Hernández, L., Simonini, S., Hansen, M.H., Paredes, E.B., Bressendorff, S., Dong, Y., et al. (2020). Recurrent requirement for the m6A-ECT2/ECT3/ECT4 axis in the control of cell proliferation during plant organogenesis. Dev. 147. doi:10.1242/dev.189134.

Baer, M.L., Houser, F., Loesch-Fries, L.S., and Gehrke, L. (1994). Specific RNA binding by amino-terminal peptides of alfalfa mosaic virus coat protein. EMBO J. 13, 727–735. doi:10.1002/j.1460-2075.1994.tb06312.x.

Bayoumi, M., Rohaim, M.A., and Munir, M. (2020). Structural and Virus Regulatory Insights Into Avian N6-Methyladenosine (m6A) Machinery. Front. Cell Dev. Biol. 8, 543. doi:10.3389/fcell.2020.00543.

Boccaletto, P., MacHnicka, M.A., Purta, E., Pitkowski, P., Baginski, B., Wirecki, T.K., et al. (2018). MODOMICS: A database of RNA modification pathways. 2017 update. Nucleic Acids Res. 46, D303–D307. doi:10.1093/nar/gkx1030.

Bodi, Z., Zhong, S., Mehra, S., Song, J., Graham, N., Li, H., et al. (2012). Adenosine Methylation in Arabidopsis mRNA is Associated with the 3′ End and Reduced Levels Cause Developmental Defects. Front. Plant Sci. 3, 48. doi:10.3389/fpls.2012.00048.

Bol, J. F. (2005). Replication of Alfamo- and Ilarviruses: Role of the Coat Protein. Annu. Rev. Phytopathol. 43, 39–62. doi:10.1146/annurev.phyto.43.101804.120505.

Bujarski, J., Gallitelli, D., García-Arenal, F., Pallás, V., Palukaitis, P., Krishna Reddy, M., et al. (2019). ICTV virus taxonomy profile: Bromoviridae. J. Gen. Virol. 100, 1206–1207. doi:10.1099/jgv.0.001282.

Calabretta, S., and Richard, S. (2015). Emerging Roles of Disordered Sequences in RNA-Binding Proteins. Trends Biochem. Sci. 40, 662–672. doi:10.1016/j.tibs.2015.08.012.

Castello, A., Fischer, B., Eichelbaum, K., Horos, R., Beckmann, B.M., Strein, C., et al. (2012). Insights into RNA Biology from an Atlas of Mammalian mRNA-Binding Proteins. Cell 149, 1393–1406. doi:10.1016/j.cell.2012.04.031.

Chen, Y., and Varani, G. (2013). Engineering RNA-binding proteins for biology. FEBS J. 280, 3734–3754. doi:10.1111/febs.12375.

Cléry, A., Jayne, S., Benderska, N., Dominguez, C., Stamm, S., and Allain, F.H.T. (2011). Molecular basis of purine-rich RNA recognition by the human SR-like protein Tra2-β1. Nat. Struct. Mol. Biol. 18, 443–451. doi:10.1038/nsmb.2001.

Covelo-Molares, H., Bartosovic, M., and Vanacova, S. (2018). RNA methylation in nuclear pre-mRNA processing. Wiley Interdiscip. Rev. RNA 9. doi:10.1002/wrna.1489.

Dang, W., Xie, Y., Cao, P., Xin, S., Wang, J., Li, S., et al. (2019). N6-methyladenosine and viral infection. Front. Microbiol. 10, 417. doi:10.3389/fmicb.2019.00417.

Daròs, J.A., and Carrington, J.C. (1997). RNA binding activity of NIa proteinase of tobacco etch potyvirus. Virology 237, 327–336. doi:10.1006/viro.1997.8802.

Martínez de Alba, A.E., Moreno, A. B., Gabriel, M., Mallory, A.C., Christ, A., Bounon, R., et al. (2015). In plants, decapping prevents RDR6-dependent production of small interfering RNAs from endogenous mRNAs. Nucleic Acids Res. 43, 2902–2913. doi:10.1093/nar/gkv119.

Dimock, K., and Stoltzfus, C.M. (1977). Sequence Specificity of Internal Methylation in B77 Avian Sarcoma Virus RNA Subunits. Biochemistry 16, 471–478. doi:10.1021/bi00622a021.

Duan, H.C., Wei, L.H., Zhang, C., Wang, Y., Chen, L., Lu, Z., et al. (2017). ALKBH10B is an RNA N6-methyladenosine demethylase affecting Arabidopsis floral transition. Plant Cell 29, 2995–3011. doi:10.1105/tpc.16.00912.

Frankel, A.D. (1999). If the loop fits... Nat. Struct. Biol. 6, 1081–1083. doi:10.1038/70002.

Furuichi, Y., Morgan, M., Shatkin, A. J., and Darnell, J.E. (1976). The Methylation of Adenovirus-Specific Nuclear and Cytoplasmic aRNA. Nucleic Acids Res. 3, 749–766. doi:10.1093/nar/3.3.749.

Gilks, N., Kedersha, N., Ayodele, M., Shen, L., Stoecklin, G., Dember, L. M., et al. (2004). Stress granule assembly is mediated by prion-like aggregation of TIA-1. Mol. Biol. Cell 15, 5383–5398. doi:10.1091/mbc.E04-08-0715.

Glisovic, T., Bachorik, J.L., Yong, J., and Dreyfuss, G. (2008). RNA-binding proteins and post-transcriptional gene regulation. FEBS Lett. 582, 1977–1986. doi:10.1016/j.febslet.2008.03.004.

Gsponer, J., and Madan Babu, M. (2009). The rules of disorder or why disorder rules. Prog. Biophys. Mol. Biol. 99, 94–103. doi:10.1016/j.pbiomolbio.2009.03.001.

Guogas, L.M., Laforest, S.M., and Gehrke, L. (2005). Coat Protein Activation of Alfalfa Mosaic Virus Replication Is Concentration Dependent. J. Virol. 79, 5752–5761. doi:10.1128/jvi.79.9.5752-5761.2005.

Herranz, M.C., and Pallás, V. (2004). RNA-binding properties and mapping of the RNA-binding domain from the movement protein of Prunus necrotic ringspot virus. J. Gen. Virol. 85, 761–768. doi:10.1099/vir.0.19534-0.

Herranz, M.C., Pallas, V., and Aparicio, F. (2012). Multifunctional roles for the N-terminal basic motif of Alfalfa mosaic virus coat protein: Nucleolar/cytoplasmic shuttling, modulation of RNA-binding activity, and virion formation. Mol. Plant-Microbe Interact. 25, 1093–1103. doi:10.1094/MPMI-04-12-0079-R.

Huang, H., Weng, H., and Chen, J. (2020). The Biogenesis and Precise Control of RNA m6A Methylation. Trends Genet. 36, 44–52. doi:10.1016/j.tig.2019.10.011.

Huong, T.T., Ngoc, L.N.T., and Kang, H. (2020). Functional Characterization of a Putative RNA Demethylase ALKBH6 in Arabidopsis Growth and Abiotic Stress Responses. Int. J. Mol. Sci. 21, 6707. doi:10.3390/ijms21186707.

Ingelfinger, D., Arndt-Jovin, D.J., Lührmann, R., and Achsel, T. (2002). The human LSm1-7 proteins colocalize with the mRNA-degrading enzymes Dcp1/2 and Xrnl in distinct cytoplasmic foci. RNA 8, 1489–1501. Available at: https://rnajournal.cshlp.org/content/8/12/1489.short [Accessed February 1, 2021].

Ishida, T., and Kinoshita, K. (2007). PrDOS: Prediction of disordered protein regions from amino acid sequence. Nucleic Acids Res. 35. doi:10.1093/nar/gkm363.

Jonas, S., and Izaurralde, E. (2013). The role of disordered protein regions in the assembly of decapping complexes and RNP granules. Genes Dev. 27, 2628–2641. doi:10.1101/gad.227843.113.

Kato, M., Han, T.W., Xie, S., Shi, K., Du, X., Wu, L. C., et al. (2012). Cell-free formation of RNA granules: Low complexity sequence domains form dynamic fibers within hydrogels. Cell 149, 753–767. doi:10.1016/j.cell.2012.04.017.

Kawai, Y., Ono, E., and Mizutani, M. (2014). Evolution and diversity of the 2-oxoglutarate-dependent dioxygenase superfamily in plants. Plant J. 78, 328–343. doi:10.1111/tpj.12479.

Kedersha, N., Panas, M.D., Achorn, C.A., Lyons, S., Tisdale, S., Hickman, T., et al. (2016). G3BP-Caprin1-USP10 complexes mediate stress granule condensation and associate with 40S subunits. J. Cell Biol. 212, 845–860. doi:10.1083/jcb.201508028.

Krug, R.M., Morgan, M.A., and Shatkin, A.J. (1976). Influenza viral mRNA contains internal N6-methyladenosine and 5'-terminal 7-methylguanosine in cap structures. J. Virol. 20, 45–53. doi:10.1128/jvi.20.1.45-53.1976.

Lee, D.H., Kim, D.S., and Hwang, B.K. (2012). The pepper RNA-binding protein CaRBP1 functions in hypersensitive cell death and defense signaling in the cytoplasm. Plant J. 72, 235–248. doi:10.1111/j.1365-313X.2012.05063.x.

Lee, K., and Kang, H. (2016). Emerging roles of RNA-binding proteins in plant growth, development, and stress responses. Mol. Cells 39, 179–185. doi:10.14348/molcells.2016.2359.

Li, D., Zhang, H., Hong, Y., Huang, L., Li, X., Zhang, Y., et al. (2014). Genome-Wide Identification, Biochemical Characterization, and Expression Analyses of the YTH Domain-Containing RNA-Binding Protein Family in Arabidopsis and Rice. Plant Mol. Biol. Report. 32, 1169–1186. doi:10.1007/s11105-014-0724-2.

Li, Z., Shi, J., Yu, L., Zhao, X., Ran, L., Hu, D., et al. (2018). N6-methyl-adenosine level in Nicotiana tabacum is associated with tobacco mosaic virus. Virol. J. 15, 87. doi:10.1186/s12985-018-0997-4.

Lin, Y., Protter, D.S.W., Rosen, M.K., and Parker, R. (2015). Formation and Maturation of Phase-Separated Liquid Droplets by RNA-Binding Proteins. Mol. Cell 60, 208–219. doi:10.1016/j.molcel.2015.08.018.

Liu, J., Yue, Y., Han, D., Wang, X., Fu, Y., Zhang, L., et al. (2014). A METTL3-METTL14 complex mediates mammalian nuclear RNA N6-adenosine methylation. Nat. Chem. Biol. 10, 93–95. doi:10.1038/nchembio.1432.

Liu, N., Dai, Q., Zheng, G., He, C., Parisien, M., and Pan, T. (2015). N6-methyladenosine-dependent RNA structural switches regulate RNA-protein interactions. Nature 518, 560–564. doi:10.1038/nature14234.

Lorković, Z.J., and Barta, A. (2002). Genome analysis: RNA recognition motif (RRM) and K homology (KH) domain RNA-binding proteins from the flowering plant Arabidopsis thaliana. Nucleic Acids Res. 30, 623–635. doi:10.1093/nar/30.3.623.

Lunde, B.M., Moore, C., and Varani, G. (2007). RNA-binding proteins: Modular design for efficient function. Nat. Rev. Mol. Cell Biol. 8, 479–490. doi:10.1038/nrm2178.

Luo, S., and Tong, L. (2014). Molecular basis for the recognition of methylated adenines in RNA by the eukaryotic YTH domain. Proc. Natl. Acad. Sci. U. S. A. 111, 13834–13839. doi:10.1073/pnas.1412742111.

Marcos, J.F., Vilar, M., Pérez-Payá, E., and Pallás, V. (1999). *In vivo* detection, RNA-binding properties and characterization of the RNA-binding domain of the p7 putative movement protein from carnation mottle carmovirus (CarMV). Virology 255, 354–365. doi:10.1006/viro.1998.9596.

Martínez-Pérez, M., Aparicio, F., López-Gresa, M.P., Bellés, J.M., Sánchez-Navarro, J.A., and Pallás, V. (2017). Arabidopsis m6A demethylase activity modulates viral infection of a plant virus and the m6A abundance in its genomic RNAs. Proc. Natl. Acad. Sci. U. S. A. 114, 10755–10760. doi:10.1073/pnas.1703139114.

Meyer, K.D., and Jaffrey, S.R. (2017). Annual Review of Cell and Developmental Biology Rethinking m6A Readers, Writers, and Erasers. doi:10.1146/annurev-cellbio-100616.

Meyer, K.D., Patil, D.P., Zhou, J., Zinoviev, A., Skabkin, M.A., Elemento, O., et al. (2015). 5′ UTR m6A Promotes Cap-Independent Translation. Cell 163, 999–1010. doi:10.1016/j.cell.2015.10.012.

Mielecki, D., Zugaj, D.Ł., Muszewska, A., Piwowarski, J., Chojnacka, A., Mielecki, M., et al. (2012). Novel AlkB Dioxygenases—Alternative Models for In Silico and *In vivo* Studies. PLoS One 7, e30588. doi:10.1371/journal.pone.0030588.

Pallas, V., Aparicio, F., Herranz, M.C., Sanchez-Navarro, J.A. and Scott, S.W. (2013). The molecular biology of ilarviruses. Adv. Virus Res. 87, 139–183.

Pallas, V., and Gómez, G. (2013). Phloem RNA-binding proteins as potential components of the long-distance RNA transport system. Front. Plant Sci. 4, 130. doi:10.3389/fpls.2013.00130.

Pallas, V., Más, P., and Sánchez-Navarro, J.A. (1998). Detection of plant RNA viruses by nonisotopic dot-blot hybridization. Methods Mol. Biol. 81, 461–468. doi:10.1385/0-89603-385-6:461.

Ping, X.L., Sun, B. F., Wang, L., Xiao, W., Yang, X., Wang, W.J., et al. (2014). Mammalian WTAP is a regulatory subunit of the RNA N6-methyladenosine methyltransferase. Cell Res. 24, 177–189. doi:10.1038/cr.2014.3.

Prall, W., Sharma, B., and Gregory, B. D. (2019). Transcription Is Just the Beginning of Gene Expression Regulation: The Functional Significance of RNA-Binding Proteins to Post-transcriptional Processes in Plants. Plant Cell Physiol. 60, 1939–1952. doi:10.1093/pcp/pcz067.

Protter, D.S.W., and Parker, R. (2016). Principles and Properties of Stress Granules. Trends Cell Biol. 26, 668–679. doi:10.1016/j.tcb.2016.05.004.

Re, A., Joshi, T., Kulberkyte, E., Morris, Q., and Workman, C.T. (2014). "RNA–Protein Interactions: An Overview," in Methods in molecular biology (Clifton, N.J.) (Methods Mol Biol), 491–521. doi:10.1007/978-1-62703-709-9_23.

Reijns, M.A.M., Alexander, R.D., Spiller, M.P., and Beggs, J.D. (2008). A role for Q/N-rich aggregation-prone regions in P-body localization. J. Cell Sci. 121, 2463–2472. doi:10.1242/jcs.024976.

Ries, R.J., Zaccara, S., Klein, P., Olarerin-George, A., Namkoong, S., Pickering, B.F., et al. (2019). m6A enhances the phase separation potential of mRNA. Nature 571, 424–428. doi:10.1038/s41586-019-1374-1.

Růžička, K., Zhang, M., Campilho, A., Bodi, Z., Kashif, M., Saleh, M., et al. (2017). Identification of factors required for m6A mRNA methylation in Arabidopsis reveals a role for the conserved E3 ubiquitin ligase HAKAI. New Phytol. 215, 157–172. doi:10.1111/nph.14586.

Scutenaire, J., Deragon, J.M., Jean, V., Benhamed, M., Raynaud, C., Favory, J.J., et al. (2018). The YTH Domain Protein ECT2 Is an m6A Reader Required for Normal Trichome Branching in Arabidopsis. Plant Cell 30, 986–1005. doi:10.1105/tpc.17.00854.

Shen, L., Liang, Z., Gu, X., Chen, Y., Teo, Z.W.N., Hou, X., et al. (2016). N6-Methyladenosine RNA Modification Regulates Shoot Stem Cell Fate in Arabidopsis. Dev. Cell 38, 186–200. doi:10.1016/j.devcel.2016.06.008.

Skuzeski, J.M., and Morris, T.J. (1995). Quantitative Analysis of the Binding of Turnip Crinkle Virus Coat Protein to RNA Fails to Demonstrate Binding Specificity but Reveals a Highly Cooperative Assembly Interaction. Virology 210, 82–90. doi:10.1006/viro.1995.1319.

Spector, D.L. (2006). Clastosome: A subtype of nuclear body enriched in 19S and 20S proteasomes, ubiquitin, and protein substrates of proteasome. Nat. Rev. Mol. Cell Biol 172, 887–898. doi:10.1016/j.cell.2006.11.026.

Terribilini, M., Lee, J. H., Yan, C., Jernigan, R.L., Honavar, V., and Dobbs, D. (2006). Prediction of RNA binding sites in proteins from amino acid sequence. RNA 12, 1450–1462. doi:10.1261/rna.2197306.

Thandapani, P., O'Connor, T.R., Bailey, T.L., and Richard, S. (2013). Defining the RGG/RG Motif. Mol. Cell 50, 613–623. doi:10.1016/j.molcel.2013.05.021.

Varadi, M., Zsolyomi, F., Guharoy, M., Tompa, P., and Levy, Y.K. (2015). Functional advantages of conserved intrinsic disorder in RNA-binding proteins. PLoS One 10. doi:10.1371/journal.pone.0139731.

Wan, Y., Tang, K., Zhang, D., Xie, S., Zhu, X., Wang, Z., et al. (2015). Transcriptome-wide high-throughput deep m6A-seq reveals unique differential m6A methylation patterns between three organs in Arabidopsis thaliana. Genome Biol. 16, 1–26. doi:10.1186/s13059-015-0839-2.

Wang, X., Lu, Z., Gomez, A., Hon, G.C., Yue, Y., Han, D., et al. (2014). N6-methyladenosine-dependent regulation of messenger RNA stability. Nature 505, 117–120. doi:10.1038/nature12730.

Wei, C.M., and Moss, B. (1975). Methylated nucleotides block 5' terminus of vaccinia virus messenger RNA. Proc. Natl. Acad. Sci. U. S. A. 72, 318–322. doi:10.1073/pnas.72.1.318.

Williams, G.D., Gokhale, N.S., and Horner, S.M. (2019). Regulation of Viral Infection by the RNA Modification N6-Methyladenosine. Annu. Rev. Virol. 6, 235–253. doi:10.1146/annurev-virology-092818-015559.

Xiang, S., Kato, M., Wu, L.C., Lin, Y., Ding, M., Zhang, Y., et al. (2015). The LC Domain of hnRNPA2 Adopts Similar Conformations in Hydrogel Polymers, Liquid-like Droplets, and Nuclei. Cell 163, 829–839. doi:10.1016/j.cell.2015.10.040.

Xiao, W., Adhikari, S., Dahal, U., Chen, Y.S., Hao, Y.J., Sun, B.F., et al. (2016). Nuclear m6A Reader YTHDC1 Regulates mRNA Splicing. Mol. Cell 61, 507–519. doi:10.1016/j.molcel.2016.01.012.

Xu, C., Liu, K., Tempel, W., Demetriades, M., Aik, W.S., Schofield, C.J., et al. (2014). Structures of human ALKBH5 demethylase reveal a unique binding mode for specific single-stranded N6-methyladenosine RNA demethylation. J. Biol. Chem. 289, 17299–17311. doi:10.1074/jbc.M114.550350.

Zhao, X., Yang, Y., Sun, B.F., Shi, Y., Yang, X., Xiao, W., et al. (2014). FTO-dependent demethylation of N6-methyladenosine regulates mRNA splicing and is required for adipogenesis. Cell Res. 24, 1403–1419. doi:10.1038/cr.2014.151.

Zheng, G., Dahl, J. A., Niu, Y., Fedorcsak, P., Huang, C. M., Li, C.J., et al. (2013). ALKBH5 Is a Mammalian RNA Demethylase that Impacts RNA Metabolism and Mouse Fertility. Mol. Cell 49, 18–29. doi:10.1016/j.molcel.2012.10.015.

Zhong, S., Li, H., Bodi, Z., Button, J., Vespa, L., Herzog, M., et al. (2008). MTA is an Arabidopsis messenger RNA adenosine methylase and interacts with a homolog of a sex-specific splicing factor. Plant Cell 20, 1278–1288. doi:10.1105/tpc.108.058883.

Zhou, Z., Lv, J., Yu, H., Han, J., Yang, X., Feng, D., et al. (2020). Mechanism of RNA modification N6-methyladenosine in human cancer. Mol. Cancer 19, 1–20. doi:10.1186/s12943-020-01216-3.

Chapter II

Impact of the potential m^{6}A modification sites at the 3'UTR of alfalfa mosaic virus RNA3 in the viral infection

Manuscript in preparation

Abstract

We have previously reported the presence of m^6A in the AMV (Alfamovirus, *Bromoviridae*) genome. Interestingly, two of these putative m^6A-sites are in hairpin (hp) structures in the 3'UTR of the viral RNA3. One site ($_{2012}$AAACU$_{2016}$) is in the loop of hpB, within the coat protein binding site 1 (CPB1), while the other ($_{1900}$UGm^6ACC$_{1904}$) is in the lower-stem of hpE, a loop previously associated with AMV negative-strand RNA synthesis. Knowing that m^6A can induce structural alterations in RNA and that m^6A-levels in the AMV genome regulate infection, we have performed *in vivo* experiments to assess the role of these putative m^6A-sites in the AMV cycle by introducing compensatory point mutations to interfere or abolish the m^6A-tag of these sites. Our results suggest that the loop of hpB could be involved in viral replication/accumulation. Meanwhile, $_{1900}$UGACC$_{1904}$ motif in hpE appears to be dispensable for AMV plus-strand accumulation, although $_{1902}$A residue identity and the maintenance of the lower-stem hpE structure are necessary to obtain wild-type plus strand accumulation *in vivo.* These results extend our understanding of the requirements for hpE in the AMV infection cycle, indicating that both the residue identity and the base-pairing capacity in this structure are essential for positive-strand synthesis.

Keywords: N^6-methyladenosine, RNA covalent modifications, plant viruses, alfamovirus, DRACH motif, *in vivo* AMV replication, 3'UTR.

Introduction

Alfalfa mosaic virus (AMV) is the only member of the Alfamovirus genus in the Bromoviridae family (Bujarski et al., 2019). AMV presents a tripartite single-stranded RNA genome of messenger-sense polarity that are capped (m^7G) at the 5' end and lack poly A tail at the 3' terminus. RNAs 1 and 2 encode the replicase subunits P1 and P2, respectively, whereas RNA 3 encodes the movement protein (MP) and serves as a template for the synthesis of the subgenomic RNA 4 (sgRNA 4), which encodes the coat protein (CP) (Bol, 2008). Like ilarviruses, AMV requires the presence of the CP to initiate infection (Pallas et al., 2013). The terminal 145 residues in the 3' untranslated regions (UTR) is > 80% homologous in the three AMV RNAs and can fold into a similar secondary structure consisting in a linear array of stem-loop structures flanked by AUGC motifs (Koper-Zwarthoff et al., 1979), which contains several independent high-affinity binding sites for CP (Houser-Scott et al., 1994) (Figure 1A). Thus, by *in vitro* binding assays, it was found that hairpins A and B (hpA and hpB) and the flanking AUGC motif 1, 2 and 3 represent the minimal CP binding site 1 (CPB1), whereas hairpins F and G (hpF and hpG) and AUGC motifs 4 and 5 conform the CPB2 (Reusken and Bol, 1996). Binding of the CP to the 3'UTR is critical for AMV to initiate infection and stimulates translation of AMV RNAs by most probably mimicking the function of the poly(A)-binding protein (Neeleman et al., 2004; Krab et al., 2005). Moreover, CP is a component of the AMV replicase (Reichert et al., 2007). Besides the binding sites for the CP, hairpin E (hpE) was found to be essential for minus-strand synthesis *in vitro* (Olsthoorn and Bol, 2002).

N^6-methyladenosine (m^6A) is a widespread modification on cellular RNAs of different organisms, including the genomes of some viruses that are dynamically regulated, and can impact many cellular processes and pathways (Baquero-Perez et al., 2021). In plants, m^6A methylation is mainly installed by a methylation complex containing several proteins: mRNA adenosine methylase A (MTA), MTB, FKBP12 INTERACTING PROTEIN 37KD (FIP37), VIRILIZER (VIR), and HAKAI. Most recently, FIONA1 (FIO1), a human METTL16 ortholog, was also described as a m^6A methyltransferase that modulates floral transition in

Arabidopsis (Růžička et al., 2017; Xu et al., 2022). Moreover, this modification is removed by demethylases of the AlkB family (Marcinkowski et al., 2020; Alvarado-Marchena et al., 2021), and members of the EVOLUTIONARI-LY CONSERVED C-TERMINAL REGIONS (ECT) family are the best described proteins that recognize and process m^6A-modified RNAs (Arribas-Hernández and Brodersen, 2020). In *Arabidopsis*, m^6A controls plant development at embryonic stage, vegetative growth and flowering (Arribas-Hernández and Brodersen, 2020). Remarkably diverse studies have demonstrated that, in addition to its involvement in physiological processes, m^6A pathway also modulates viral infections in mammals (Williams et al., 2019).

We previously reported the presence of m^6A along the RNAs of AMV, and that suppression of the m^6A demethylase *Arabidopsis* protein ALKBH9B increases the abundance of m^6A on the viral genome. Furthermore, the systemic infection capability of the virus was clearly reduced in *alkbh9b* plants, nearly blocking floral stems invasion (Martínez-Pérez et al., 2017, 2021). Additionally, by a methylated-RNA immuno-precipitation sequencing experiment, we mapped several discrete peaks distributed along the AMV genome susceptible to be m^6A methylated. Two of these sites are located in two hairpin structures in the 3'UTR of the genomic RNA 3. Interestingly, one site ($_{2012}$AAACU$_{2016}$) is positioned within the CPB1, in the loop of hpB, whereas the other ($_{1900}$UGACC$_{1904}$) is located in the lower-stem of hpE, both presenting the canonical m^6A motif DRACH (D= A, G or U, R = G/A, H = A/U/C) (Bayoumi and Munir, 2021) (Figure 1).

Previous studies have shown that the structural integrity of hpB and hpE on RNA 3 is essential for AMV replication cycle through their role in CP binding and minus strand synthesis, respectively (Bol, 2008). Furthermore, it has been found that m^6A methylation can affect A-U base pairing, which may lead to alter putative RNA-protein interactions (Liu et al., 2017), and m^6A levels on AMV genome regulate viral infection (Martínez-Pérez et al., 2017a). Although the impact of m^6A on RNA structure and function has been clearly demonstrated in animal viruses, its significance remains to be firmly established in the case of plant RNA viruses. Thus, we carried out *in vivo* experiments to evaluate the role of these

two putative m^6A-sites in AMV cycle by introducing compensatory point mutations to interfere or abolish the m^6A methylation of these sites.

Materials and Methods

Viral Constructs

For infection with viral transcripts, RNA 1, 2 and 3 of the AMV PV0196 isolate (Plant Virus Collection, DSMZ) were cloned into pTZ57R/T (Thermo Scientific™), generating the plasmids ptZ/cDNA1, ptZ/cDNA2 and ptZ/cDNA3. Using ptZ/cDNA3, mutagenic PCRs was performed to disable the putative DRACH sites located at loop hpB and stem hpE. Thus, specific primers (Supplementary Table 1) were designed with point mutations to change i) the putative $_{2014}m^6A$ residue in loop hpB for a guanosine residue (A to G), ii) the putative $_{1902}m^6A$ in the lower-stem hpE for cytosine (A to C), and iii) the $_{1903}C$ residue next to the $_{1902}m^6A$ for a guanosine (C to G). Compensatory mutations were also introduced to preserve the hairpin structure in mutations located at positions 1902 and 1903 (Figure 1 and Supplementary Table 1). After the treatment with Esp3I and DpnI endonucleases to digest the restriction sites and the parental DNA template, PCR products were ligated and transformed in *Escherichia coli* DH5α cells and mutation-containing plasmids. ptZ/cDNA3 mutants (ptZ/cDNA3$_{2014}$; ptZ/cDNA3$_{1902}$ and ptZ/cDNA3$_{1903}$) were confirmed by sequencing. Then, 300 ng of each plasmid that compose the viral RNA of AMV were linearized with PstI and transcribed with T7 RNA polymerase (Takara™). Viral RNAs (vRNAs) were m^7G-capped (m^7G-vRNAs) using Scriptcap™ m^7G Capping System (Epicentre® Biotechnologies) according to the manufacturer's instructions.

For infection with AMV/PV0196-infectious clone, RNA 1, 2 and 3 were cloned into a pBluescript SK(+) (AddGene®): pSK/cDNA1, pSK/cDNA2, pSK/cDNA3. The cDNAs were inserted between the Cauliflower mosaic virus (CaMV) 35S promoter and the Hepatitis delta virus (HDV) ribozyme sequence since the inclusion of this ribozyme at the end of the viral cDNAs was previously shown to enhance their infectivity (Balasubramaniam et al., 2006). To obtain the mutant pSK/cDNA3, the procedure described above was carried out.

Additionally, three new mutations were developed in: i) the $_{2012}$A$_{2013}$A residues next to the $_{2014}$A for guanosines (AA to GG), ii) the $_{1901}$G residue next to the $_{1902}$A for an adenosine (G to A), and iii) the $_{1922}$GGUCA$_{1926}$ residues in lower-stem hpE for AACAC nucleosides. The mutation located at position 1901 required another compensatory mutation to preserve the hairpin structure (Figure 1 and Supplementary Table 1). pSK/cDNA3 mutants (pSK/cDNA3$_{2014}$; pSK/cDNA3$_{1902}$; pSK/cDNA3$_{2012\text{-}13}$; pSK/cDNA3$_{1903}$; pSK/cDNA3$_{1901}$; pSK/cDNA3$_{1922\text{-}26}$) were confirmed by sequencing. Finally, each expression cassette of the plasmid pSK [35S::RNA1::Rz::PoPit], [35S::RNA2::Rz::PoPit] and pSK [35S::RNA3wt or mutant::Rz::PoPit] was introduced into the pMOG800 binary vector using a unique HindIII restriction site. Then, all binary vectors were transformed into *Agrobacterium tumefaciens* C58 cells.

Infection and Viral RNA Analysis

Infectious transcripts and cDNAs were evaluated in 2-week-old *Nicotiana benthamiana* plants. The AMV m^{7}G-vRNAs were mechanically inoculated with a mixture of 1 ug of m^{7}G-RNA1 and m^{7}G-RNA2, and the corresponding m^{7}G-RNA3 (wild-type or mutants) plus 1.9 µg of AMV 6XHis-CP (previously described in Martínez-Pérez et al., 2017) in 30 mM of sodium phosphate buffer, pH 7.0. Three biological replicates were performed, every replicate consisted in three *N. benthamiana* plants inoculated with each m^{7}G-vRNA123 combinations. Meanwhile, for the agroinfiltration infections, AMV infectious clones were mixed at an optical density at 600 nm of 0.15 each, in infiltration solution (10 mM MES, pH 5.5, and 10 mM $MgCl_2$) and infiltrated (three plants with each pMOG/cDNA123 combination). In all experiments, total RNA was extracted using EXTRAzol® (BLIRT S.A.). The detection of viral RNAs (vRNAs) was carried out by Northern blot analysis as previously described (Aparicio et al., 2003), using a digoxigenin-labeled probe to detect the multipartite genome of AMV (DigAMV). Viral RNA detection was conducted using CSPD chemiluminescent substrate. Densitometry was performed using ImageJ 1.53c. Statistical significances at the 95% confidence level ($\alpha = 0.05$) were determined using Minitab 18 ($P < 0.05$) through one-

way analysis of variance and Fisher's least significant difference (LSD) test for multiple comparisons.

Electrophoretic Mobility Shift Assay (EMSA)

To evaluate if these mutations interfered with the RNA/CP interaction, we performed EMSA experiments. For this, the 3'UTR of the corresponding pSK/cDNA3's plasmids were amplified using a forward primer located at the end of the CP open reading frame, containing the sequence of the T7 promoter and a reverse primer located at the 3' 20 last residues (Supplementary Table 1). To perform EMSA experiments, PCR products were used as templates to synthetize plus-strand RNAs corresponding to the 3'UTR region of the RNA3 *wt* and mutants ($3'UTR_{wt}$, $3'UTR_{2014}$, $3'UTR_{1902}$ and $3'UTR_{2012\text{-}13}$), which were incubated with increased concentrations of AMV CP as described in Aparicio et al., (2003). For this, we expressed and purified the CP protein using a N-terminal histidine tag (6xHis-CP) in a bacterial system as previously described in Martínez-Pérez et al., (2017).

Results and Discussion

In a previous study we mapped several discrete peaks distributed along the AMV genome susceptible to be m^6A methylated (Martínez-Pérez et al., 2017). Some of the potentially methylated bases are located in the 3'UTR of the RNA 3 at positions 1902 and 2014 from the 5' end forming part of a DRACH motif located in the lower-stem of hpE ($_{1900}$UGACC$_{1904}$) and in the hpB loop ($_{2012}$AAACU$_{2016}$) (Figure 1A). In this work, we have analyzed their putative role in AMV infection cycle by introducing point mutations that affect different key residues in both DRACH sites (Figure 1B).

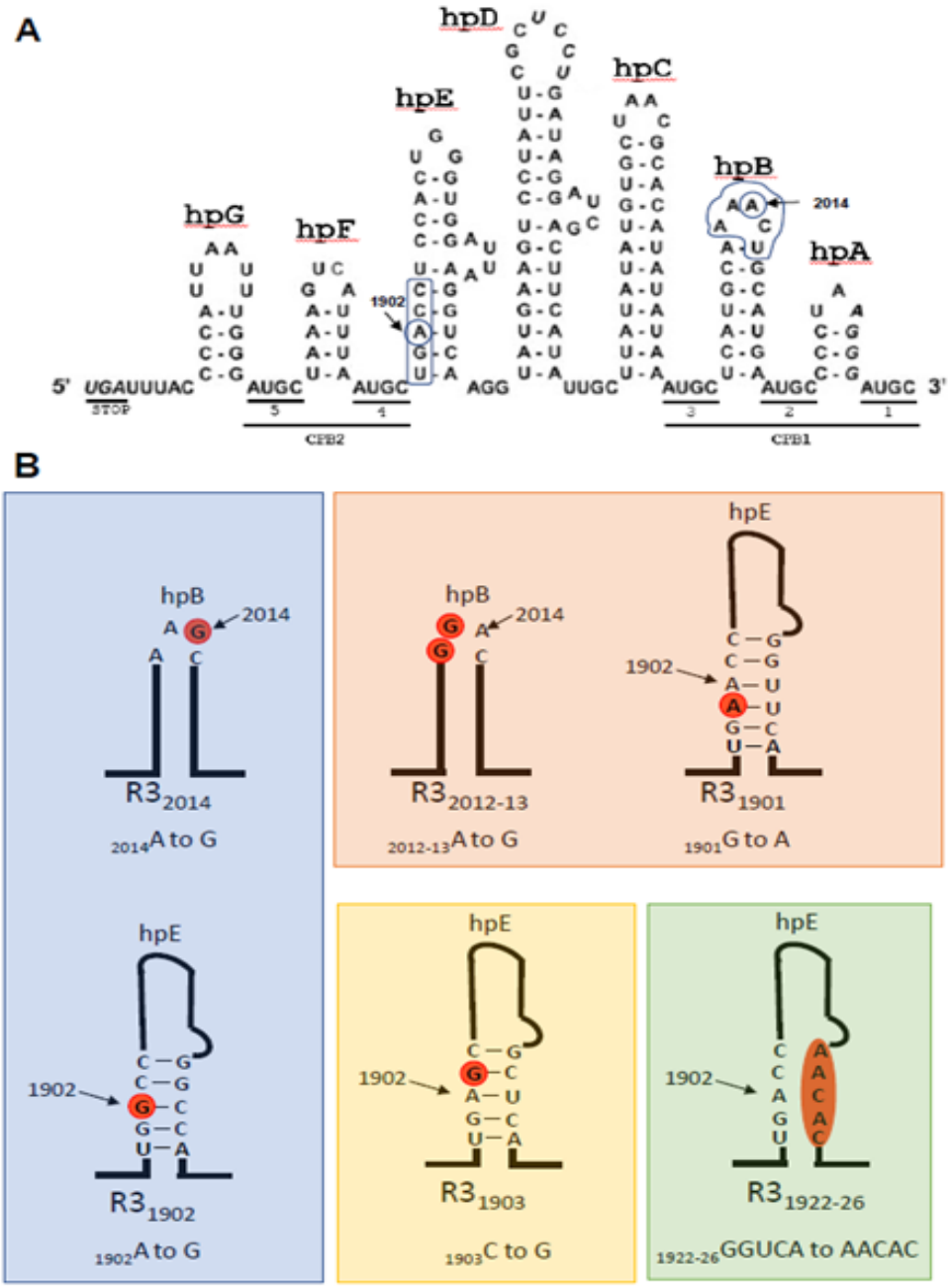

Figure 1. Schematic representation of the strucutre and mutants in 3'UTR of the AMV RNA3 analyzed in this study. (A) Linear secondary structure conformation proposed for the 3′UTR of RNA3. AUGC-sequence motifs and minimal CP-binding sites are underlined. Hairpins (hp) are labeled A to E. The nucleotides in the RNA 3 sequence are numerated from the first 5' residue of the full-length RNA 3. Putative DRm^{6}ACH in hpB and hpE are indicated. Adenosine residues at postions 1902 and 2012 susceptible to be modified are shown. (B) Schematic representation of the different mutations on hpB and hpE strutures. Mutant names are indicated at the bottom of each mutant. Mutated nucleotides are indicated in orange circles.

Thus, *N. benthamiana* leaves were inoculated with a mixture of capped transcripts of the RNA 1, RNA2 and RNA 3 wild-type (*wt*) or mutated versions of the potential m^6A residues (Figure 1B, blue box, $R3_{2014}$ and $R3_{1902}$ mutants) in the presence of the AMV-CP. Northern blot assays showed that plants inoculated with wild-type m^7G-vRNAs showed 100% infection effectiveness (Figure 2A and 2B: lanes m^7G-vRNA123_{wt}), which demonstrates that the inoculum was fully functional to initiate the infection cycle and perform systemic movement. Contrarily, we found that in plants inoculated with the mixture m^7G-vR123_{2014} only one sample out of three accumulated viral RNAs (vRNAs) in the inoculated and non-inoculated leaves, whereas the inoculum m^7G-vR123_{1902} failed to accumulate both in inoculate and upper non-inoculated leaves (Figure 2A and 2B: lanes m^7G-vRNA123_{2014} and m^7G-vRNA123_{1902}). The same results were consistently observed in three independent trials (Supplementary Table 2). Overall, these results indicate that the elimination of the residue A in these DRACH sites interfered with early stages of AMV replication.

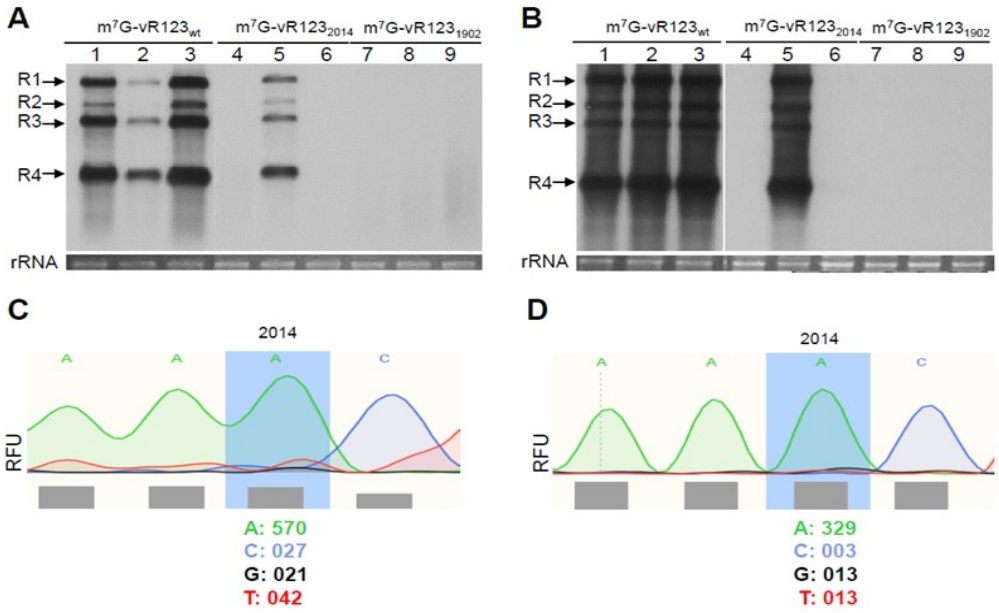

Figure 2. Effect of mutations in DRACH motives in the 3'UTR-RNA 3 using RNA transcript inoculation procedure. Representative Northern blots assays from inoculated (A) and upper non-inoculated leaves (B) of *N. benthamiana* plants at 6- and 13- days post-inoculation, respectively. Three plants were mechanically inoculated with different mixtures of the three RNAs plus CP (indicated at the top of the panels). Positions of the vRNAs are indicated on the left. Ethidium bromide staining of ribosomal RNAs was used as RNA loading controls. (C-D) Representative electropherogram of the $_{2012}$DRACH$_{2016}$-motif located in the hpB of the 3'UTR-RNA 3 in inoculated (C) and upper non-inoculated leaves (D) with m^{7}G-vRNA123$_{2014}$. RFU values of the predominant nucleotides are indicated for each position is indicated at the bottom of the mutated position.

A nucleotide reversion at the mutated site could be the reason why only one of three plants inoculated with m^{7}G-vR123$_{2014}$ inoculum resulted in local and systemic infection. To check this possibility, an RT-PCR was carried out with specific primers to amplify the 3'UTR of the RNA 3 from the total RNAs extracted from infected plants. Direct sequencing of the PCR product showed the nucleotide reversion of the G$_{2014}$ mutation to A in both inoculated and non-inoculated tissue (Fig. 2C and 2D: Relative fluorescence units – RFU – detected was 86.4% and 91.9% of A, compared to 3.2% and 3.6% of G).

As stated above, in the case of alfamovirus, inoculation with transcripts requires that vRNAs are capped and either RNA 4 or CP must be present in the inoculum. All these requirements could interfere with the effectiveness of the inoculation procedure as it is reflected in plants inoculated with the wild-type transcripts, in which different accumulation levels were

observed (Figure 2A, lanes m^7G-vRNA123$_{wt}$). In addition, it is well known that *Agrobacterium*-based inoculation methods are much more efficient than transcript-based procedures (Prol et al., 2021; Peyret and Lomonossoff, 2015). Thus, to circumvent the necessity of preparing *in vitro* transcripts and to avoid as much as possible failures on the infection process, the three cDNAs of AMV were cloned into binary vectors driven by the 35S promoter of Cauliflower mosaic virus.

To confirm the ability of the AMV cDNAs to initiate the infection cycle, a mixture of *Agrobacterium* cells transformed with each binary vector was agroinfiltrated in *N. benthamiana* plants. As shown in Figure 3A, this approach resulted in a 100% infection effectiveness accumulating the four RNAs (Figure 3A, lanes cDNA123$_{wt}$). Then, the infection efficiency of R3$_{2014}$ and R3$_{1902}$ mutants (Figure 1B) was evaluated using this same approach.

In contrast to the RNA inoculation procedure, agroinfiltration with the mixture cDNA123$_{2014}$ rendered the infection of all agroinfiltrated plants, although with a reduction in viral accumulation of 12.6 ± 5% (Figure 3, panels A and B, cDNA123$_{2014}$). Interestingly, sequencing of 3'UTR showed the reversion of the mutated nucleotide to the wild-type in all plants (Figure 3C, left panel: RFU detected was 60% of A compared to 29% of G). Furthermore, all plants agroinfiltrated with the mixture cDNA123$_{1902}$ were infected, although viral accumulation in upper non-inoculated leaves showed a reduction of 21.7 ± 1.7% (Figure 3, panels A and B, cDNA123$_{1902}$). Overall, our results suggest that the identity of these residues are important for AMV infection. Regarding the DRACH motif in hpB structure, the upstream $_{2012}$A$_{2013}$A residues were changed for G (Figure 1B, R3$_{2012\text{-}13}$ mutant) and northern blot analysis of plants agroinfiltrated with this mutant showed a reduction of 19.5 ± 5.8% respect to the *wt* virus (Figure 3A and 3B, cDNA123$_{2012\text{-}13}$). Furthermore, sequencing of the 3'UTR region showed a reversion of the mutated nucleotides to the wild-type (Figure 3C, right panel: RFU detected was 65.8% of $_{2012}$A compared to 20% of G and 66.7% of $_{2013}$A compared to 32% of G). These results suggest that the $_{2012}$A$_{2013}$A and $_{2014}$A residues conforming the DRACH motif in hpB are an important structural requirement for *in vivo*

viral replication and/or accumulation. Similar effects have been reported in dengue virus, in which point mutations in the upper loop of the hairpin A (SLA) of the 5'UTR were found to produce non-replicating RNAs, and nucleotide reversions within the SLA are sufficient to restore promoter activity (Filomatori et al., 2006). Moreover, point changes in the third base of the stem-loop of the mouse histone H2a-614 gene have been shown to greatly reduce the expression of histone mRNA; and also, a similar reduction was found in the ability to process the same mutant pre-mRNAs *in vitro* (Pandey et al., 1994).

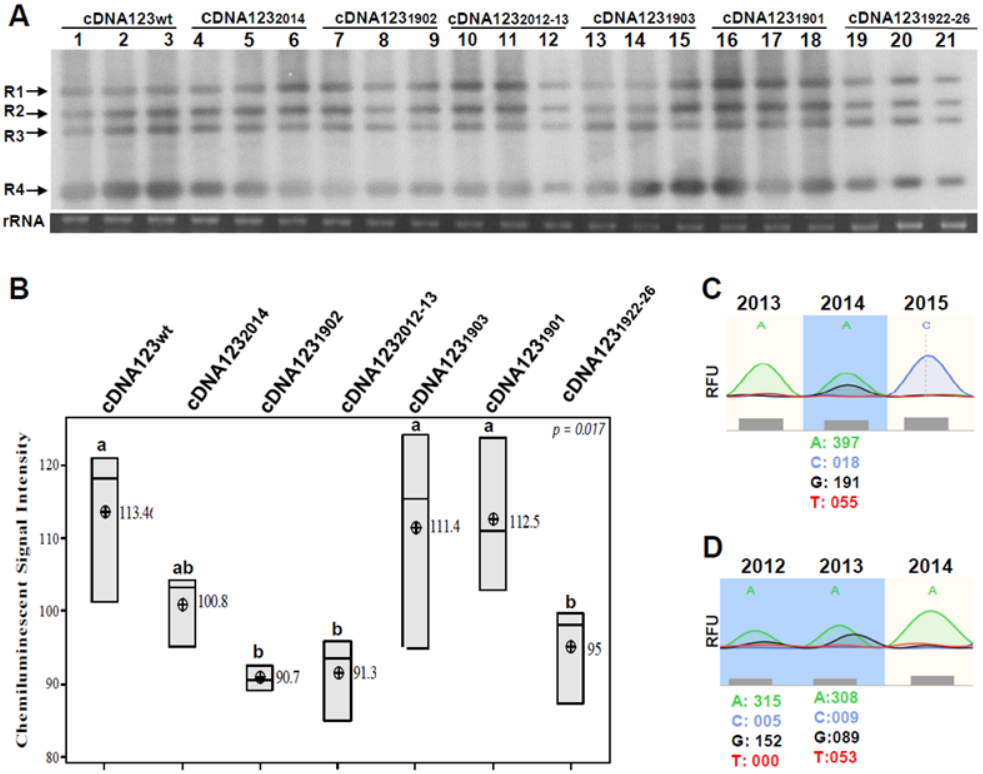

Figure 3. Effect of mutations in DRACH motifs of the 3'UTR-RNA 3 using the agroinfiltration procedure. (A) Representative northern blot assays from upper non-infiltrated leaves of *N. benthamiana* plants at 5 days post-agroinfiltration. Three plants were agroinfiltrated with different mixtures of cDNAs (indicated at the top of the panels). Positions of the vRNAs are indicated on the left. Ethidium bromide of ribosomal RNAs was used as RNA loading controls. (B) Boxplots of the densitometric analysis of AMV vRNA's accumulation. The lower and upper limits of the boxes are plotting the min and max values, respectively, whereas the lines dividing them represent the median values. Points inside boxes represent the mean from the three replicates. $P < 0.05$ indicates statistical significance. Means that do not share a letter are significantly different. (C-D) Representative electropherograms of the $_{2012}$DRACH$_{2016}$ motif located in the hpB of the 3'UTR-RNA 3 in agroinfiltrated plants with cDNA123$_{2014}$ (C) and cDNA123$_{2012\text{-}13}$ (D). RFU values of the predominant nucleotide is indicated for each position at the bottom of the mutated position.

It has been found that the binding of the CP to the CPB1 region in the RNA3 is critical to establish AMV infection cycle (Choi et al., 2003). We then evaluated if the mutations on hpB_{2014} and $hpB_{2012\text{-}13}$ were interfering with the interaction of the CP with the full-length 3'UTR of the AMV RNA3, which would explain the reduced infectivity of the inoculums containing these mutated RNA3. Additionally, we included mutant hpE_{1902} (Figure 1A and 1B). EMSA analysis showed a decrease of the free RNA at increasing concentrations of suggesting a similar formation of protein–RNA complexes in all 3'UTR versions (Figure 4). Previous studies reported that the loop of hpB would not disturb CP binding to the last 39 nt fragment of the 3'UTR (Reusken and Bol, 1996). Similarly, our results indicate that neither the DRACH-sequence located in hpB loop nor in hpE are involved in sequence-specific interactions with the CP *per se*. However, we cannot rule out the possibility that they could play other roles in the AMV infection cycle by inducing RNA structural modifications that interfere with other RNA-protein interactions.

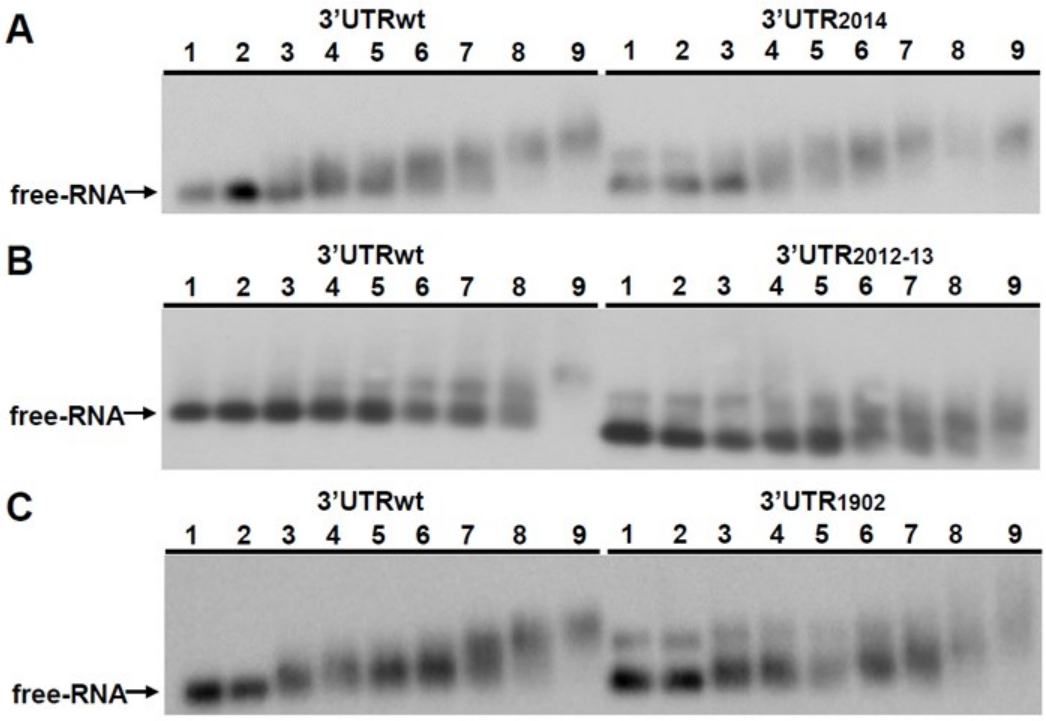

Figure 4. Analysis of RNA–protein complexes formed between purified 6xHis-CP protein and the 3'UTR transcript of AMV-RNA and mutants. (A-C) EMSA after incubation with 5 ng of 3'UTRs transcript *wt* or the indicated mutant without protein (lanes 1, 2, 10 and 11) or with 1, 2, 3, 5, 20, 50 and 100 ng of 6xHis-CP (lanes 3 to 9 and 12 to 18) corresponding to 0.004, 0.008, 0.01, 0.02, 0.08, 0.20, and 0.41 μM, respectively.

On the other hand, it is well known that m^6A-U base pair is weaker than A-U base pair, which can lead to destabilization of stem-loop structures and consequently altering putative RNA-protein interactions (reviewed in Zaccara et al. 2019). Thus, to evaluate if the observed effects in $R3_{1902}$ mutation are due to the m^6A-site substitution or a structural alteration of this stem structure, we generated a series of mutants altering the DRACH consensus site but keeping the A residues susceptible to be methylated. Thus, $_{1901}$G and $_{1903}$C residues in hpE were changed for A and G, respectively (Figure 1B, $R3_{1901}$ and $R3_{1903}$ yellow shaded). Compensatory mutations were also introduced to preserve the hairpin structure in this mutant. Surprisingly, plants agroinfiltrated with these constructs accumulated vRNAs at similar levels than plants agroinfiltrated with the wild-type infectious clone as well (Figure 3A and 3B, $cDNA123_{1901}$ and $cDNA123_{1903}$), suggesting that hpE structure, but not sequence identity, would be important for *in vivo* AMV infection. To corroborate this hypothesis,

$_{1922}$GGUCA$_{1926}$ residues in lower-stem hpE were changed to AACAC residues, disrupting the base pairing (Figure 1B, mutant hpE$_{1922\text{-}26}$, green shaded). Plants agroinfiltrated with this mutant showed a vRNAs reduction of the 16.3 ± 6.7% (Figure 3A and 3B, cDNA123$_{1922\text{-}26}$). Finally, direct sequencing of the 3'UTRs showed that, in contrast with mutants in hpB, all mutations on hpE stem-loop remained unaltered. A previous study showed that hpE is a crucial element for AMV minus-strand *in vitro* synthesis (Pandey et al., 1994). Furthermore, the identity and base-pairing capability of the upper-stem (Figure 1A, just below of the UCG triloop) was essential in this process, whereas, when the nucleotide sequence DRACH was eliminated, minus-strand synthesis was reduced around 60% (Pandey et al., 1994). Our results show that both $_{1902}$A residue and that base-pairing capability of the hpE lower-stem are critical for AMV plus-strand *in vivo* synthesis, whereas the DRACH motif identity is not. It has been proposed that hpE must consist on an interrupted 10 bp stem-base pairing to be functional (Olsthoorn et al., 2004). Altering the base-pairing capability of the hpE in cDNA3$_{1922\text{-}26}$ mutant causes a reduction in stem-size, a key structural requirement for hpE-promoting activity.

Conclusions

In this work we have evaluated the *in vivo* role of two DRACH motifs located in the hpB loop and hpE stem of the RNA 3 3'UTR that, interestingly, led to discover hot-sites involved in the initiation of *in vivo* AMV replication. The reversion of the mutated nucleotides observed in hpB$_{2014}$ and hpB$_{2012\text{-}13}$ mutants indicates that the identity of the residues conforming the loop hpB ($_{2012}$AAACU$_{2016}$) is a key structural requirement for *in vivo* viral replication. In this context, it is important to highlight that, as far as we know, this is the first time that the loop of hpB is shown to be involved in viral replication/accumulation. However, we cannot rule out the possibility that N^6-adenosine methylation of this site would modify the hpB structural conformation altering the *in vivo* binding of the CP or another viral or host proteins to this stem-loop. Contrarily, the putative UGm^{6}ACC motif in hpE seems to be dispensable for AMV plus-strand accumulation. Interestingly, both ^{1902}A residue identity and the maintenance of the lower-stem hpE structure keeping a 10 bp length-stem are necessary

to obtain wild-type plus strand accumulation *in vivo*. These results extend our knowledge on the requirement of hpE in AMV infection cycle, so that both identity and base-pairing capability of bases in this structure are essential for minus strand (Pandey et al., 1994) and plus strand synthesis.

Supplementary Material

Supplementary Table 1. Primers used in this study.

Primer	Sequence
ss/R3-3'UTR	5'- TAATACGACTCACTATAGACGATCTTGATCGTCAATGA -3'
as/R3-3'UTR	5'- TATAGTGAGTCGTATTAGCATCCCTTAGGGGCATTCA -3'
ss/mut_2014	5'- AGTCCGTCTCCTCATGCAAAGCTGCATGAATGC -3'
as/mut_2014	5'- AGTCCGTCTCCATGAGCATTTATATATGTGCGTTAG -3'
ss/mut_1902	5'- AGTCCGTCTCGGGTGGATTAAGGGCAAGGTATGAAGT -3'
as/mut_1902	5'- AGTCCGTCTCCCACCCAGTGGAGGGCAGCATTAAATGA -3'
ss/mut_2012-13	5'- ACTGCGTCTCGGACTGCATGAATGCCCCTAAG -3'
as/mut_2012-13	5'- AGTCCGTCTCCAGTCCTGCATGAGCATTTATATATGTGCGT -3'
ss/mut_1903	5'- AGTCCGTCTCGTGGATTAAGCTCAAGGTATGAAGTCCTATTCG -3'
as/mut_1903	5'- AGTCCGTCTCATCCACCCAGTGGAGCTCAGCATTAAAT -3'
ss/mut_1901	5'- AGTCCGTCTCACCTCCACTGGGTGGATTAAGGTTAAGG -3'
as/mut_1901	5'- AGTCCGTCTCGGAGGTTAGCATTAAATGACTTTAGCATCCC -3'
ss/mut_1922-26	5'- ACTGCGTCTCAACACAGGTATGAAGTCCTATTCGCTCC -3'
as/mut_1922-26	5'- AGTCCGTCTCTGTGTTTTAATCCACCCAGTGGAGGTCAG -3'

Supplementary Table 2. Detection of AMV by Northern blot assays in three biological replicates performed in *N. benthamiana* after inoculation with infectious transcripts (wild-type and mutants).

	Biological replicate No. 1			**Biological replicate No. 2**			**Biological replicate No. 3**		
	Plant 1	*Plant 2*	*Plant 3*	*Plant 1*	*Plant 2*	*Plant 3*	*Plant 1*	*Plant 2*	*Plant 3*
m^7G-vR123$_{wt}$	+ / +	+ / +	+ / +	+ / +	+ / +	+ / +	+ / +	+ / +	+ / +
m^7G-vR123$_{2014}$	+ / +	- / -	- / -	- / -	+ / +	- / -	+ / +	- / -	- / -
m^7G-vR123$_{1902}$	- / -	- / -	- / -	- / -	- / -	- / -	- / -	- / -	- / -
m^7G-vR123$_{1903}$	+ / -	- / -	- / -	+ / -	- / -	- / -	- / -	- / -	+ / -

+ / + AMV was detected in inoculated and systemic tissues.
- / - AMV was neither detected in inoculated nor in systemic tissues.
+ / - AMV was detected in inoculated tissue but not in systemic tissues.

References

Alvarado-Marchena, L., Marquez-Molins, J., Martinez-Perez, M., Aparicio, F., and Pallás, V. (2021). Mapping of Functional Subdomains in the atALKBH9B m6A-Demethylase Required for Its Binding to the Viral RNA and to the Coat Protein of Alfalfa Mosaic Virus. Front. Plant Sci. 12, 1–12. doi:10.3389/fpls.2021.701683.

Aparicio, F., Vilar, M., Perez-Payá, E., and Pallás, V. (2003). The coat protein of prunus necrotic ringspot virus specifically binds to and regulates the conformation of its genomic RNA. Virology 313, 213–223. doi:10.1016/S0042-6822(03)00284-8.

Arribas-Hernández, L., and Brodersen, P. (2020). Occurrence and functions of m6A and other covalent modifications in plant mRNA. Plant Physiol. 182, 79–96. doi:10.1104/pp.19.01156.

Balasubramaniam, M., Ibrahim, A., Kim, B. S., and Loesch-Fries, L. S. (2006). Arabidopsis thaliana is an asymptomatic host of Alfalfa mosaic virus. Virus Res. 121, 215–219. doi:10.1016/J.VIRUSRES.2006.04.005.

Baquero-Perez, B., Geers, D., and Díez, J. (2021). From A to m6A: The Emerging Viral Epitranscriptome. Viruses 13. doi:10.3390/V13061049.

Bayoumi, M., and Munir, M. (2021). Evolutionary conservation of the DRACH signatures of potential N6-methyladenosine (m6A) sites among influenza A viruses. Sci. Reports 2021 111 11, 1–12. doi:10.1038/s41598-021-84007-0.

Bol, J. F. (2008). "Alfalfa Mosaic Virus," in Encyclopedia of Virology, 81–87. doi:10.1016/B978-012374410-4.00635-X.

Bujarski, J., Gallitelli, D., García-Arenal, F., Pallás, V., Palukaitis, P., Krishna Reddy, M., et al. (2019). ICTV virus taxonomy profile: Bromoviridae. J. Gen. Virol. 100, 1206–1207. doi:10.1099/jgv.0.001282.

Choi, J., Kim, B. S., Zhao, X., and Loesch-Fries, S. (2003). The Importance of Alfalfa Mosaic Virus Coat Protein Dimers in the Initiation of Replication. Virology 305, 44–49. doi:10.1006/VIRO.2002.1756.

Filomatori, C. V., Lodeiro, M. F., Alvarez, D. E., Samsa, M. M., Pietrasanta, L., and Gamarnik, A. V. (2006). A 5′ RNA element promotes dengue virus RNA synthesis on a circular genome. Genes Dev. 20, 2238–2249. doi:10.1101/gad.1444206.

Houser-Scott, F., Baer, M., Liem, K., Cai, J., and Gehrke, L. (1994). Nucleotide sequence and structural determinants of specific binding of coat protein or coat protein peptides to the 3' untranslated region of alfalfa mosaic virus RNA 4. J. Virol. 68, 2194–2205. doi:10.1128/JVI.68.4.2194-2205.1994.

Koper-Zwarthoff, E. C., Brederod, F. T., Walstra, P., and Bol, J. F. (1979). Nucleotide sequence of the 3′-noncoding region of alfalfa mosaic virus RNA 4 and its homology with the genomic RNAs. Nucleic Acids Res. 7, 1887–1900. doi:10.1093/nar/7.7.1887.

Krab, I. M., Caldwell, C., Gallie, D. R., and Bol, J. F. (2005). Coat protein enhances translational efficiency of Alfalfa mosaic virus RNAs and interacts with the elF4G component of initiation factor elF4F. J. Gen. Virol. 86, 1841–1849. doi:10.1099/VIR.0.80796-0.

Liu, N., Zhou, K. I., Parisien, M., Dai, Q., Diatchenko, L., and Pan, T. (2017). N6-methyladenosine alters RNA structure to regulate binding of a low-complexity protein. Nucleic Acids Res. 45, 6051–6063. doi:10.1093/nar/gkx141.

Marcinkowski, M., Pilžys, T., Garbicz, D., Steciuk, J., Zugaj, D., Mielecki, D., et al. (2020). Human and Arabidopsis alpha-ketoglutarate-dependent dioxygenase homolog proteins—New players in important regulatory processes. IUBMB Life 72, 1126–1144. doi:10.1002/IUB.2276.

Martínez-Pérez, M., Aparicio, F., López-Gresa, M. P., Bellés, J. M., Sánchez-Navarro, J. A., and Pallás, V. (2017). Arabidopsis m6A demethylase activity modulates viral infection of a plant virus and the m6A abundance in its genomic RNAs. Proc. Natl. Acad. Sci. U. S. A. 114, 10755–10760. doi:10.1073/pnas.1703139114.

Martínez-Pérez, M., Gómez-Mena, C., Alvarado-Marchena, L., Nadi, R., Micol, J. L., Pallas, V., et al. (2021). The m6A RNA Demethylase ALKBH9B Plays a Critical Role for Vascular Movement of Alfalfa Mosaic Virus in Arabidopsis. Front. Microbiol. 12. doi:10.3389/fmicb.2021.745576.

Neeleman, L., Linthorst, H., and Bol, J. (2004). Efficient translation of alfamovirus RNAs requires the binding of coat protein dimers to the 3' termini of the viral RNAs. J. Gen. Virol. 85, 231–240. doi:10.1099/VIR.0.19581-0.

Olsthoorn, R., and Bol, J. (2002). Role of an essential triloop hairpin and flanking structures in the 3' untranslated region of Alfalfa mosaic virus RNA in *in vitro* transcription. J. Virol. 76, 8747–8756. doi:10.1128/JVI.76.17.8747-8756.2002.

Olsthoorn, R. C. L., Haasnoot, P. C. J., and Bol, J. F. (2004). Similarities and Differences between the Subgenomic and Minus-Strand Promoters of an RNA Plant Virus. J. Virol. 78, 4048–4053. doi:10.1128/JVI.78.8.4048-4053.2004.

Pallas, V., Aparicio, F., Herranz, M. C., Sanchez-Navarro, J. A., and Scott, S. W. (2013). "The Molecular Biology of Ilarviruses," in Advances in Virus Research (Academic Press Inc.), 139–181. doi:10.1016/B978-0-12-407698-3.00005-3.

Pandey, N., Niranjan, B., Williams, A., Sun, J., Brown, V., Bond, U., et al. (1994). Point Mutations in the Stem-Loop at the 3' End of Mouse Histone mRNA Reduce Expression by Reducing the Efficiency of 3' End Formation. Mol. Cell. Biol. 14, 1709–1720.

Peyret, H., and Lomonossoff, G. P. (2015). When plant virology met Agrobacterium: the rise of the deconstructed clones. Plant Biotechnol. J. 13, 1121–1135. doi:10.1111/PBI.12412.

Prol, F. V., Márquez-Molins, J., Rodrigo, I., López-Gresa, M. P., Bellés, J. M., Gómez, G., et al. (2021). Symptom Severity, Infection Progression and Plant Responses in Solanum Plants Caused by Three

Pospiviroids Vary with the Inoculation Procedure. Int. J. Mol. Sci. 2021, Vol. 22, Page 6189 22, 6189. doi:10.3390/IJMS22126189.

Reichert, V. L., Choi, M., Petrillo, J. E., and Gehrke, L. (2007). Alfalfa mosaic virus coat protein bridges RNA and RNA-dependent RNA polymerase *in vitro*. Virology 364, 214–226. doi:10.1016/J.VIROL.2007.02.026.

Reusken, C. B. E. M., and Bol, J. F. (1996). Structural elements of the 3'-terminal coat protein binding site in alfalfa mosaic virus RNAs. Nucleic Acids Res. 24, 2660. doi:10.1093/NAR/24.14.2660.

Růžička, K., Zhang, M., Campilho, A., Bodi, Z., Kashif, M., Saleh, M., et al. (2017). Identification of factors required for m6A mRNA methylation in Arabidopsis reveals a role for the conserved E3 ubiquitin ligase HAKAI. New Phytol. 215, 157–172. doi:10.1111/nph.14586.

Williams, G. D., Gokhale, N. S., and Horner, S. M. (2019). Regulation of Viral Infection by the RNA Modification N6 -Methyladenosine. Annu. Rev. Virol. 6, 235–253. doi:10.1146/annurev-virology-092818-015559.

Xu, T., Wu, X., Wong, C. E., Fan, S., Zhang, Y., Zhang, S., et al. (2022). FIONA1-Mediated m6A Modification Regulates the Floral Transition in Arabidopsis. Adv. Sci. 2103628, 1–12. doi:10.1002/advs.202103628.

Zaccara, S., Ries, R. J., and Jaffrey, S. R. (2019). Reading, writing and erasing mRNA methylation. Nat. Rev. Mol. Cell Biol. 2019 2010 20, 608–624. doi:10.1038/s41580-019-0168-5.

Chapter III

Evaluation of the effect of *Arabidopsis* m^6A RNA-MTases on Alfalfa Mosaic Virus replication

Abstract

N^6-methyladenosine (m^6A) is a widespread modification on cellular RNAs of different organisms and can impact many cellular processes and pathways. The m^6A abundance and effects are determined by dynamic interactions between its methyltransferases, demethylases, and binding proteins; also called "writers", "erasers" and "readers", respectively. This modification is also present in the genomic RNAs of viruses and transcripts of DNA viruses, and in many cases, it plays an essential role in the biology of the virus. However, most of these studies have been carried out in mammalian viruses, while in plant viruses there are very few studies on the regulatory activity of m^6A during infection cycles. We previously reported the presence of m^6A along the RNAs of AMV, and that suppression of the *Arabidopsis* m^6A-eraser protein, ALKBH9B, increases the abundance of m^6A on the viral genome. Furthermore, the systemic infection capability of the virus was clearly reduced in *alkbh9b* plants, nearly blocking floral stems invasion. Due to the functional relevance of m^6A-levels in AMV-vRNAs, we analyzed the implication in AMV infection *in vivo* of the *Arabidopsis* proteins with m^6A-methyltransferase activity MTA and MTB and the proteins encoded by the AT4G28830 and AT1G78190 genes; putative homolog of human METTL5 and TRMT112, respectively. The results obtained in this work indicate that the loss of function of MTA in *Arabidopsis* ABI3prom:MTA mutant-plants does not interfere positively or negatively in the biology of AMV. This effect was also observed when overexpressing the *Arabidopsis* MTA:MTB and METTL5-*like*:TRMT112-*like* proteins in *N. benthamiana* plants. This raises the possibility that the MTases evaluated here are not responsible for causing the m^6A-modification in the AMV genome; and that, since research on the regulatory activity of m^6A in plant viruses is scarce, there could be other proteins with the capacity to catalyze m^6A not yet identified in the *Arabidopsis* genome.

Keywords: N^6-methyladenosine, RNA covalent modifications, epitranscriptomics, RNA-methyltransferases, plant viruses, alfamovirus.

Introduction

N^6-methyladenosine (m^6A) is the most commonly occurring internal post-transcriptional modification on messenger RNA (mRNA) in eukaryotic cells (Arribas-Hernández and Brodersen, 2020; Zhou et al., 2020; Jiang et al., 2021), and was recently discovered in bacterial (Deng et al., 2015). This chemical modification is involved in multiple processes, including stability (Wang et al., 2014), splicing (Bartosovic et al., 2017), translation (Meyer et al., 2015), structure, export and decay (Yue et al., 2019) and protein/RNA interactions (Liu et al., 2015).

In mammals, the m^6A-mRNA modification is catalyzed co-transcriptionally by a multicomponent m^6A RNA methyltransferase complex (MTC also known as "writers") (Liu et al., 2014; Ping et al., 2014). The heterodimer, composed of METTL3 and METTL14, is the core component of MTC (Huang et al., 2020). Other regulatory subunits of MTC have also been identified, including WTAP, KIAA1429, RBM15, and RBM15B that likely involved in the selective methylation of m^6A-sites (Schwartz et al., 2014; Patil et al., 2016). m^6A is removed by RNA demethylases, "erasers", including FTO and ALKBH5 (Aik et al., 2014; Xu et al., 2014), and it is recognized by the m^6A RNA-binding proteins YTHDF1/2/3, YTHDC1/2 IGF2BP1/2/3 and HNRNPA2B1, also known as "readers" (Luo and Tong, 2014; Wang et al., 2015; Xiao et al., 2016; Jiang et al., 2021). It is yet to be determined whether writer, eraser and reader protein systems exist for m^6A in other types of RNA. To date, it is known that in humans, METTLTRANSFERASE-LIKE 5 (METTL5) bound to the known activator tRNA MTase SUBUNIT 11–2 (TRMT112) and the monomeric protein ZCCHC4 are the enzymes responsible for adding the m^6A-tag on 18S rRNAs and 28S, respectively (Van Tran et al., 2018; Ma et al., 2019; Ren et al., 2019; Pinto et al., 2020; Oerum et al., 2021). Moreover, structured RNAs that contains the sequence UAC(A)GAGAA are methylated by METHYLTRANSFERASE-LIKE 16 (METTL16), which also appears to bind to U6 small nuclear RNAs (snRNAs), pre-RNAs, mature mRNAs, and other non-coding RNAs (ncRNAs) and long non-coding RNAs (lncRNAs) (Pendleton et al., 2017; Shima et al., 2017; Warda et al., 2017; Mendel et al., 2018).

In plants, the catalytic core of the main MTC is formed by two MTA-70 family proteins, METHYLTRANSFERASE A (MTA, AT4G10760) - homolog of METTL3 - (Zhong et al., 2008) and METHYLTRANSFERASE B (MTB, AT4G09980) - homolog of METTl14 - (Růžička et al., 2017). Furthermore, several additional factors have been identified to participate in m^6A-deposition (Arribas-Hernández and Brodersen, 2020). These include FKBP12 interacting protein 37 (FIP37, AT3G54170) - homolog of WTAP - (Zhong et al., 2008; Shen et al., 2016), VIRILIZER (VIR, AT3G05680) - homolog of human KIAA1429 - (Schwartz et al., 2014; Růžička et al., 2017) and the putative ubiquitin E3 ligase (HAKAI, AT5G01160) - homolog of human CBLL1 -. Additionally, it was recently shown that *Arabidopsis* FIONA1 (FIO1, AT2G21070) - homolog of METLL16 - (Pendleton et al., 2017), installs m^6A in U6 snRNA and a small subset of poly(A) RNA (Wang et al., 2022). Contrarily, orthologs of mammal METLL5 and ZCCHC4 have not yet been found in plants (Oerum et al., 2021). Moreover, *Arabidopsis* genome encodes 14 homologs of Alk B family of "erasers" proteins (ALKBH1A-D, ALKBH2, ALKBH6, ALKBH8A-B, ALKBH9A-C and ALKBH10A-B) (Mielecki et al., 2012; Kawai et al., 2014), of which, ALKBH9B and ALKBH10B, have been shown to present m^6A demethylase activity *in vitro* and m^6A-related functions *in vivo* (Duan et al., 2017; Martínez-Pérez et al., 2017). In addition, plants also contain proteins that contain the YTH-domain: eleven YTHDF proteins called: EVOLUTIONARILY CONSERVED C-TERMINAL REGION 1 to 11 (ECT1-11) (Bai, 2022), one classical YTHDC1-type protein (AT4G11970) and one YTHDC-like protein, unusual because it also contains additional folded domains: CLEAVAGE AND POLYADENYLATION SPECIFICITY FACTOR 30 (CPSF30) and the 30-kD subunit involved in pre-mRNA clavage and 3'end formation (Thomas et al., 2012; Bruggeman et al., 2014; Pontier et al., 2019). To date, only ECT2, ECT3 and ECT4 have been described as m^6A-readers, which perform redundant functions in the m^6A-dependent control of developmental timing and leaf morphogenesis (Arribas-Hernández et al., 2018).

m^6A is also present in genomic RNAs of viruses and transcripts of DNA viruses (Manners et al., 2019; Imam et al., 2020). Recent studies of viral epitransciptomics have revealed an

equally important role of m^6A during virus infection (Baquero-Perez et al., 2021); however, there is no global pro- or anti-viral role of m^6A-methylation that can be generalized (Thiel, 2020). In HIV-1, two independent research groups have concluded that METTL3/14 writers promote virus replication, while ALKBH5 and FTO erasers suppress it (Lichinchi et al., 2016; Tirumuru et al., 2016). However, hepatitis C virus (HCV) and Zika virus (ZIKV) infection were positively and negatively regulated, respectively, by siRNA-mediated depletion of the METTL3/14 and FTO (Gokhale et al., 2016; Lichinchi et al., 2016). Furthermore, depletion of YTHDF proteins exhibited a pro-viral effect in ZIKA and HCV (Gokhale et al., 2016; Lichinchi et al., 2016), while in the case of HIV-1, both pro-viral (Kennedy et al., 2016) and anti-viral (Tirumuru et al., 2016) effects have been reported. Then, a global reduced methylation response has also been observed in Influenza A Virus (IAV) and Kaposi sarcoma–associated herpesvirus (KSHV) caused by chemical inhibitor 3DAA or METTL3 knockdown (Courtney et al., 2017; Ye, 2018).

In plant viruses, there are few studies of the regulatory activity of m^6A during the infection cycles. *Nicotiana tabacum* plants infected with Tobacco mosaic virus (TMV) exhibited increased levels of m^6A-mRNAs, in addition, a potential demethylase (orthologue of human ALKBH5) and MTases were induced and repressed, respectively, compared to non-infected plants (Li et al., 2018). Other studies have reported putative AlkB domains in positive single-stranded RNA viruses (+)ssRNA of the families Alphaflexiviridae, Betaflexiviridae and Closteroviridae (Martelli et al., 2007), which have the ability to reverse methylation-induced lesions (van den Born et al., 2008).

Alfalfa mosaic virus (AMV) belongs to the *Bromoviridae* family and, as the rest of the members of this family, its genome consists of three (+)ssRNA (Bujarski et al., 2019). RNA1 and RNA2 encode the replicase subunits (P1 and P2), whereas RNA3 encodes the movement protein (MP) and serves as a template for the synthesis of subgenomic RNA4 (sgRNA4), which encodes the coat protein (CP) (Bol, 2005). AMV contains several m^6A-sites throughout its genome. CP can recruit the host m^6A-demethylase atALKBH9B (orthologue of human ALKBH5) to reduce m^6A levels. This demethylation is a key factor for infection

because the systemic spread of the virus towards flower stems is severely hampered in *Arabidopsis* ALKBH9B knockout (Martínez-Pérez et al., 2017, 2021). Due to the functional relevance of m^6A levels in AMV-vRNAs, we analyzed the implication in AMV infection *in vivo* of the *Arabidopsis* proteins with m^6A-methyltransferase activity MTA and MTB and the proteins encoded by the AT4G28830 and AT1G78190 genes (putative homolog of METTL5 and TRMT112), respectively. Transitory expression of these MTases in *Nicotiana benthamiana* plants, and the subsequent mechanical inoculation of AMV virions suggested that the overexpression of MTA plus MTB and the METTL5-like plus TRMT112-like proteins do not interfere positively or negatively in AMV infection. The non-interference oftMTA in the AMV viral replication was also observed in *Arabidopsis* MTA knockdown plants.

Materials and Methods

Plant growth conditions

N. benthamiana and *Arabidopsis* ecotype Col-0 wild-type (wt) and *mta* (ABI3prom:MTA complemented mta SALK_074069 allele) (Bodi et al., 2012) plants were grown in 6- and 2.5-cm diameter pots, respectively, in a growth chamber at 24°C with a photoperiod of 24°C - 16 h light/20°C - 8 h dark. Plants were mechanically inoculated with purified virions (1 mg/mL) of AMV PV0196 isolate (Plant Virus Collection, DSMZ) in 30 mM sodium phosphate buffer pH 7.0 (Martínez-Pérez et al., 2017).

Analysis of proteins homologous to human METTL5, TRMT122 and ZCCHC4 in *Arabidpsis*

A Position-Specific Iterated (PSI) was carried out in the Basic Local Alignment Search Tool (BLAST) (Altschul et al., 1997) with the amino acid (aa) sequence of human METTL5 (Uniprot: Q9NRN9), TRMT122 (Uniprot: Q9UI30) and ZCCHC4 (Uniprot: Q9H5U6). The *Arabidopsis* accessions with the highest query cover and percent identity were selected as

putative homologs. Then, a sequence alignment was performed with the ClustalW tool (Hung and Weng, 2016) to identify the level of similarity and the conserved domains.

Recombinant plasmids for transient expression

Full-length of MTA (AT4G10760) and MTB (AT4G09980) ORFs were cloned between the cauliflower mosaic virus 35S promoter and the terminator sequence of the *Solanum tuberosum* proteinase inhibitor II gene in the binary vector pMOG800 (Genovés et al., 2006). The 3' ends of these MTases were fused in frame to the human influenza hemagglutinin (HA) tag. A similar procedure was performed for METTL5-like and TRMT112-like, but without the HA-tag. The resulting pMOG800 plasmids were called: p/MTA, p/MTB, p/METTL5-like and p/TRMT112-like.

Agrobacterium tumefaciens (strain C58) transformed with the corresponding binary vector, was grown overnight in a shaking incubator at 28°C in Luria-Bertani (LB) medium supplemented with the appropriate antibiotic. p/MTA plus p/MTB, and p/METTL5-like plus p/TRMT112-like were used at an optical density at 600 nm (OD600) of 0.6 each, in infiltration solution (10 mM MES, pH 5.5, and 10 mM MgCl2) and infiltrated in 2-week-old *N. benthamiana* leaves. The 35S:mCherry:Popit expression cassette into pMOG800 was used as MOCK. Western blot analysis using anti-HA (Roche) antibodies were conducted following the manufacturer's recommendations to corroborate the expression of HA:MTA and HA:MTB proteins.

Virus inoculation and Viral RNA Analysis

In *N. benthamiana* plants, the same agroinfiltrated leaves were mechanically inoculated with AMV virions 12 hours post-agroinfiltration (hpa). The detection of vRNAs was performed 3 days post-agroinfiltration (3 dpa) on these same leaves. *Arabidopsis* plants were inoculated when they were 20 days old. The upper non-inoculated leaves were analyzed at 11 days post-inoculation (dpi). Total RNA was extracted using EXTRAzol® (BLIRT S.A.). AMV vRNAs was carried out by Northern blot analysis as described in (Aparicio et al., 2003), using a digoxigenin-labeled probe to detect the multipartite genome of AMV (DigAMV). vRNAs

detection was conducted using CSPD chemiluminescent substrate. Densitometry was performed using ImageJ 1.53c. Statistical significances at the 95% confidence level (α = 0.05) were determined using Minitab 18 ($P < 0.05$) through one-way analysis of variance and Fisher's least significant difference (LSD) test for multiple comparisons.

Results and Discussion

In plants, the m^6A-catalitic core is formed by two proteins of the MTA-70 family, MTA and MTB. Other regulatory subunits associated with the m^6A-writer complex have also been identified, including FIP37 (AT3G54170, WTAP homolog), VIRILIZER (AT3G05680, KIAA1429 homolog) and homologue of human HAKAI (AT5G01160) (Zhong et al., 2008; Shen et al., 2016; Růžička et al., 2017). *Arabidopsis* knockdown plants for *mta*, *mtb*, *fip37* and *virilizer* showed reduced m^6A levels in mRNAs associated with different developmental defects such as atypical organ morphology, defective trichome branching, loss of apical dominance, malfunctioning gravitropic responses and abnormal development of lateral roots and vasculature (Vespa et al., 2004; Bodi et al., 2012; Růžička et al., 2017).

In addition to m^6A roles in regulating biological cellular processes, this modification is also implicated in viral infections. This has caused that in recent years the elucidation of the epitranscriptome derived from m^6A in viral infections is one of the main focuses of attention (Tan and Gao, 2018; Dang et al., 2019; Wu et al., 2019). In general, the most common approach to study m^6A- epitranscriptome of virus and cells is to manipulate the m^6A *writer*, *eraser*, and/or *reader* machinery (depletion or overexpression) and then, map the m^6A-sites along the RNAs (Linder and Jaffrey, 2019b). However, unlike in mammals, there are very few examples of m^6A involvement in plant viruses (Arribas-Hernández and Brodersen, 2020). For example, TMV-infected *Nicotiana tabacum* plants exhibited increased levels of m^6A-mRNAs and additionally, expression of a potential demethylase (orthologue of human ALKBH5) and MTases was induced and repressed, respectively, compared to non-infected plants (Li et al., 2018). In *Solanum tuberosum* plants exposed to single and combined treatments (PVY infection and heat) generate drastic changes in the expression of many

lncRNAs, RNA methylation and alternative splicing (Glushkevich et al., 2022). In virus-susceptible rice plants, it was found that m^6A-levels increased in response to infection by Rice black-streaked dwarf virus (RBSDV) and Rice stripe virus (RSV), and that m^6A-methylation is mainly associated with genes that are not actively expressed in virus-infected rice plants (Zhang et al., 2021b).

Due to the functional relevance of m^6A-levels in AMV vRNAs, we decided to evaluate whether the loss of cellular methylation capability interferes with the infectious cycle of AMV. For this, we used *mta Arabidopsis* plants (ABI3prom:MTA complemented mta SALK_074069 allele) (Bodi et al., 2012). We decided to work with this mutant-line because the null mutation in MTA caused embryonic lethality (Zhong et al., 2008). The ABI3prom:MTA line was developed by complementing an MTA-knockout mutant with an MTA coding sequence under the control of the ABI3-promoter. This allows for high expression of MTA-protein as well as complete m^6A-methylation during the embryonic stage, but very low activity after germination (Bodi et al., 2012). This loss of MTA function during post-embryonic development gives as a result reduced root growth and aberrant gravitropic responses in plants (see Figure 6 in Růžička et al., 2017). In this context, northern blot analysis using DigAMV showed an equal accumulation of AMV vRNAs in wild-type and ABI3prom:MTA plants (Figure 1 A & B), indicating that viral replication is not affected in *mta* plants.

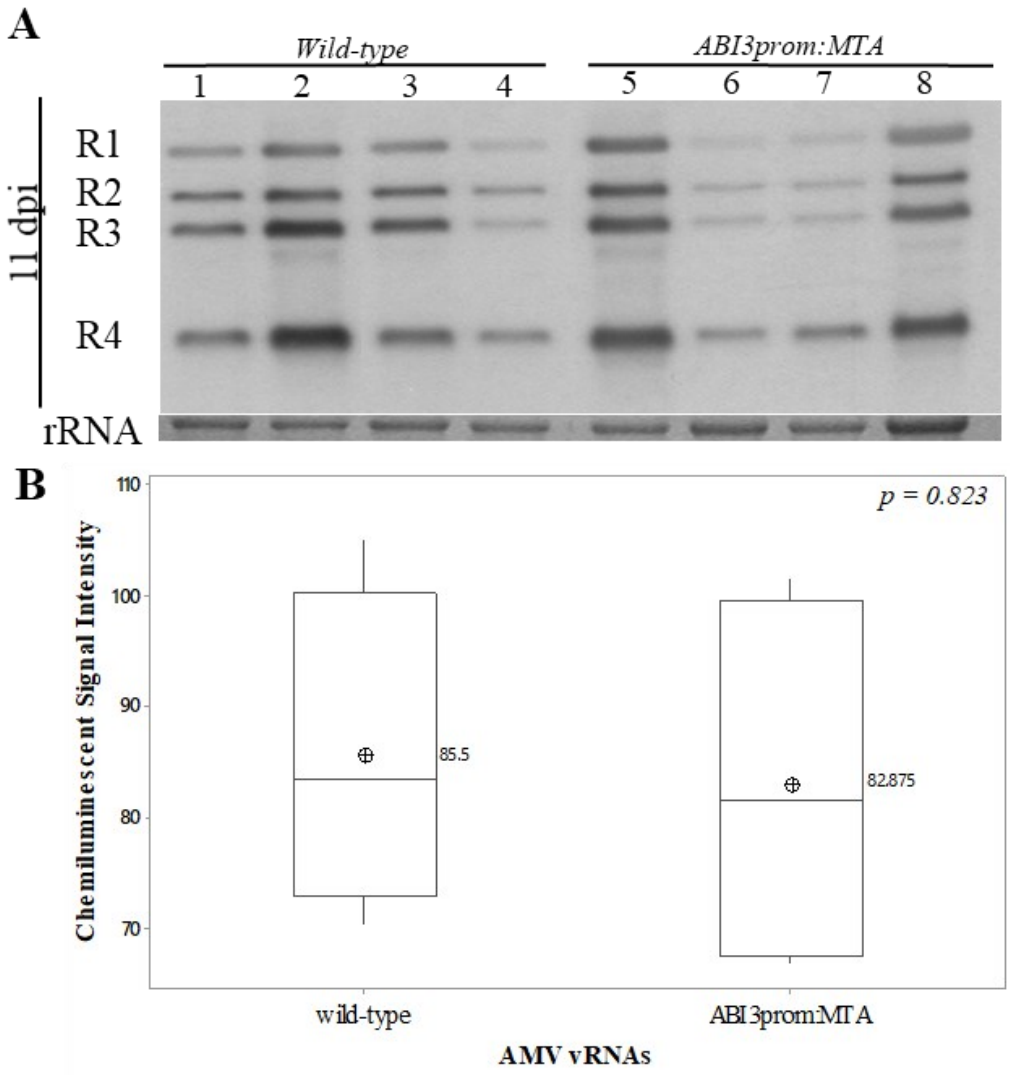

Figure 1. AMV-vRNA analysis in *Arabidopsis* wt and ABI3prom:MTA plants. (a) Representative Northern blots assays from non-inoculated leaves at 11 dpi. Each lane represents an individual plant. Positions of the vRNAs are indicated on the left. Ethidium bromide of ribosomal RNAs were used as RNA loading controls. (B) Boxplots of the densitometric analysis of AMV vRNA's accumulation. The lower and upper limits of the boxes are plotting the min and max values, respectively, whereas the lines dividing them represent the median values. Points inside boxes represent the mean from the three replicates. $P < 0.05$ indicates statistical significance.

Next, we evaluated how the overexpression of MTA would affect to the AMV infection cycle. Since there are no mutant or transgenic *Arabidopsis* plants that overexpress MTA, we decided to co-agroinfiltrate this MTase with MTB protein in *N. benthamiana* to transiently

express the m^{6}A-catalitic core. These agroinfiltrated plants were subsequently inoculated with AMV and viral accumulation was analyzed by northern blot. As shown in Figure 2, no significant differences in AMV accumulation were found with respect to MOCK (Figure 2 A & B). MTA and MTB expression were corroborated by western blot (Figure 2 C). Overall, our results suggest that the AMV infection cycle would not be affected by the suppression of MTA, nor by the overexpression of the MTA-MTB complex.

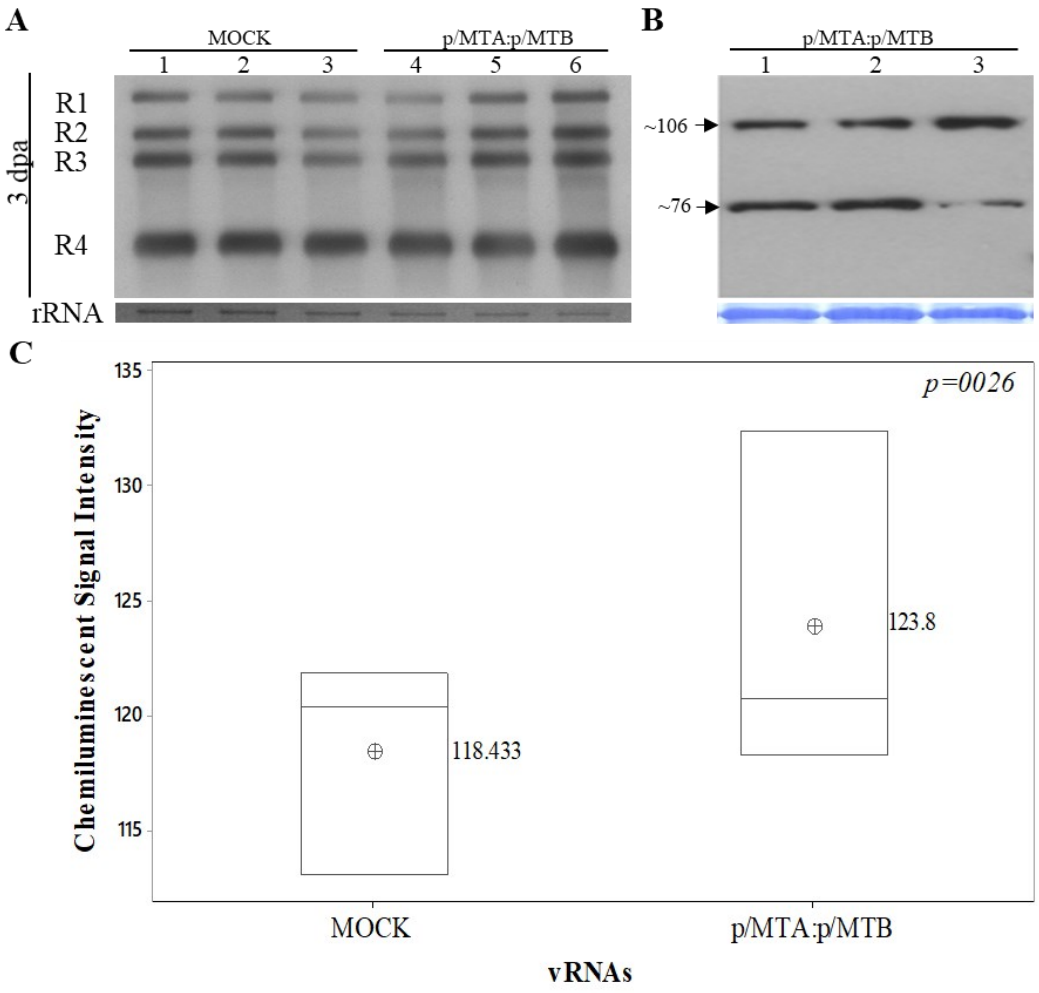

Figure 2. AMV-vRNA analysis in *N. benthamiana* plants agroinfiltrated with MOCK and p/MTA plus p/MTB. (a) Representative Northern blots assays from inoculated leaves of *N. benthamiana* plants at 3 dpa. Each lane represents an individual plant. Positions of the vRNAs are indicated on the left. Ethidium bromide of ribosomal RNAs were used as RNA loading controls. (B) Western blot assays to confirm protein expression of co-infiltrated constructs of atMTA plus atMTB (line 1 to 3). The approximate size of the proteins evaluated is

shown on the left in kDa. (C) Boxplots of the densitometric analysis of AMV vRNA's accumulation. The lower and upper limits of the boxes are plotting the min and max values, respectively, whereas the lines dividing them represent the median values. Points inside boxes represent the mean from the three replicates. $P < 0.05$ indicates statistical significance.

On the other hand, taking advantage of the recent discovery of METTL5 (Q9NRN9) and ZCCHC4 (Q9H5U6) m^6A-writers in humans (Oerum et al., 2021), we decided to search putative homologs of these MTases in *Arabidopsis* for evaluation in AMV infections. We defined as "selection criteria" the proteins that presented the highest percentage of their aligned sequence (query cover), as well as identical bases (identity percentage), in relation to the sequence in reference. Also, we performed a sequence alignment to identify the level of similarity and conserved domains (Altschul et al., 1997). PSI-BLAST analyzes showed a potential protein-homolog for hsMETLL5 (AT4G28830: query cover: 97% and ident percentage: 54.37%), while for hsZCCHC4 no protein with significant similarity was found. For this reason, we decided to continue our study only with the putative hsMETTL5-homolog protein.

It has been reported that hsMETTL5 contains the three m^6A RNA-methyltransferase loops that surround the active site pocket: (i) the active site loop (ASL: $_{16}$V to T_{31}), (ii) the substrate binding loop (SBL: $_{185}$D to D_{199}), rich in positively charged and hydrophobic residues ($_{190}$YKFHKKK$_{196}$), which are associated with rRNA-binding, and (iii) the catalytic loop (CL: $_{126}$N to G_{136}) that contains the catalytic $_{126}$NPPF$_{129}$ motif (Van Tran et al., 2019). Interestingly, these three regions are also strongly conserved in the protein encoded by AT4G28830, especially the rRNA-binding and the catalytic motifs (Figure 3A).

A

```
hsMETLL5        MKKVRLKELESRLQQVDGFEKPKLLLEQYPTRPHIAACMLYTIHNTYDDIENKVVADLGC
AT4G28830       ---MKLKQLEGLLGDLEQFSNPKVEFEQYPTGPHIASRMLFTAENSYGDITDKVVADFGC
                   ::**:**. * ::: *.:**: :***** **** : **:* .*:*.** :*****:**

hsMETLL5        GCGVLSIGTAMLGAGLCVGFDIDEDALEIFNRNAEEFELTNIDMVQCDVCLLSNRMSKSF
AT4G28830       GCGTLSAAAALLDAASVIGFDIDPESLETATLNAEELEVE-IDFVQCDITKLELKG-LIV
                ***.** .:*:*.*.  :***** ::**  . ****:*:  **:****:  *. :    .

hsMETLL5        DTVIMNPPFGTKNNKGTDMAFLKTALEMARTAVYSLHKSSTREHVQKKAAEWK--IKIDI
AT4G28830       DTVVMNPPFGTRK-KGADMEFLSAAMKVASKAVYSLHKTSTREHIKRAALRDFNAKSAEV
                ***:*******:: **:** **.:*:::* .*******:*****::: * .     . ::

hsMETLL5        IAELRYDLPASYKFHKKKSVDIEVDLIRFSF---
AT4G28830       ICELRYDLPKLYKFHKRKEVDIAVDLWRFEPRQN
                *.*******  *****:*.*** *** **.
```

B

```
hsTRMT112        MKLLTHNLLSSHVRGVGSRGFPLRLQATEVRICPVEFNPNFVARMIPKVEWSAFLEAADN
AT1G78190        MRLIVHNMLSCNIKGVVNK-FPLRIEAEKVTVKEVDFNPDFLRYMFAKIDWKALVDGARS
                 *:*:.**:**.:::** .: ****::* :* :  *:***:*:  *:.*::*.*:::.* .

hsTRMT112        LRLIQVPKGP--VEGYEENEEFLRTMHHLLLEVEVIEGTLQCPESGRMFPISRGIPNMLL
AT1G78190        MEYTELPDNAPDTTTLESDETFLRKFHHALLELHLEEGSLVCPETGRKFSVSKGIPNMLL
                 :.  ::*...  .   *.:* ***.:** ***:.: **:* ***:** *.:*:*******

hsTRMT112        SEEETES
AT1G78190        HEDEV--
                  *:*.
```

Figure 3. Protein alignment using ClustalW. (A) hsMETTL5:AT4G28830 alignment. The m^6A RNA-methyltransferase loops of hsMETTL5 are shown in: grey (CL), green (SBL) and cyan (ASL). The underlined nucleotides in CL and SBL corresponding to the catalytic and rRNA-binding motifs. The amino acids underlined in red corresponds to the binding sites with hsTRMT112. (B) hsTRMT112:AT1G78190 alignment. In red, the aa involved in METTL5-binding. Asterisk, colon and dot symbols corresponds to: indetic aa, conserved substitution of aa and semi-conserved substitution of aa, respectively.

On the other hand, the catalytic activity of hsMETTL5 has been reported to be increased ~100-fold in the presence of hsTRMT112 (Chen et al., 2020). This increased metabolic stability of METTL5 in cells is due to: TRMT112 hides a large hydrophobic patch on METTL5 improving its solubility; and increases the affinity of METTL5 with the SAM cofactor (Van Tran et al., 2019). For this reason, we also decided to search for a homolog protein of hsTRM112 in *Arabidopsis* using the PSI-BLAST tool. This analysis showed a possible protein-homolog for hsMETLL5 (AT1G78190: query cover: 97% and ident percentage: 43.55%).

The human METTL5:TRMT112 binding interface is characterized by the presence of a large central hydrophobic core composed of METTL5 residues V_{54}, L_{76}, V_{78}, F_{80}, M_{104}, V_{105}, M_{116}, and F_{120} and L_4, L_8, L_9, V_{35}, F_{41}, M_{45}, L_{89}, I_{113}, P_{114}, M_{116} and L_{117} of TRMT112 (Van Tran et al., 2019). It was observed that the amino acids that make up the binding interface in the protein encoded by AT4G28830 (putative homolog of hsMETTL5) are: 37.5% identical, 25% conserved substitutions, and 12.5% semi-conserved substitutions. The remaining 25% of the aa did not show any similarity with the referenced amino acid (Figure 3A). Meanwhile, in the protein encoded by AT1G78190 (putative homolog of hsTRMT112) 81.9% of the aa are identical, and the remaining 18.2% are conserved substitutions (Figure 3B). Based on these results, we decided to assess the effect of the AT4G28830 and AT1G78190 -encoded proteins as putative homologs of hsMETTL5 and hsTRMT112, respectively.

For this, the CDS of AT4G28830 (atMETTL5-*like*) and AT1G78190 (atTRMT112-*like*) genes were transiently co-expressed in *Nicotiana benthamiana* plants. To avoid modifying and/or altering the stability/integrity of these proteins, which are 24 and 14 KDa, respectively, we decided not to add any tags to their polypeptide sequences. Northern blot analysis showed no significant differences in AMV replication between plants agroinfiltrated with MOCK and p/ atMETTL5-like plus p/ atTRMT112-like (Figure 4); suggesting that the enrichment of this MTase-complex does not interfere with AMV replication.

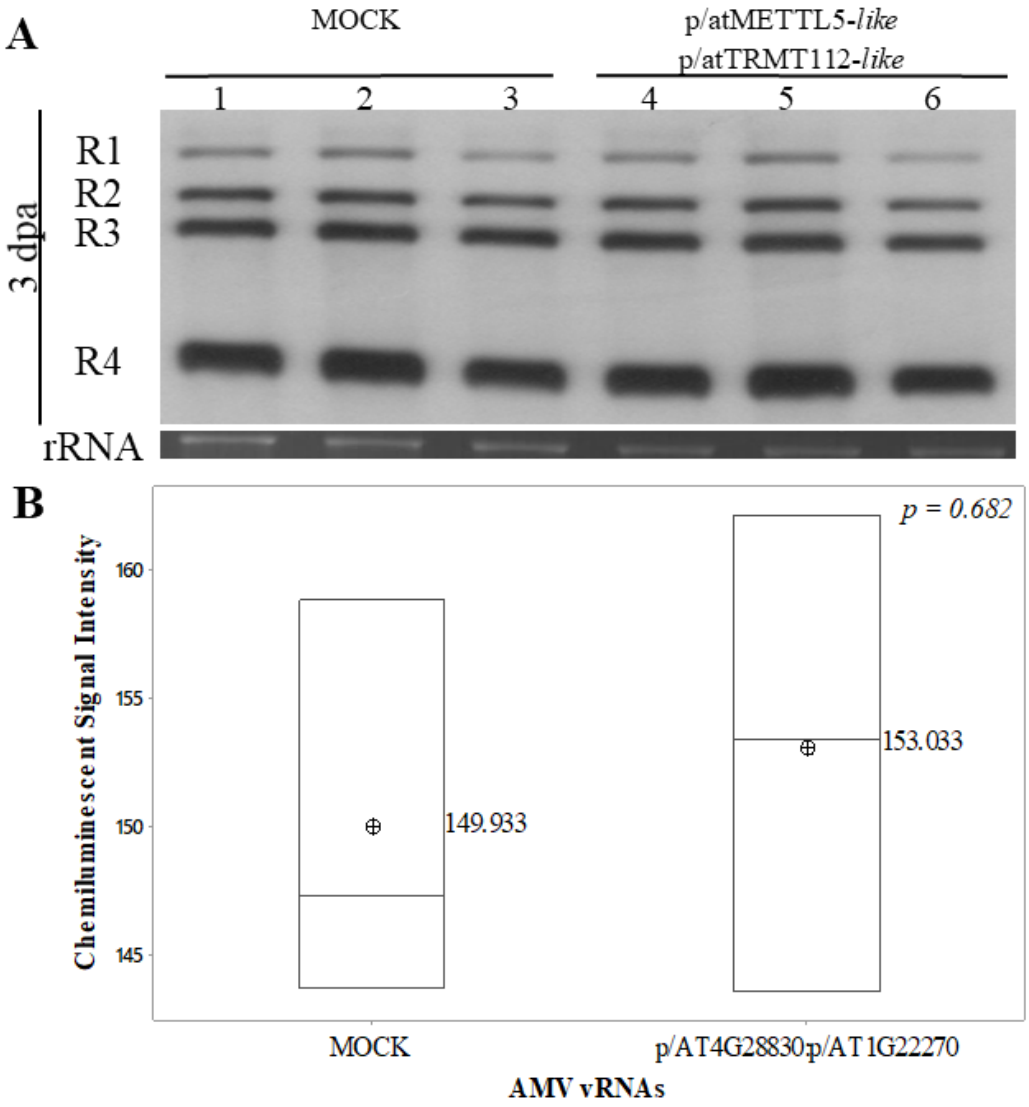

Figure 4. AMV-vRNA analysis in *N. benthamiana* plants agroinfiltrated with MOCK and p/atMETTL5-like plus p/atTRMT112-like. (A) Representative Northern blots assays from inoculated leaves of *N. benthamiana* plants at 3 dpa. Each lane represents an individual plant. Positions of the vRNAs are indicated on the left. Ethidium bromide of ribosomal RNAs were used as RNA loading controls. (B) Boxplots of the densitometric analysis of AMV vRNA's accumulation. The lower and upper limits of the boxes are plotting the min and max values, respectively, whereas the lines dividing them represent the median values. Points inside boxes represent the mean from the three replicates. $P < 0.05$ indicates statistical significance.

The proviral, antiviral or neutral effect of m^6A depends on: (i) the type of virus, (ii) the stage of the life cycle in which the virus is found and (iii) the type of cell used (Williams et al., 2019; Lisy et al., 2021). The results presented here suggest that the methylation complex to

which MTA belongs would not be responsible for causing the m^{6}A-modification in the AMV genome.

Previous studies, using the agroinfiltration methodology, have determined that the transient expression of MTA from *Arabidopsis* in tobacco plants not only regulates the m^{6}A-mark in mRNA, but also positively mediates the maturation of microRNAs (miRNA) (Bhat et al., 2019). In that study, it was determined by northern blot assay that miR393b, a miRNA involved in the regulation of the auxin response, exhibited ~2.3-fold increase when MTA was agroinfiltrated, whereas this effect was largely abolished when a catalytically inactive version of MTA was transiently expressed (see Figure 5c in Bhat et al., 2019). This result suggests that an MTA enzymatically functional version can be expressed by agroinfiltration in plants of the genus *Nicotiana*. In our experiment, although western blot results showed the correct expression of MTA and MTB (Figure 2 B), the overall m^{6}A levels on mRNAs of agroinfiltrated plants or in AMV genome were not determined. Thus, it might be possible that the overexpressed MTA-MTB complex was not functional. Furthermore, we also found that the AMV replicative cycle was not affected in an *Arabidopsis* line transformed with the construct ABI3prom:MTA. We cannot rule out that some residual expression of MTA in these plants gives rise to sufficient methylation activity level to maintain viral yield unaltered.

On the other hand, the neutral effect of *Arabidopsis* METTL5-*like*:TRMT112-*like* complex on AMV infection may be due to other different reasons. First, despite the functional similarity between the amino acid sequences of human METTL5 and TRMT112 with AT4G28830 and AT1G78190, respectively, it is unknown whether these *Arabidopsis* proteins interact with each other, and whether AT4G28830 exhibits m^{6}A-writing activity. Second, the proteins encoded by AT4G28830 and AT1G78190 have a size of 24 and 14 kDa, respectively. To avoid possible structural alterations in the folding of these proteins, we did not include any recognition tag; therefore, we cannot guarantee the correct expression of these proteins. Third, it has been reported that the non-generalization of the proviral or antiviral role of m^{6}A in viral infections could be attributed to the intracellular localization of vRNAs and thus the availability of host proteins that respond to m^{6}A-RNAs (Tan and Gao,

2018). In this context, another possible explanation might be that the AMV viral replication complex (formed by P1 and P2) associates with the tonoplast membrane during the infection (Heijden et al., 2001; Ibrahim et al., 2012), while the human METTL5:TRMT112 complex is located in the nucleolus (Van Tran et al., 2019).

Finally, it has been recently shown that *Arabidopsis* FIONA1 (FIO1, AT2G21070) - homolog of METLL16 - (Pendleton et al., 2017), installs m^6A in a small subset of poly(A) RNAs and at the UAC<u>A</u>GAGAA motif of U6 snRNA (Wang et al., 2022) (the putative adenosine target for m^6A deposition is underlined). Interestingly, at least two C<u>A</u>GAGAA motifs are present in the negative strand of the RNA1 and RNA2 of several AMV isolates. Thus, there might be other proteins asides of MTA-MTB complex with the capacity to install m^6A in AMV genome. Further studies are necessary to identify the writer-complex which mediate m^6A deposition in the AMV genome.

References

Aik, W., Scotti, J. S., Choi, H., Gong, L., Demetriades, M., Schofield, C. J., et al. (2014). Structure of human RNA N6-methyladenine demethylase ALKBH5 provides insights into its mechanisms of nucleic acid recognition and demethylation. Nucleic Acids Res. 42, 4741–4754. doi:10.1093/nar/gku085.

Altschul, S. F., Madden, T. L., Schäffer, A. A., Zhang, J., Zhang, Z., Miller, W., et al. (1997). Gapped BLAST and PSI-BLAST: A new generation of protein database search programs. Nucleic Acids Res. 25, 3389–3402. doi:10.1093/nar/25.17.3389.

Aparicio, F., Vilar, M., Perez-Payá, E., and Pallás, V. (2003). The coat protein of prunus necrotic ringspot virus specifically binds to and regulates the conformation of its genomic RNA. Virology 313, 213–223. doi:10.1016/S0042-6822(03)00284-8.

Arribas-Hernández, L., Bressendorff, S., Hansen, M. H., Poulsen, C., Erdmann, S., and Brodersen, P. (2018). An m6A-YTH module controls developmental timing and morphogenesis in arabidopsis. Plant Cell 30, 952–967. doi:10.1105/TPC.17.00833.

Arribas-Hernández, L., and Brodersen, P. (2020). Occurrence and functions of m6A and other covalent modifications in plant mRNA. Plant Physiol. 182, 79–96. doi:10.1104/pp.19.01156.

Bai, B. (2022). An update on principles of m6A targeting. Trends Plant Sci. 27, 224–226. doi:10.1016/J.TPLANTS.2021.12.007.

Baquero-Perez, B., Geers, D., and Díez, J. (2021). From A to m6A: The Emerging Viral Epitranscriptome. Viruses 2021, Vol. 13, Page 1049 13, 1049. doi:10.3390/V13061049.

Bartosovic, M., Molares, H. C., Gregorova, P., Hrossova, D., Kudla, G., and Vanacova, S. (2017). N6-methyladenosine demethylase FTO targets pre-mRNAs and regulates alternative splicing and 3′-end processing. Nucleic Acids Res. 45, 11356–11370. doi:10.1093/NAR/GKX778.

Bhat, S. S., Bielewicz, D., Grzelak, N., Gulanicz, T., Bodi, Z., Szewc, L., et al. (2019). mRNA adenosine methylase (MTA) deposits m6A on pri-miRNAs to modulate miRNA biogenesis in Arabidopsis thaliana. bioRxiv. doi:10.1101/557900.

Bodi, Z., Zhong, S., Mehra, S., Song, J., Graham, N., Li, H., et al. (2012). Adenosine methylation in Arabidopsis mRNA is associated with the 3′ end and reduced levels cause developmental defects. Front. Plant Sci. 3. doi:10.3389/fpls.2012.00048.

Bol, J. F. (2005). Replication of Alfamo- and Ilarviruses: Role of the Coat Protein. Annu. Rev. Phytopathol. 43, 39–62. doi:10.1146/annurev.phyto.43.101804.120505.

Bruggeman, Q., Garmier, M., de Bont, L., Soubigou-Taconnat, L., Mazubert, C., Benhamed, M., et al. (2014). The polyadenylation factor subunit CLEAVAGE AND POLYADENYLATION SPECIFICITY FACTOR30: A key factor of programmed cell death and a regulator of immunity in arabidopsis. Plant Physiol. 165, 732–746. doi:10.1104/PP.114.236083.

Bujarski, J., Gallitelli, D., García-Arenal, F., Pallás, V., Palukaitis, P., Krishna Reddy, M., et al. (2019). ICTV virus taxonomy profile: Bromoviridae. J. Gen. Virol. 100, 1206–1207. doi:10.1099/jgv.0.001282.

Chen, H., Liu, Q., Yu, D., Natchiar, K., Zhou, C., Hsu, C., et al. (2020). METTL5, an 18S rRNA-specific m6A methyltransferase, modulates expression of stress response genes. bioRxiv, 2020.04.27.064162. doi:10.1101/2020.04.27.064162.

Courtney, D. G., Kennedy, E. M., Dumm, R. E., Bogerd, H. P., Tsai, K., Heaton, N. S., et al. (2017). Epitranscriptomic Enhancement of Influenza A Virus Gene Expression and Replication. Cell Host Microbe 22, 377-386.e5. doi:10.1016/J.CHOM.2017.08.004/ATTACHMENT/54EE395B-3B1F-415B-99BE-D47E9445EE6D/MMC1.PDF.

Dang, W., Xie, Y., Cao, P., Xin, S., Wang, J., Li, S., et al. (2019). N6-methyladenosine and viral infection. Front. Microbiol. 10, 417. doi:10.3389/fmicb.2019.00417.

Deng, X., Chen, K., Luo, G.-Z., Weng, X., Ji, Q., Zhou, T., et al. (2015). Widespread occurrence of N 6-methyladenosine in bacterial mRNA. Nucleic Acids Res. 43, 6557–6567. doi:10.1093/nar/gkv596.

Duan, H. C., Wei, L. H., Zhang, C., Wang, Y., Chen, L., Lu, Z., et al. (2017). ALKBH10B is an RNA N6-methyladenosine demethylase affecting arabidopsis floral transition. Plant Cell 29, 2995–3011. doi:10.1105/tpc.16.00912.

Genovés, A., Navarro, J. A., and Pallás, V. (2006). Functional analysis of the five melon necrotic spot virus genome-encoded proteins. J. Gen. Virol. 87, 2371–2380. doi:10.1099/VIR.0.81793-0/CITE/REFWORKS.

Glushkevich, A., Spechenkova, N., Fesenko, I., Knyazev, A., Samarskaya, V., Kalinina, N. O., et al. (2022). Transcriptomic Reprogramming, Alternative Splicing and RNA Methylation in Potato (Solanum tuberosum L.) Plants in Response to Potato Virus Y Infection. Plants 11, 635. doi:10.3390/PLANTS11050635.

Gokhale, N. S., McIntyre, A. B. R., McFadden, M. J., Roder, A. E., Kennedy, E. M., Gandara, J. A., et al. (2016). N6-Methyladenosine in Flaviviridae Viral RNA Genomes Regulates Infection. Cell Host Microbe 20, 654–665. doi:10.1016/j.chom.2016.09.015.

Heijden, M. W. Van Der, Carette, J. E., Reinhoud, P. J., Haegi, A., and Bol, J. F. (2001). Alfalfa Mosaic Virus Replicase Proteins P1 and P2 Interact and Colocalize at the Vacuolar Membrane. J. Virol. 75, 1879. doi:10.1128/JVI.75.4.1879-1887.2001.

Huang, H., Weng, H., and Chen, J. (2020). The Biogenesis and Precise Control of RNA m6A Methylation. Trends Genet. 36, 44–52. doi:10.1016/j.tig.2019.10.011.

Hung, J. H., and Weng, Z. (2016). Sequence Alignment and Homology Search with BLAST and ClustalW. Cold Spring Harb. Protoc. 2016, pdb.prot093088. doi:10.1101/PDB.PROT093088.

Ibrahim, A., Hutchens, H. M., Berg, R. H., and Loesch-Fries, L. S. (2012). Alfalfa mosaic virus replicase proteins, P1 and P2, localize to the tonoplast in the presence of virus RNA. doi:10.1016/j.virol.2012.08.018.

Imam, H., Kim, G.-W., and Siddiqui, A. (2020). Epitranscriptomic(N6-methyladenosine) Modification of Viral RNA and Virus-Host Interactions. Front. Cell. Infect. Microbiol. 0, 730. doi:10.3389/FCIMB.2020.584283.

Jiang, X., Liu, B., Nie, Z., Duan, L., Xiong, Q., Jin, Z., et al. (2021). The role of m6A modification in the biological functions and diseases. Signal Transduct. Target. Ther. 2021 61 6, 1–16. doi:10.1038/s41392-020-00450-x.

Kawai, Y., Ono, E., and Mizutani, M. (2014). Evolution and diversity of the 2-oxoglutarate-dependent dioxygenase superfamily in plants. Plant J. 78, 328–343. doi:10.1111/tpj.12479.

Kennedy, E. M., Bogerd, H. P., Kornepati, A. V. R., Kang, D., Ghoshal, D., Marshall, J. B., et al. (2016). Posttranscriptional m6A Editing of HIV-1 mRNAs Enhances Viral Gene Expression. Cell Host Microbe 19, 675–685. doi:10.1016/J.CHOM.2016.04.002.

Li, Z., Shi, J., Yu, L., Zhao, X., Ran, L., Hu, D., et al. (2018). N 6 -methyl-adenosine level in Nicotiana tabacum is associated with tobacco mosaic virus. Virol. J. 15. doi:10.1186/S12985-018-0997-4.

Lichinchi, G., Gao, S., Saletore, Y., Gonzalez, G. M., Bansal, V., Wang, Y., et al. (2016). Dynamics of the human and viral m(6)A RNA methylomes during HIV-1 infection of T cells. Nat. Microbiol. 1, 16011. doi:10.1038/nmicrobiol.2016.11.

Linder, B., and Jaffrey, S. R. (2019). Discovering and Mapping the Modified Nucleotides That Comprise the Epitranscriptome of mRNA. Cold Spring Harb. Perspect. Biol. 11. doi:10.1101/CSHPERSPECT.A032201.

Lisy, S., Rothamel, K., and Ascano, M. (2021). RNA Binding Proteins as Pioneer Determinants of Infection: Protective, Proviral, or Both? Viruses 2021, Vol. 13, Page 2172 13, 2172. doi:10.3390/V13112172.

Liu, J., Yue, Y., Han, D., Wang, X., Fu, Y., Zhang, L., et al. (2014). A METTL3-METTL14 complex mediates mammalian nuclear RNA N6-adenosine methylation. Nat. Chem. Biol. 10, 93–95. doi:10.1038/nchembio.1432.

Liu, N., Dai, Q., Zheng, G., He, C., Parisien, M., and Pan, T. (2015). N6 -methyladenosine-dependent RNA structural switches regulate RNA-protein interactions. Nature 518, 560–564. doi:10.1038/NATURE14234.

Luo, S., and Tong, L. (2014). Molecular basis for the recognition of methylated adenines in RNA by the eukaryotic YTH domain. Proc. Natl. Acad. Sci. U. S. A. 111, 13834–13839. doi:10.1073/PNAS.1412742111.

Ma, H., Wang, X., Cai, J., Dai, Q., Natchiar, S. K., Lv, R., et al. (2019). N 6-Methyladenosine methyltransferase ZCCHC4 mediates ribosomal RNA methylation. Nat. Chem. Biol. 15, 88–94. doi:10.1038/S41589-018-0184-3.

Manners, O., Baquero-Perez, B., and Whitehouse, A. (2019). m6A: Widespread regulatory control in virus replication. Biochim. Biophys. Acta. Gene Regul. Mech. 1862, 370. doi:10.1016/J.BBAGRM.2018.10.015.

Martelli, G. P., Adams, M. J., Kreuze, J. F., and Dolja, V. V. (2007). Family Flexiviridae: A Case Study in Virion and Genome Plasticity. http://dx.doi.org/10.1146/annurev.phyto.45.062806.094401 45, 73–100. doi:10.1146/ANNUREV.PHYTO.45.062806.094401.

Martínez-Pérez, M., Aparicio, F., López-Gresa, M. P., Bellés, J. M., Sánchez-Navarro, J. A., and Pallás, V. (2017). Arabidopsis m6A demethylase activity modulates viral infection of a plant virus and the m6A

abundance in its genomic RNAs. Proc. Natl. Acad. Sci. U. S. A. 114, 10755–10760. doi:10.1073/pnas.1703139114.

Martínez-Pérez, M., Gómez-Mena, C., Alvarado-Marchena, L., Nadi, R., Micol, J. L., Pallas, V., et al. (2021). The m6A RNA Demethylase ALKBH9B Plays a Critical Role for Vascular Movement of Alfalfa Mosaic Virus in Arabidopsis. Front. Microbiol. 12. doi:10.3389/FMICB.2021.745576.

Mendel, M., Chen, K. M., Homolka, D., Gos, P., Pandey, R. R., McCarthy, A. A., et al. (2018). Methylation of Structured RNA by the m6A Writer METTL16 Is Essential for Mouse Embryonic Development. Mol. Cell 71, 986-1000.e11. doi:10.1016/j.molcel.2018.08.004.

Meyer, K. D., Patil, D. P., Zhou, J., Zinoviev, A., Skabkin, M. A., Elemento, O., et al. (2015). 5′ UTR m6A Promotes Cap-Independent Translation. Cell 163, 999–1010. doi:10.1016/J.CELL.2015.10.012.

Mielecki, D., Zugaj, D. Ł., Muszewska, A., Piwowarski, J., Chojnacka, A., Mielecki, M., et al. (2012). Novel AlkB Dioxygenases—Alternative Models for In Silico and *In vivo* Studies. PLoS One 7, e30588. doi:10.1371/journal.pone.0030588.

Oerum, S., Meynier, V., Catala, M., and Tisne, C. (2021). A comprehensive review of m6A/m6Am RNA methyltransferase structures. Nucleic Acids Res. 49, 7239–7255. doi:10.1093/NAR/GKAB378.

Patil, D. P., Chen, C. K., Pickering, B. F., Chow, A., Jackson, C., Guttman, M., et al. (2016). m6A RNA methylation promotes XIST-mediated transcriptional repression. Nat. 2016 5377620 537, 369–373. doi:10.1038/nature19342.

Pendleton, K. E., Chen, B., Liu, K., Hunter, O. V., Xie, Y., Tu, B. P., et al. (2017). The U6 snRNA m6A Methyltransferase METTL16 Regulates SAM Synthetase Intron Retention. Cell 169, 824-835.e14. doi:10.1016/J.CELL.2017.05.003.

Ping, X. L., Sun, B. F., Wang, L., Xiao, W., Yang, X., Wang, W. J., et al. (2014). Mammalian WTAP is a regulatory subunit of the RNA N6-methyladenosine methyltransferase. Cell Res. 24, 177–189. doi:10.1038/cr.2014.3.

Pinto, R., Vågbø, C. B., Jakobsson, M. E., Kim, Y., Baltissen, M. P., O'Donohue, M. F., et al. (2020). The human methyltransferase ZCCHC4 catalyses N6-methyladenosine modification of 28S ribosomal RNA. Nucleic Acids Res. 48, 830–846. doi:10.1093/NAR/GKZ1147.

Pontier, D., Picart, C., El Baidouri, M., Roudier, F., Xu, T., Lahmy, S., et al. (2019). The m6A pathway protects the transcriptome integrity by restricting RNA chimera formation in plants. Life Sci. Alliance 2. doi:10.26508/lsa.201900393.

Ren, W., Lu, J., Huang, M., Gao, L., Li, D., Greg Wang, G., et al. (2019). Structure and regulation of ZCCHC4 in m6A-methylation of 28S rRNA. Nat. Commun. 10. doi:10.1038/S41467-019-12923-X.

Růžička, K., Zhang, M., Campilho, A., Bodi, Z., Kashif, M., Saleh, M., et al. (2017). Identification of factors required for m 6 A mRNA methylation in Arabidopsis reveals a role for the conserved E3 ubiquitin ligase HAKAI. New Phytol. 215, 157–172. doi:10.1111/nph.14586.

Schwartz, S., Mumbach, M. R., Jovanovic, M., Wang, T., Maciag, K., Bushkin, G. G., et al. (2014). Perturbation of m6A writers reveals two distinct classes of mRNA methylation at internal and 5' sites. Cell Rep. 8, 284–296. doi:10.1016/J.CELREP.2014.05.048/ATTACHMENT/1DA5BCC7-7D40-4B7E-A117-689EE0A26C2E/MMC6.XLSX.

Shen, L., Liang, Z., Gu, X., Chen, Y., Teo, Z. W. N., Hou, X., et al. (2016). N6-Methyladenosine RNA Modification Regulates Shoot Stem Cell Fate in Arabidopsis. Dev. Cell 38, 186–200. doi:10.1016/J.DEVCEL.2016.06.008.

Shima, H., Matsumoto, M., Ishigami, Y., Ebina, M., Muto, A., Sato, Y., et al. (2017). S-Adenosylmethionine Synthesis Is Regulated by Selective N6-Adenosine Methylation and mRNA Degradation Involving METTL16 and YTHDC1. Cell Rep. 21, 3354–3363. doi:10.1016/J.CELREP.2017.11.092.

Tan, B., and Gao, S. J. (2018). RNA epitranscriptomics: Regulation of infection of RNA and DNA viruses by N6-methyladenosine (m6A). Rev. Med. Virol. 28, e1983. doi:10.1002/RMV.1983.

Thiel, V. (2020). Viral RNA in an m 6 A disguise. Nat. Microbiol. 2020 54 5, 531–532. doi:10.1038/s41564-020-0689-x.

Thomas, P. E., Wu, X., Liu, M., Gaffney, B., Ji, G., Li, Q. Q., et al. (2012). Genome-wide control of polyadenylation site choice by CPSF30 in arabidopsisC W OA. Plant Cell 24, 4376–4388. doi:10.1105/TPC.112.096107.

Tirumuru, N., Zhao, B. S., Lu, W., Lu, Z., He, C., and Wu, L. (2016). N6-methyladenosine of HIV-1 RNA regulates viral infection and HIV-1 Gag protein expression. Elife 5. doi:10.7554/eLife.15528.

van den Born, E., Omelchenko, M. V., Bekkelund, A., Leihne, V., Koonin, E. V., Dolja, V. V., et al. (2008). Viral AlkB proteins repair RNA damage by oxidative demethylation. Nucleic Acids Res. 36, 5451–5461. doi:10.1093/nar/gkn519.

Van Tran, N., Ernst, F. G. M., Hawley, B. R., Zorbas, C., Ulryck, N., Hackert, P., et al. (2019). The human 18S rRNA m6A methyltransferase METTL5 is stabilized by TRMT112. Nucleic Acids Res. 47, 7719–7733. doi:10.1093/NAR/GKZ619.

Van Tran, N., Muller, L., Ross, R. L., Lestini, R., Létoquart, J., Ulryck, N., et al. (2018). Evolutionary insights into Trm112-methyltransferase holoenzymes involved in translation between archaea and eukaryotes. Nucleic Acids Res. 46, 8483–8499. doi:10.1093/NAR/GKY638.

Vespa, L., Vachon, G., Berger, F., Perazza, D., Faure, J. D., and Herzog, M. (2004). The Immunophilin-Interacting Protein AtFIP37 from Arabidopsis Is Essential for Plant Development and Is Involved in Trichome Endoreduplication. Plant Physiol. 134, 1283. doi:10.1104/PP.103.028050.

Wang, C., Yang, J., Song, P., Zhang, W., Lu, Q., Yu, Q., et al. (2022). FIONA1 is an RNA N6-methyladenosine methyltransferase affecting Arabidopsis photomorphogenesis and flowering. Genome Biol. 2022 231 23, 1–29. doi:10.1186/S13059-022-02612-2.

Wang, X., Lu, Z., Gomez, A., Hon, G. C., Yue, Y., Han, D., et al. (2014). N 6-methyladenosine-dependent regulation of messenger RNA stability. Nature 505, 117–120. doi:10.1038/nature12730.

Wang, X., Zhao, B. S., Roundtree, I. A., Lu, Z., Han, D., Ma, H., et al. (2015). N6-methyladenosine modulates messenger RNA translation efficiency. Cell 161, 1388–1399. doi:10.1016/J.CELL.2015.05.014/.

Warda, A. S., Kretschmer, J., Hackert, P., Lenz, C., Urlaub, H., Höbartner, C., et al. (2017). Human METTL16 is a N 6 -methyladenosine (m 6 A) methyltransferase that targets pre-mRNAs and various non-coding RNAs . EMBO Rep. 18, 2004–2014. doi:10.15252/EMBR.201744940.

Williams, G. D., Gokhale, N. S., and Horner, S. M. (2019). Regulation of Viral Infection by the RNA Modification N6 -Methyladenosine. Annu. Rev. Virol. 6, 235–253. doi:10.1146/annurev-virology-092818-015559.

Wu, F., Cheng, W., Zhao, F., Tang, M., Diao, Y., and Xu, R. (2019). Association of N6-methyladenosine with viruses and related diseases. Virol. J. 16, 1–10. doi:10.1186/S12985-019-1236-3/TABLES/1.

Xiao, W., Adhikari, S., Dahal, U., Chen, Y. S., Hao, Y. J., Sun, B. F., et al. (2016). Nuclear m6A Reader YTHDC1 Regulates mRNA Splicing. Mol. Cell 61, 507–519. doi:10.1016/J.MOLCEL.2016.01.012.

Xu, C., Liu, K., Tempel, W., Demetriades, M., Aik, W. S., Schofield, C. J., et al. (2014). Structures of human ALKBH5 demethylase reveal a unique binding mode for specific single-stranded N6-methyladenosine RNA demethylation. J. Biol. Chem. 289, 17299–17311. doi:10.1074/jbc.M114.550350.

Ye, F. (2018). RNA N6-Adenosine Methylation (m6A) Steers Epitranscriptomic Control of Herpesvirus Replication. Inflamm. Cell Signal. 4. doi:10.14800/ics.1604.

Yue, H., Nie, X., Yan, Z., and Weining, S. (2019). N6-methyladenosine regulatory machinery in plants: composition, function and evolution. Plant Biotechnol. J. 17, 1194–1208. doi:10.1111/pbi.13149.

Zhang, K., Zhuang, X., Dong, Z., Xu, K., Chen, X., Liu, F., et al. (2021). The dynamics of N 6-methyladenine RNA modification in interactions between rice and plant viruses. Genome Biol. 22. doi:10.1186/S13059-021-02410-2.

Zhong, S., Li, H., Bodi, Z., Button, J., Vespa, L., Herzog, M., et al. (2008). MTA is an Arabidopsis messenger RNA adenosine methylase and interacts with a homolog of a sex-specific splicing factor. Plant Cell 20, 1278–1288. doi:10.1105/TPC.108.058883.

Zhou, Z., Lv, J., Yu, H., Han, J., Yang, X., Feng, D., et al. (2020). Mechanism of RNA modification N6-methyladenosine in human cancer. Mol. Cancer 19, 1–20. doi:10.1186/s12943-020-01216-3.

General discussion

As a reversible modification, m^6A plays key roles in a series of biological processes in plants including embryo development, flowering-time control, microspore generation and fruit ripening. Recent results have revealed that RNA m^6A modification is critical to control plant growth, and its modulation provides a new, promising approach to substantially elevate crop production. As a significant breakthrough it has been demonstrated that RNA demethylation increases the yield and biomass of rice and potato plants in field trials being one of the first examples showing that the epitranscriptome can be engineered to stimulate crop production (Yu et al., 2021). By the other hand, increasing evidence links epitranscriptomic dynamic changes with plant response to abiotic and biotic stresses. Indeed, epitranscriptomics can be considered as an additional regulatory layer in plants' development and stress response (Shoaib et al., 2022). Transcripts encoding proteins required for salt and osmotic stress responses are targeted by m^6A modification leading to more stable RNAs and eventually increasing the protein levels (e.g. Hu et al., 2021; Zhang et al., 2021). Unfortunately, the study of the implication of the m^6A modification in the infection of plants by pathogens has not received much attention.

During the last decades, however, it has been clearly demonstrated a strong correlation between m^6A and virus infection in mammals (Glushkevich et al., 2022). In plants, there is still little evidence on the role of m^6A in viral infection although an emerging picture is showing up where m^6A might play a dual role. In response to viral infection, plants would activate a kind of immune response consisting in the m^6A methylation of the viral RNAs what would interfere with viral replication or translation. Plant viruses would counteract this response by regulating m^6A-related proteins accumulation or activity to overcome that host immune system (Yue et al., 2022). In this context, it has been recently shown that: (i) in TMV-infected *N. tabacum* plants exhibit elevated levels of m^6A-mRNAs and, in addition, exhibit a repression of a potential demethylase (ortholog of human ALKBH5) and MTases, respectively, compared to uninfected plants (Li et al., 2018); (ii) *Solanum tuberosum* plants exposed to single and combined stress treatments (PVY and heat) generate drastic changes in the expression of many lncRNAs, RNA methylation and alternative splicing (Glushkevich

et al., 2022); (iii) in susceptible rice plants, it was found that m^6A-levels increased in response to infection by Rice black-streaked dwarf virus (RBSDV) and Rice stripe virus (RSV), and that m^6A-methylation is mainly associated with genes that are not actively expressed in virus-infected rice plants (Zhang et al., 2021b). Additionally, viruliferous small brown planthopper (SBPH) of RBSDV were reported to have a lower level of m^6A compared to non-viruliferous insects. Inhibition of m^6A by silencing LsMETTL3 and LsMETTL14 increased viral titers in SBPH gut cells; aspect that suggests that m^6A can negatively modulate virus replication and prevent severe damage to insect vectors; however, RBSDV can suppress the m^6A-modification, allowing the virus to persist in the insect vector (Tian et al., 2021). Then (iv) in wheat, m^6A profiling of the entire transcriptome of two varieties with different resistance to wheat yellow mosaic virus (WYMV) revealed that many genes related to plant defense responses and plant-pathogen interaction were significantly changed in both m^6A and mRNA levels (Zhang et al., 2021c); and finally, (v) in watermelon, global m^6A levels are reduced in response to Cucumber green mottle mosaic virus (CGMMV) infection; implying that a global hypomethylation of m^6A likely activates watermelon defense responses early in CGMMV infection (He et al., 2021).

m^6A-modification is regulated by writers, erasers and readers that would define the final status of the RNA population both at the cellular or at the viral level. In the case of AMV infection, one of the key players in this homeostatic scenario is the α-ketoglutarate dependent dioxygenase homolog 9B (ALKBH9B). This protein was identified as the first demethylase in plants and it was shown that interacts with the coat protein of AMV (Martínez-Pérez et al., 2017). However, its biochemical properties remained unsolved. Thus, one of the main objectives of this Thesis was to map the regions of this protein that interact with either AMV CP or viral RNA, as well as to determine its subcellular location. By the other hand, although m^6A modification sites in viral RNAs were identified, their potential impact in the infection cycle have been poorly studied. As a first approximation to this topic, we have carried out a series of mutations in the 3'UTR end of AMV RNAs that harbors several of the potential sites of modification by m^6A. Finally, although methylases have been proven to be involved in

abiotic stress tolerance in plants, no report describing their potential involvement in plant virus-host interactions has been made. We decided to explore this possibility and, if positive, deepening into their potential modes of action.

Mapping of functional subdomains in the atALKBH9B m^{6}A-Demethylase

As previously stated, the m^{6}A pathway relies on the dynamic interactions between methyltransferases, demethylases and m^{6}A binding proteins (writers, erasers and readers, respectively). A previous study carried out in the laboratory where this work was carried out trying to find host proteins interacting the AMV CP identified the *Arabidopsis* protein ALKBH9B as one of the CP interactors. Later on, *in vitro* demethylation assays identified this protein as the first plant m^{6}A RNA demethylase (Martínez-Pérez et al., 2017). Furthermore, AMV-infection based studies using *alkbh9b* mutant plants demonstrated that ALKBH9B regulates m^{6}A abundance on vRNAs and systemic invasion of floral stems (Martínez-Pérez et al., 2017, 2021). This regulation seems to be specific of ALKBH9B since ALKBH9A and ALKBH9C were observed not to be involved in the AMV cycle (Martínez-Pérez et al., 2021). Furthermore, a deeper characterization of the AMV RNA/CP-ALKBH9B interaction led us to propose that AMV phloem loading in *alkbh9b* knockdown plants is restricted (Martínez- Pérez et al., 2021). A working model was proposed for the involvement of this demethylase in the viral cycle of AMV (Figure 1, for more details see Martínez-Pérez 2020, Doctoral Thesis).

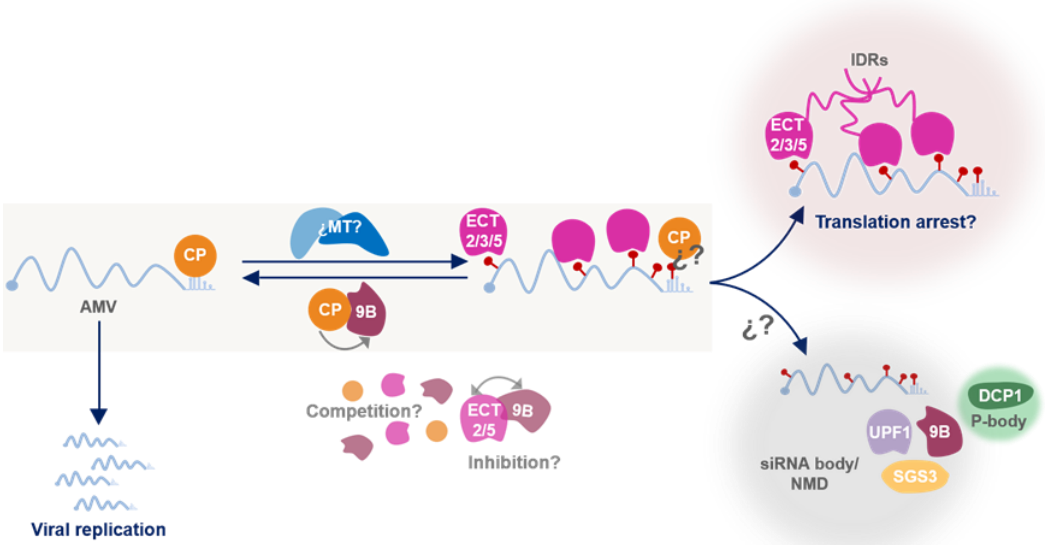

Figure 1. Schematic representation of the hypothetical model of m^{6}A-mediated AMV regulation in *Arabidopsis*. vRNAs would be methylated by an unidentified m^{6}A methyltransferase. Diverse ECTs would recognize the m^{6}A poly-methylated vRNAs and the interaction among their IDRs would undergo phased separation that favor the localization of m^{6}A-modified vRNAs to RNA granules such as SGs and or siRNA bodies. In turn, AMV-CP would hijack the atALKBH9B to demethylate the viral genome and avoid ECTs sequestration, enhancing the viral replication. Moreover, m^{6}A might potentially affect the CP binding to the 3'UTR of viral RNAs. m^{6}A residues are represented as red circles. Adapted from Martínez-Pérez, (2020).

Due to the functional relevance of ALKBH9B on viral infection in this thesis we carried out a detailed mapping of the protein to dissect the functional activity of ALKBH9B in plant-virus infection. Thus, we delimited the region between residues 427 and 467 as an RNA binding domain (RBD) critical for binding *in vitro* to the sgRNA4. Moreover, the kinetic parameters obtained for the interaction of the full length ALKBH9B with the viral RNA indicate that the protein binds efficiently viral RNA in a cooperative manner. Computational analysis of the ALKBH9B sequence revealed no obvious structured RBD that could justify the RNA-binding properties. Interestingly, we found that about 78% of the RBD identified in ALKBH9B is contained in a C-terminal intrinsically disorder region (IDR) (see Figure 4 in chapter 2). IDRs are protein disordered domains that lack a stable structure in solution which have found to be involved in protein-protein and protein-RNA interactions (Castello et al., 2012). In this sense, it has been proposed that the capability to specifically target

different RNAs in RNA binding proteins (RBPs) containing IDRs is due to conformational flexibility as well as the establishment of extended conserved electrostatic interfaces with RNAs (Varadi et al., 2015). In this thesis work, it is proposed that the RNA motif $_{459}$RGxxxRGG$_{466}$ within the RBD could induce the formation of a flexible structure that allows additional contacts through RG residues at positions 473-474 and 496-497, and YG residues at 506-507, improving the binding affinity and the specificity of the interaction. This has been observed in the splicing factor Tra2-β1 that presents IDRs in the N- and C-terminal region of the RRM. In the protein-RNA interface, this region adopts a folded structure, forming extensive contacts (Cléry et al., 2011).

On other hand, IDRs are frequently localized in proteins that undergo liquid-liquid phase separation (LLPS), a process that likely contributes to the formation and stability of RNA granules (Alberti et al., 2019). This has been shown in YTHDF1, YTHDF2 and YTHDF3, m^{6}A-readers, which undergo LLPS in the presence of poly-methylated mRNAs. The resulting mRNA-YTHDF complexes form P-bodies and stress granules (Ries et al., 2019). Computational predictions indicate that around of 45.4% of the ALKBH9B amino acid sequence is in a IDR conformation. These IDRs are located at the N-terminal region, within the internal domain like *AlkB* and at the C-terminal region. In this context, as has been reported in other RBPs (Jonas and Izaurralde, 2013; Protter and Parker, 2016), the IDRs of ALKBH9B, as well as the folded domains that mediate RNA binding and oligomerization, could act together with RNAs to produce and maintain biomolecular condensates, as it has been reported for other RBPs (Jonas and Izaurralde, 2013; Protter and Parker, 2016),. In this sense, here we found that deletion of some IDR regions (the first 20 N-terminal residues or the last 40 C-terminal amino acids), blocks the capability of the protein to accumulate in siRNA bodies.

Once demonstrated the proviral activity of ALKBH9B (Martínez-Pérez et al., 2017, 2021) and mapped its RNA and CP binding motifs (this work), it would be very interesting to study whether both RBD and CP binding domain are essential for viral infection and if IDRs are

playing essential functions in this potential modulation by promoting viral accumulation in stress RNA granules.

Impact of the putative DRACH-motifs located in the hpB loop and the lower-stem of hpE in the 3'UTR RNA 3 in the AMV infection cycle

In agreement with early biochemical studies of animal, viral, and plant mRNA, transcriptome-wide mapping of m^6A has identified DR[m^6A]CH (D=A/G/U, R=A/G, H=A/C/U) as the most significantly enriched motif in m^6A peaks of all eukaryotes analyzed to date including plants (see Arribas-Hernández and Brodersen, 2020, for a review). In addition to its presence in a defined consensus motif, m^6A was predominantly found in the 3'UTR of mRNAs in eukaryotes.

A methylated-RNA immunoprecipitation sequencing experiment carried out previously to this doctoral Thesis reported the presence of m^6A in AMV vRNAs. Interestingly, two of these putative m^6A-sites are located in the 3'UTR of the genomic RNA 3 (Martínez-Pérez et al., 2017). In AMV, similar to ilarviruses, the 3'UTR of all genomic RNAs have a high homology (>80%), and can form two mutually exclusive conformers that are believed to act as a molecular switch from translation to replication (Koper-Zwarthoff et al., 1979; Aparicio et al., 2003; Chen and Olsthoorn, 2010; Pallas et al., 2013). One conformation is believed to consist in a linear array of several hairpin structures (hpA to hpE) flanked by AUGC-motifs, representing specific CP binding (CPB) sites (Reusken and Bol, 1996).The alternative conformation would consist of a tRNA-like structure (TLS) generated by base pairing between the UCCU and AGGG sequences of hpD and hpA, respectively (Olsthoorn et al., 1999). According to the switch model, 3'UTR-TLS conformer would favor negative vRNA synthesis, while 3'UTR-CPB conformation would facilitate protein translation (Olsthoorn et al., 1999; Chen and Olsthoorn, 2010). Interestingly, one putative m^6A-site ($_{2012}$AAACU$_{2016}$) is positioned within the CPB1, in the loop of hpB, whereas the other ($_{1900}$UGACC$_{1904}$) is located in the lower-stem of hpE, both presenting the canonical m^6A motif DRACH (D= A, G or U, R = G/A, H = A/U/C) (Bayoumi and Munir, 2021). Previous studies have shown that

the integrity of hpB and hpE structures are essential for AMV replication cycle through their role in CP-binding and minus strand synthesis, respectively (Bol, 2008). Because m^6A methylation can affect A-U base pairing, which may led to alter putative RNA-protein interactions (Liu et al., 2017), and m^6A levels of AMV genome regulate viral infection (Martínez-Pérez et al., 2017) we reasoned that these two putative m^6A-sites could have significant roles in the AMV cycle. To address this issue, a mutational analysis was carried out by generating a series of AMV RNA 3 clones with compensatory point mutations in order to interfere or abolish the m^6A-methylation of these sites.

In this context, our results indicated that the identity of residues $_{2012}$A, $_{2013}$A and $_{2014}$A in the hpB loop appears to be a key structural requirement for AMV replication and/or accumulation since reversal of mutated nucleotides is necessary to restore the wild-type genotype. Similar effects have been observed in dengue virus, where point mutations in the upper loop of hairpin A (SLA) of the 5'UTR generated non-replicating RNAs. Nucleotide reversal in SLA is sufficient to restore its promoter activity (Filomatori et al., 2006). However, in the other pathosystem where this effect was studied it was observed that m^6A minimally affects the structure, dynamics, of the Rev response element (RRE) stem IIB in human immunodeficiency virus-1 (Chu et al., 2019). This is not surprising since m^6A modification has a opposite regulatory effect on the replication of different viruses, and virus infection can also regulate the level of host m^6A modification (Yue et al., 2022).

Regarding hpE, a previous study (Pandey et al., 1994), carried out under *in vitro* conditions, showed that: (i) hpE is a crucial element for the minus-strand synthesis *in vitro* in AMV; (ii) that the identity and base pairing capacity of the hpE upper-stem is also essential for this process, and that (iii) when the DRACH nucleotide sequence is removed, minus-strand synthesis was reduced by up to 60%. In addition, in this thesis work it was determined that the putative m^6A-residue $_{1902}$A, as well as the base pairing of the lower-stem of hpE, are also essential requirements for the *in vivo* plus-strand synthesis in AMV. Regarding base-pairing, it has been proposed that hpE must consist on an interrupted 10 bp stem-base pairing to be functional (Olsthoorn et al., 2004). In this context, the alteration of the base-pairing capacity

of hpE in the cDNA3$_{1922\text{-}26}$ mutant caused a reduction in stem-size, a key structural requirement for hpE promoter activity. Our results are consistent with the growing evidence that the impact of m^{6}A on RNA depends on sequence context and secondary structure.

Exploring the potential involvement of RNA methylases in the viral infection cycle

As stated before, m^{6}A-modification plays a critical role in both viral pathogenesis and host defense response, however, this mechanism is complex and still needs to be elucidated (Williams et al., 2019; He et al., 2021; McFadden and Horner, 2021).

The activity of METTL3 and METTL14 complex-writer has been associated with m^{6}A deposition on RNAs of different mammal infecting viruses. Thus, depletion or overexpression of these methylases has been shown to have either an antiviral or a proviral effect in mammalian viruses depending on the particular virus studied (Manners et al., 2019). However, any m^{6}A methyltransferase has been identified yet targeting viral RNAs in plant infections. The involvement of m^{6}A mechanism in the AMV infection cycle has been clearly demonstrated (Martínez-Pérez et al., 2017, 2021) and in the present Thesis we have performed a series of preliminary studies to identify the m^{6}A methylases that could account for the methylated status of the AMV RNA. Thus, due to the functional relevance of m^{6}A-levels in AMV vRNAs, we analyzed the *in vivo* role of *Arabidopsis* MTA (homolog of METTL3, Zhong et al., 2008) and MTB (homolog of METTl14, Růžička et al., 2017), and the proteins encoded by the AT4G28830 and AT1G78190 genes (putative homolog of METTL5 and TRMT112, respectively) during AMV infection by two different approaches, e.g., transient overexpression in *N. benthamiana* plants and use of the *Arabidopsis* ABI3prom:MTA line. This transgenic plant was developed by complementing an MTA-knockout mutant with an MTA coding sequence under the control of the ABI3-promoter allowing high expression of MTA-protein as well as complete m^{6}A-methylation during the embryonic stage, but very low activity after germination (Bodi et al., 2012).

The results obtained in this thesis indicate that function of *Arabidopsis* MTA/MTB complex would not play any role in the biology of AMV. This result is quite surprising given that the

viral RNA of AMV, and other viruses, has been shown to be methylated. In any case, we cannot rule out that the agro-overexpressed MTA-MTB complex was not functional in *N. benthamiana* plants or some residual expression of MTA would rely in Arabidopsis ABI3prom:MTA plants. Alternatively, we decided to search putative homologs of the recent discovers m^6A-writers in humans METTL5 (Q9NRN9) and ZCCHC4 (Q9H5U6) (Oerum et al., 2021). Again, no effect was either observed when overexpressing atMETTL5-*like*:atTRMT112-*like* in *N. benthamiana* plants. It is necessary to extend these preliminary studies to corroborate whether MTA/MTB complex mediate m^6A deposition in the AMV genome or if not, to identify other potential methyltransferase candidates to complete the global picture on the m^6A mechanism in the viral cycle of plant viruses.

Conclusions

- Electrophoretic Mobility Shift Assays (EMSA) revealed that ALKBH9B binds RNA *in vitro*. The apparent constant dissociation (K_d) of the RNA–ALBKH9B interaction was estimated to be 0.30 μM.
- A mutational analysis of ALKBH9B revealed that the residues between 427 and 467 positions are critical for *in vitro* binding to the AMV RNA. This region represents an RNA binding domain that contains an RGxxxRGG motif. Furthermore, residues located between 387 and 427 positions in ALKBH9B are critical for the interaction with the AMV CP. Previous studies had indicated that this interaction is critical for modulating the viral infection process.
- A deletion analysis showed that both N-terminal first 20 residues and the C-terminal last 40 amino acids seem to be required for proper accumulation of ALKBH9B in siRNA bodies.
- The IDRs and the RBD of *Arabidopisis* ALKBH9B could act cooperatively to promote the formation of RNA granules, where the IDRs, as well as the folded domains that mediate RNA binding and oligomerization, act together with the RNAs to produce and maintain biomolecular condensates. Nonetheless, the mechanisms underlying the cooperativity of the folded domain in IDRs and their potential regulation need further examination.
- Our results suggest that the identity of residues $_{2012}$A, $_{2013}$A and $_{2014}$A that make up the DRACH-motif in hpB are a key structural requirement for AMV replication and/or accumulation. Likewise, the putative m^{6}A-residue $_{1902}$A, as well as the base pairing of the lower-stem in hpE, appears to be critical for the *in vivo* plus-strand synthesis in AMV. Nonetheless, we cannot rule out the possibility that mutations of the putative m^{6}A-residues and surrounding sequences may alter vRNA structure, thus the biology of the virus.
- Preliminary results suggest that neither the m^{6}A methyltransferase MTA/MTB complex nor the *Arabidopsis* homolog METTL5:TRMT112 complex would modulate AMV replication cycle. However, further and much extensive studies are

required to corroborate these results and to undoubtedly identify the m^6A methyltransferase activity responsible for installing m^6A on AMV viral genome

References

Adams, J., and Cory, S. (1975). Modified nucleosides and bizare 5'-termini in mouse myeloma mRNA. *Nature* 255, 28–33.

Agarwala, S. D., Blitzblau, H. G., Hochwagen, A., and Fink, G. R. (2012). RNA methylation by the MIS complex regulates a cell fate decision in yeast. *PLoS Genet.* 8. doi:10.1371/JOURNAL.PGEN.1002732.

Al-Saleh, M. A., and Amer, M. A. (2013). Biological and Molecular Variability of Alfalfa mosaic virus Affecting Alfalfa Crop in Riyadh Region. *Plant Pathol. J.* 29, 410. doi:10.5423/PPJ.OA.05.2013.0050.

Alarcón, C. R., Lee, H., Goodarzi, H., Halberg, N., and Tavazoie, S. F. (2015). N6-methyladenosine marks primary microRNAs for processing. *Nature* 519, 482–485. doi:10.1038/NATURE14281.

Alberti, S., Gladfelter, A., and Mittag, T. (2019). Considerations and Challenges in Studying Liquid-Liquid Phase Separation and Biomolecular Condensates. *Cell* 176, 419–434. doi:10.1016/j.cell.2018.12.035.

Anders, M., Chelysheva, I., Goebel, I., Trenkner, T., Zhou, J., Mao, Y., et al. (2018). Dynamic m6A methylation facilitates mRNA triaging to stress granules. *Life Sci. Alliance* 1. doi:10.26508/LSA.201800113.

Anderson, P., and Kedersha, N. (2008). Stress granules: the Tao of RNA triage. *Trends Biochem. Sci.* 33, 141–150. doi:10.1016/J.TIBS.2007.12.003.

Ansel-McKinney, P., Scott, S. W., Swanson, M., Ge, X., and Gehrke, L. (1996). A plant viral coat protein RNA binding consensus sequence contains a crucial arginine. *EMBO J.* 15, 5077–5084. doi:10.1002/J.1460-2075.1996.TB00888.X.

Aparicio, F., and Pallás, V. (2017). The coat protein of *Alfalfa mosaic virus* interacts and interferes with the transcriptional activity of the bHLH transcription factor ILR3 promoting salicylic acid-dependent defence signalling response. *Mol. Plant Pathol.* 18, 173–186. doi:10.1111/mpp.12388.

Aparicio, F., Vilar, M., Perez-Payá, E., and Pallás, V. (2003). The coat protein of prunus necrotic ringspot virus specifically binds to and regulates the conformation of its genomic RNA. *Virology* 313, 213–223. doi:10.1016/S0042-6822(03)00284-8.

Aravind, L., and Koonin, E. V. (2001). The DNA-repair protein AlkB, EGL-9, and leprecan define new families of 2-oxoglutarate- and iron-dependent dioxygenases. *Genome Biol.* 2, research0007.1. doi:10.1186/GB-2001-2-3-RESEARCH0007.

Arribas-Hernández, L., Bressendorff, S., Hansen, M. H., Poulsen, C., Erdmann, S., and Brodersen, P. (2018). An m6A-YTH module controls developmental timing and morphogenesis in arabidopsis. *Plant Cell* 30, 952–967. doi:10.1105/TPC.17.00833.

Arribas-Hernández, L., and Brodersen, P. (2020). Occurrence and functions of m6A and other covalent modifications in plant mRNA. *Plant Physiol.* 182, 79–96. doi:10.1104/pp.19.01156.

Arribas-Hernández, L., Rennie, S., Schon, M., Porcelli, C., Enugutti, B., Andersson, R., et al. (2021). The Arabidopsis m6A-binding proteins ECT2 and ECT3 bind largely overlapping mRNA target sets and influence target mRNA abundance, not alternative polyadenylation. *bioRxiv*, 2021.08.01.454660. doi:10.1101/2021.08.01.454660.

Avgelis, A., and Katis, N. (1989). Identification of Alfalfa Mosaic Virus in Greek Alfalfa Crops. *J. Phytopathol.* 125, 231–237. doi:10.1111/J.1439-0434.1989.TB01064.X.

Bai, B. (2022). An update on principles of m6A targeting. *Trends Plant Sci.* 27, 224–226. doi:10.1016/J.TPLANTS.2021.12.007.

Bailiss, K. W., and Ollennu, L. A. A. (1986). Effect of alfalfa mosaic virus isolates on forage yield of lucerne (Medicago sativa) in Britain. *Plant Pathol.* 35, 162–168. doi:10.1111/J.1365-3059.1986.TB02000.X.

Balacco, D. L., and Soller, M. (2019). The m6A Writer: Rise of a Machine for Growing Tasks. *Biochemistry* 58, 363–378. doi:10.1021/acs.biochem.8b01166.

Balasubramaniam, M., Kim, B. S., Hutchens-Williams, H. M., and Loesch-Fries, L. S. (2014). The Photosystem II Oxygen-Evolving Complex Protein PsbP Interacts With the Coat Protein of Alfalfa mosaic virus and Inhibits Virus Replication. *Mol. PLant-Mol. INteract.* 27, 1107–1118. doi:10.1094/MPMI-02-14-0035-R.

Banani, S. F., Lee, H. O., Hyman, A. A., and Rosen, M. K. (2017). Biomolecular condensates: Organizers of cellular biochemistry. *Nat. Rev. Mol. Cell Biol.* 18, 285–298. doi:10.1038/nrm.2017.7.

Baquero-Perez, B., Antanaviciute, A., Yonchev, I. D., Carr, I. M., Wilson, S. A., and Whitehouse, A. (2019).

The tudor SND1 protein is an m6a RNA reader essential for replication of kaposi's sarcoma-associated herpesvirus. *Elife* 8. doi:10.7554/ELIFE.47261.

Baquero-Perez, B., Geers, D., and Díez, J. (2021). From A to m6A: The Emerging Viral Epitranscriptome. *Viruses* 13, 1049. doi:10.3390/V13061049.

Bartosovic, M., Molares, H. C., Gregorova, P., Hrossova, D., Kudla, G., and Vanacova, S. (2017). N6-methyladenosine demethylase FTO targets pre-mRNAs and regulates alternative splicing and 3′-end processing. *Nucleic Acids Res.* 45, 11356–11370. doi:10.1093/NAR/GKX778.

Bayoumi, M., and Munir, M. (2021). Evolutionary conservation of the DRACH signatures of potential N6-methyladenosine (m6A) sites among influenza A viruses. *Sci. Rep.* 11, 1–12. doi:10.1038/s41598-021-84007-0.

Beemon, K., and Keith, J. (1977). Localization of N6-methyladenosine in the Rous sarcoma virus genome. *J. Mol. Biol.* 113, 165–179. doi:10.1016/0022-2836(77)90047-X.

Beijerinck, M. W. (1898). Concerning a contagium vivum fluidum as cause of the Spot Disease of Tobacco leaves. *Verh. der K. Akad. van Wet. te Amsterdam* 65, 3–21. Available at: https://www.apsnet.org/edcenter/apsnetfeatures/Documents/1998/BeijerckSpotDiseaseTobaccoLeaves.PDF [Accessed February 10, 2022].

Bhasin, H., and Hülskamp, M. (2017). ANGUSTIFOLIA, a plant homolog of CtBP/BARS localizes to stress granules and regulates their formation. *Front. Plant Sci.* 8. doi:10.3389/FPLS.2017.01004/FULL.

Bhat, S. S., Bielewicz, D., Grzelak, N., Gulanicz, T., Bodi, Z., Szewc, L., et al. (2019). mRNA adenosine methylase (MTA) deposits m6A on pri-miRNAs to modulate miRNA biogenesis in Arabidopsis thaliana. *bioRxiv*. doi:10.1101/557900.

Bhullar, D. S., Sheahan, M. B., and Rose, R. J. (2017). RNA processing body (P-body) dynamics in mesophyll protoplasts re-initiating cell division. *Protoplasma* 254, 1627–1637. doi:10.1007/S00709-016-1053-0/FIGURES/10.

Boccaletto, P., MacHnicka, M. A., Purta, E., Pitkowski, P., Baginski, B., Wirecki, T. K., et al. (2018). MODOMICS: A database of RNA modification pathways. 2017 update. *Nucleic Acids Res.* 46, D303–D307. doi:10.1093/nar/gkx1030.

Bodi, Z., Button, J. D., Grierson, D., and Fray, R. G. (2010). Yeast targets for mRNA methylation. *Nucleic Acids Res.* 38, 5327–5335. doi:10.1093/nar/gkq266.

Bodi, Z., Zhong, S., Mehra, S., Song, J., Graham, N., Li, H., et al. (2012). Adenosine methylation in Arabidopsis mRNA is associated with the 3′ end and reduced levels cause developmental defects. *Front. Plant Sci.* 3. doi:10.3389/fpls.2012.00048.

Bokar, J. A., Rath-Shambaugh, M. E., Ludwiczak, R., Narayan, P., and Rottman, F. (1994). Characterization and partial purification of mRNA N6-adenosine methyltransferase from HeLa cell nuclei. Internal mRNA methylation requires a multisubunit complex. *J. Biol. Chem.* 269, 17697–17704. doi:10.1016/S0021-9258(17)32497-3.

Bol, J. F. (1999). Alfamovirus and Ilarviruses (Bromoviridae). *Encycl. Virol.*, 38–43. doi:10.1006/RWVI.1999.0009.

Bol, J. F. (2003). Alfalfa mosaic virus: coat protein-dependent initiation of infection. *Mol. Plant Pathol.* 4, 1–8. doi:10.1046/J.1364-3703.2003.00146.X.

Bol, J. F. (2005). Replication of Alfamo- and Ilarviruses: Role of the Coat Protein. *Annu. Rev. Phytopathol.* 43, 39–62. doi:10.1146/annurev.phyto.43.101804.120505.

Bol, J. F. (2008). "Alfalfa Mosaic Virus," in *Encyclopedia of Virology*, 81–87. doi:10.1016/B978-012374410-4.00635-X.

Bos, L. (1981). WILD PLANTS IN THE ECOLOGY OF VIRUS DISEASES. *Plant Dis. Vectors Ecol. Epidemiol.*, 1–33. doi:10.1016/B978-0-12-470240-0.50005-6.

Bratlie, M. S., and Drabløs, F. (2005). Bioinformatic mapping of AlkB homology domains in viruses. *BMC Genomics* 6. doi:10.1186/1471-2164-6-1.

Bruggeman, Q., Garmier, M., de Bont, L., Soubigou-Taconnat, L., Mazubert, C., Benhamed, M., et al. (2014). The polyadenylation factor subunit CLEAVAGE AND POLYADENYLATION SPECIFICITY FACTOR30: A key factor of programmed cell death and a regulator of immunity in arabidopsis. *Plant*

Physiol. 165, 732–746. doi:10.1104/PP.114.236083.
Bujarski, J., Gallitelli, D., García-Arenal, F., Pallás, V., Palukaitis, P., Krishna Reddy, M., et al. (2019). ICTV virus taxonomy profile: Bromoviridae. *J. Gen. Virol.* 100, 1206–1207. doi:10.1099/jgv.0.001282.
Campos-Melo, D., Hawley, Z. C. E., Droppelmann, C. A., and Strong, M. J. (2021). The Integral Role of RNA in Stress Granule Formation and Function. *Front. Cell Dev. Biol.* 9, 808. doi:10.3389/FCELL.2021.621779/BIBTEX.
Castello, A., Fischer, B., Eichelbaum, K., Horos, R., Beckmann, B. M., Strein, C., et al. (2012). Insights into RNA Biology from an Atlas of Mammalian mRNA-Binding Proteins. *Cell* 149, 1393–1406. doi:10.1016/j.cell.2012.04.031.
Chantarachot, T., and Bailey-Serres, J. (2018). Polysomes, Stress Granules, and Processing Bodies: A Dynamic Triumvirate Controlling Cytoplasmic mRNA Fate and Function. *Plant Physiol.* 176, 254–269. doi:10.1104/PP.17.01468.
Chen, J., Jin, L., Wang, Z., Wang, L., Chen, Q., Cui, Y., et al. (2020). N6-methyladenosine regulates PEDV replication and host gene expression. *Virology* 548, 59–72. doi:10.1016/J.VIROL.2020.06.008.
Chen, M., Urs, M. J., Sánchez-González, I., Olayioye, M. A., Herde, M., and Witte, C. P. (2018). M6A RNA degradation products are catabolized by an evolutionarily conserved N6-methyl-AMP deaminase in plant and Mammalian cells. *Plant Cell* 30, 1511–1522. doi:10.1105/TPC.18.00236.
Chen, S.-C., and Olsthoorn, R. C. L. (2010). In Vitro and In Vivo Studies of the RNA Conformational Switch in Alfalfa Mosaic Virus. *J. Virol.* 84, 1423–1429. doi:10.1128/jvi.01443-09.
Chu, C. C., Liu, B., Plangger, R., Kreutz, C., and Al-Hashimi, H. M. (2019). m6A minimally impacts the structure, dynamics, and Rev ARM binding properties of HIV-1 RRE stem IIB. *PLoS One* 14, e0224850. doi:10.1371/JOURNAL.PONE.0224850.
Cléry, A., Jayne, S., Benderska, N., Dominguez, C., Stamm, S., and Allain, F. H. T. (2011). Molecular basis of purine-rich RNA recognition by the human SR-like protein Tra2-β1. *Nat. Struct. Mol. Biol.* 18, 443–451. doi:10.1038/nsmb.2001.
Conti, G., Zavallo, D., Venturuzzi, A. L., Rodriguez, M. C., Crespi, M., and Asurmendi, S. (2017). TMV induces RNA decay pathways to modulate gene silencing and disease symptoms. *Plant J.* 89, 73–84. doi:10.1111/TPJ.13323.
Courtney, D. G., Kennedy, E. M., Dumm, R. E., Bogerd, H. P., Tsai, K., Heaton, N. S., et al. (2017). Epitranscriptomic Enhancement of Influenza A Virus Gene Expression and Replication. *Cell Host Microbe* 22, 377–386. doi:10.1016/J.CHOM.2017.08.004.
Covelo-Molares, H., Bartosovic, M., and Vanacova, S. (2018). RNA methylation in nuclear pre-mRNA processing. *Wiley Interdiscip. Rev. RNA* 9. doi:10.1002/wrna.1489.
Culver, J. N., and Padmanabhan, M. S. (2007). Virus-Induced Disease: Altering Host Physiology One Interaction at a Time. *Annu. Rev. Phytopath.* 45, 221–243. doi:10.1146/ANNUREV.PHYTO.45.062806.094422.
Dang, W., Xie, Y., Cao, P., Xin, S., Wang, J., Li, S., et al. (2019). N6-methyladenosine and viral infection. *Front. Microbiol.* 10, 417. doi:10.3389/fmicb.2019.00417.
Dimock, K., and Stoltzfus, C. M. (1977). Sequence Specificity of Internal Methylation in B77 Avian Sarcoma Virus RNA Subunits. *Biochemistry* 16, 471–478. doi:10.1021/bi00622a021.
Dominissini, D., Moshitch-Moshkovitz, S., Schwartz, S., Salmon-Divon, M., Ungar, L., Osenberg, S., et al. (2012). Topology of the human and mouse m6A RNA methylomes revealed by m6A-seq. *Nature* 485, 201–206. doi:10.1038/nature11112.
Dong, O. X., Meteignier, L. V., Plourde, M. B., Ahmed, B., Wang, M., Jensen, C., et al. (2016). Arabidopsis TAF15b localizes to RNA processing bodies and contributes to snc1-mediated autoimmunity. *Mol. Plant-Microbe Interact.* 29, 247–257. doi:10.1094/MPMI-11-15-0246-R/.
Dougherty, J. D., White, J. P., and Lloyd, R. E. (2011). Poliovirus-Mediated Disruption of Cytoplasmic Processing Bodies. *J. Virol.* 85, 64–75. doi:10.1128/JVI.01657-10/.
Duan, H. C., Wei, L. H., Zhang, C., Wang, Y., Chen, L., Lu, Z., et al. (2017). ALKBH10B is an RNA N6-methyladenosine demethylase affecting arabidopsis floral transition. *Plant Cell* 29, 2995–3011. doi:10.1105/tpc.16.00912.

Durbin, A. F., Wang, C., Marcotrigiano, J., and Gehrke, L. (2016). RNAs containing modified nucleotides fail to trigger RIG-I conformational changes for innate immune signaling. *MBio* 7. doi:10.1128/MBIO.00833-16/.

Edens, B. M., Vissers, C., Su, J., Arumugam, S., Xu, Z., Shi, H., et al. (2019). FMRP Modulates Neural Differentiation through m6A-Dependent mRNA Nuclear Export. *Cell Rep.* 28, 845-854.e5. doi:10.1016/J.CELREP.2019.06.072.

Escriu, F., Bernal, M., Vargas, M., Arteaga, L., and Paz, M. (2011). Síntomas, dispersión y daños del virus del mosaico de la alfalfa: un virus muy extendido en todas las zonas de producción con el que se lleva conviviendo muchos años. *Vida Rural*, 48–52. Available at: https://rica.chil.me/post/sintomas-dispersion-y-danos-del-virus-del-mosaico-de-la-alfalfa-un-virus-muy-ext-223388 [Accessed February 14, 2022].

Fedeles, B. I., Singh, V., Delaney, J. C., Li, D., and Essigmann, J. M. (2015). The AlkB Family of Fe(II)/α-Ketoglutarate-dependent Dioxygenases: Repairing Nucleic Acid Alkylation Damage and Beyond. *J. Biol. Chem.* 290, 20734–20742. doi:10.1074/JBC.R115.656462.

Filomatori, C. V., Lodeiro, M. F., Alvarez, D. E., Samsa, M. M., Pietrasanta, L., and Gamarnik, A. V. (2006). A 5′ RNA element promotes dengue virus RNA synthesis on a circular genome. *Genes Dev.* 20, 2238–2249. doi:10.1101/gad.1444206.

Fros, J. J., Domeradzka, N. E., Baggen, J., Geertsema, C., Flipse, J., Vlak, J. M., et al. (2012). Chikungunya Virus nsP3 Blocks Stress Granule Assembly by Recruitment of G3BP into Cytoplasmic Foci. *J. Virol.* 86, 10873–10879. doi:10.1128/JVI.01506-12/.

Frye, M., Jaffrey, S. R., Pan, T., Rechavi, G., and Suzuki, T. (2016). RNA modifications: what have we learned and where are we headed? *Nat. Rev. Genet. 2016 176* 17, 365–372. doi:10.1038/nrg.2016.47.

Fu, Y., Dominissini, D., Rechavi, G., and He, C. (2014). Gene expression regulation mediated through reversible m 6 A RNA methylation. *Nat. Rev. Genet.* 15, 293–306. doi:10.1038/NRG3724.

Fu, Y., and Zhuang, X. (2020). m6A-binding YTHDF proteins promote stress granule formation. *Nat. Chem. Biol. 2020 169* 16, 955–963. doi:10.1038/s41589-020-0524-y.

Garcia, D., Garcia, S., and Voinnet, O. (2014). Nonsense-Mediated Decay Serves as a General Viral Restriction Mechanism in Plants. *Cell Host Microbe* 16, 391–402. doi:10.1016/J.CHOM.2014.08.001.

Glushkevich, A., Spechenkova, N., Fesenko, I., Knyazev, A., Samarskaya, V., Kalinina, N. O., et al. (2022). Transcriptomic Reprogramming, Alternative Splicing and RNA Methylation in Potato (Solanum tuberosum L.) Plants in Response to Potato Virus Y Infection. *Plants* 11, 635. doi:10.3390/PLANTS11050635.

Gokhale, N. S., McIntyre, A. B. R., McFadden, M. J., Roder, A. E., Kennedy, E. M., Gandara, J. A., et al. (2016). N6-Methyladenosine in Flaviviridae Viral RNA Genomes Regulates Infection. *Cell Host Microbe* 20, 654–665. doi:10.1016/J.CHOM.2016.09.015.

Goldberg, N. (2012). Extension Plant Pathology "News You Can Use." Available at: www.commanster.edu [Accessed February 21, 2022].

Guogas, L. M., Laforest, S. M., and Gehrke, L. (2005). Coat Protein Activation of Alfalfa Mosaic Virus Replication Is Concentration Dependent. *J. Virol.* 79, 5752–5761. doi:10.1128/JVI.79.9.5752-5761.2005/.

Hafrén, A., Eskelin, K., and Mäkinen, K. (2013). Ribosomal Protein P0 Promotes Potato Virus A Infection and Functions in Viral Translation Together with VPg and eIF(iso)4E. *J. Virol.* 87, 4302–4312. doi:10.1128/JVI.03198-12/.

Hafrén, A., Lõhmus, A., and Mäkinen, K. (2015). Formation of Potato Virus A-Induced RNA Granules and Viral Translation Are Interrelated Processes Required for Optimal Virus Accumulation. *PLOS Pathog.* 11, e1005314. doi:10.1371/JOURNAL.PPAT.1005314.

Hao, H., Hao, S., Chen, H., Chen, Z., Zhang, Y., Wang, J., et al. (2019). N6-methyladenosine modification and METTL3 modulate enterovirus 71 replication. *Nucleic Acids Res.* 47, 362–374. doi:10.1093/NAR/GKY1007.

Hashimoto, S. I., and Green, M. (1976). Multiple methylated cap sequences in adenovirus type 2 early mRNA. *J. Virol.* 20.

Haussmann, I. U., Bodi, Z., Sanchez-Moran, E., Mongan, N. P., Archer, N., Fray, R. G., et al. (2016). M6 A potentiates Sxl alternative pre-mRNA splicing for robust Drosophila sex determination. *Nature* 540, 301–304. doi:10.1038/nature20577.

He, F., and Jacobson, A. (2015). Nonsense-Mediated mRNA Decay: Degradation of Defective Transcripts Is Only Part of the Story. *Annu. Rev. Genet.* 49, 339–366. doi:10.1146/ANNUREV-GENET-112414-054639.

He, Y., Li, L., Yao, Y., Li, Y., Zhang, H., and Fan, M. (2021). Transcriptome-wide N6-methyladenosine (m6A) methylation in watermelon under CGMMV infection. *BMC Plant Biol.* 21, 1–14. doi:10.1186/S12870-021-03289-8/FIGURES/7.

Heinlein, M. (2015). Plant virus replication and movement. *Virology* 479–480, 657–671. doi:10.1016/J.VIROL.2015.01.025.

Herranz, M. C., Pallas, V., and Aparicio, F. (2012). Multifunctional roles for the N-terminal basic motif of Alfalfa mosaic virus coat protein: Nucleolar/cytoplasmic shuttling, modulation of RNA-binding activity, and virion formation. *Mol. Plant-Microbe Interact.* 25, 1093–1103. doi:10.1094/MPMI-04-12-0079-R.

Hesser, C. R., Karijolich, J., Dominissini, D., He, C., and Glaunsinger, B. A. (2018). N6-methyladenosine modification and the YTHDF2 reader protein play cell type specific roles in lytic viral gene expression during Kaposi's sarcoma-associated herpesvirus infection. *PLoS Pathog.* 14. doi:10.1371/JOURNAL.PPAT.1006995.

Hill, J. H., and Whitham, S. A. (2014). Control of Virus Diseases in Soybeans. *Adv. Virus Res.* 90, 355–390. doi:10.1016/B978-0-12-801246-8.00007-X.

Hipper, C., Brault, V., Ziegler-Graff, V., and Revers, F. (2013). Viral and cellular factors involved in phloem transport of plant viruses. *Front. Plant Sci.* 4, 154. doi:10.3389/FPLS.2013.00154/BIBTEX.

Hofmann, N. R. (2017). Epitranscriptomics and flowering: MRNA methylation/demethylation regulates flowering time. *Plant Cell* 29, 2949–2950. doi:10.1105/TPC.17.00929.

Hofmann, S., Kedersha, N., Anderson, P., and Ivanov, P. (2021). Molecular mechanisms of stress granule assembly and disassembly. *Biochim. Biophys. Acta - Mol. Cell Res.* 1868, 118876. doi:10.1016/J.BBAMCR.2020.118876.

Hongay, C. F., and Orr-Weaver, T. L. (2011). Drosophila inducer of MEiosis 4 (IME4) is required for Notch signaling during oogenesis. *Proc. Natl. Acad. Sci. U. S. A.* 108, 14855–14860. doi:10.1073/pnas.1111577108.

Hou, Y., Sun, J., Wu, B., Gao, Y., Nie, H., Nie, Z., et al. (2021). CPSF30-L-mediated recognition of mRNA m6A modification controls alternative polyadenylation of nitrate signaling-related gene transcripts in Arabidopsis. *Mol. Plant* 14, 688–699. doi:10.1016/J.MOLP.2021.01.013.

Houwing, C. J., and Jaspars, E. M. J. (1986). Coat protein blocks the in vitro transcription of the virion RNAs of alfalfa mosaic virus. *FEBS Lett.* 209, 284–288. doi:10.1016/0014-5793(86)81128-0.

Hu, J., Cai, J., Park, S. J., Lee, K., Li, Y., Chen, Y., et al. (2021). N6-Methyladenosine mRNA methylation is important for salt stress tolerance in Arabidopsis. *Plant J.* 106, 1759–1775. doi:10.1111/TPJ.15270.

Hu, J., Manduzio, S., and Kang, H. (2019). Epitranscriptomic RNA methylation in plant development and abiotic stress responses. *Front. Plant Sci.* 10, 500. doi:10.3389/fpls.2019.00500.

Huang, J., and Yin, P. (2018). Structural Insights into N6-methyladenosine (m6A) Modification in the Transcriptome. *Genomics, Proteomics Bioinforma.* 16, 85–98. doi:10.1016/j.gpb.2018.03.001.

Hull, R. (2013). *Matthews' Plant Virology.* Academic Press.

Ibrahim, A., Hutchens, H. M., Berg, R. H., and Loesch-Fries, L. S. (2012). Alfalfa mosaic virus replicase proteins, P1 and P2, localize to the tonoplast in the presence of virus RNA. doi:10.1016/j.virol.2012.08.018.

Imai, Y., Matsuo, N., Ogawa, S., Tohyama, M., and Takagi, T. (1998). Cloning of a gene, YT521, for a novel RNA splicing-related protein induced by hypoxia/reoxygenation. *Mol. Brain Res.* 53, 33–40. doi:10.1016/S0169-328X(97)00262-3.

Imam, H., Khan, M., Gokhale, N. S., McIntyre, A. B. R., Kim, G. W., Jang, J. Y., et al. (2018). N6-methyladenosine modification of hepatitis B virus RNA differentially regulates the viral life cycle.

Proc. Natl. Acad. Sci. U. S. A. 115, 8829–8834. doi:10.1073/PNAS.1808319115.

Ivanov, P., Kedersha, N., and Anderson, P. (2019). Stress Granules and Processing Bodies in Translational Control. *Cold Spring Harb. Perspect. Biol.* 11, a032813. doi:10.1101/CSHPERSPECT.A032813.

Iwanowski, D. (1892). Concerning the mosaic disease of the tobacco plant. *St Petersb Acad Imp Sci Bul* 35, 67–70. Available at: https://www.apsnet.org/edcenter/apsnetfeatures/Documents/2008/Ivanowski1892.pdf [Accessed February 10, 2022].

Jaspars, E. M. J. (2014). Genome activation in alfamo- and ilarviruses. *Arch. Virol. 1999 1445* 144, 843–863. doi:10.1007/S007050050551.

Jia, G., Fu, Y., Zhao, X., Dai, Q., Zheng, G., Yang, Y., et al. (2011). N6-Methyladenosine in nuclear RNA is a major substrate of the obesity-associated FTO. *Nat. Chem. Biol.* 7, 885–887. doi:10.1038/nchembio.687.

Jonas, S., and Izaurralde, E. (2013). The role of disordered protein regions in the assembly of decapping complexes and RNP granules. *Genes Dev.* 27, 2628–2641. doi:10.1101/gad.227843.113.

Jones, R. (2014). Plant virus ecology and epidemiology: historical perspectives, recent progress and future prospects. *Ann. Appl. Biol.* 164, 320–347. doi:10.1111/AAB.12123.

Jones, R. A. C. (2009). Plant virus emergence and evolution: Origins, new encounter scenarios, factors driving emergence, effects of changing world conditions, and prospects for control. *Virus Res.* 141, 113–130. doi:10.1016/J.VIRUSRES.2008.07.028.

Jones, R. A. C. (2016). Future Scenarios for Plant Virus Pathogens as Climate Change Progresses. *Adv. Virus Res.* 95, 87–147. doi:10.1016/BS.AIVIR.2016.02.004.

Jones, R. A. C., and Naidu, R. A. (2019). Global Dimensions of Plant Virus Diseases: Current Status and Future Perspectives. *Annu. Rev. Virol.* 6, 387–409. doi:10.1146/ANNUREV-VIROLOGY-092818-015606.

Jouannet, V., Moreno, A. B., Elmayan, T., Vaucheret, H., Crespi, M. D., and Maizel, A. (2012). Cytoplasmic Arabidopsis AGO7 accumulates in membrane-associated siRNA bodies and is required for ta-siRNA biogenesis. *EMBO J.* 31, 1704. doi:10.1038/EMBOJ.2012.20.

Jurczyszak, D., Zhang, W., Terry, S. N., Kehrer, T., Bermúdez González, M. C., McGregor, E., et al. (2020). HIV protease cleaves the antiviral m6A reader protein YTHDF3 in the viral particle. *PLOS Pathog.* 16, e1008305. doi:10.1371/JOURNAL.PPAT.1008305.

Kane, S. E., and Beemon, K. (1985). Precise localization of m6A in Rous sarcoma virus RNA reveals clustering of methylation sites: implications for RNA processing. *Mol. Cell. Biol.* 5, 2298–2306. doi:10.1128/mcb.5.9.2298.

Karikó, K., Buckstein, M., Ni, H., and Weissman, D. (2005). Suppression of RNA recognition by Toll-like receptors: The impact of nucleoside modification and the evolutionary origin of RNA. *Immunity* 23, 165–175. doi:10.1016/J.IMMUNI.2005.06.008/.

Kasteel, D. T. J., Van Der Wel, N. N., Jansen, K. A. J., Goldbach, R. W., and Van Lent, J. W. M. (1997). Tubule-forming capacity of the movement proteins of alfalfa mosaic virus and brome mosaic virus. *J. Gen. Virol.* 78 (Pt 8), 2089–2093. doi:10.1099/0022-1317-78-8-2089.

Kawai, Y., Ono, E., and Mizutani, M. (2014). Evolution and diversity of the 2-oxoglutarate-dependent dioxygenase superfamily in plants. *Plant J.* 78, 328–343. doi:10.1111/tpj.12479.

Ke, S., Alemu, E. A., Mertens, C., Gantman, E. C., Fak, J. J., Mele, A., et al. (2015). A majority of m6A residues are in the last exons, allowing the potential for 3'UTR regulation. *Genes Dev.* 29, 2037–2053. doi:10.1101/gad.269415.115.9.

Kennedy, E. M., Bogerd, H. P., Kornepati, A. V. R., Kang, D., Ghoshal, D., Marshall, J. B., et al. (2016). Posttranscriptional m6A Editing of HIV-1 mRNAs Enhances Viral Gene Expression. *Cell Host Microbe* 19, 675–685. doi:10.1016/J.CHOM.2016.04.002.

Kenyon, L., Kumar, S., Tsai, W. S., and Hughes, J. d. A. (2014). Virus Diseases of Peppers (Capsicum spp.) and Their Control. *Adv. Virus Res.* 90, 297–354. doi:10.1016/B978-0-12-801246-8.00006-8.

Khaperskyy, D. A., Hatchette, T. F., and McCormick, C. (2012). Influenza A virus inhibits cytoplasmic stress granule formation. *FASEB J.* 26, 1629–1639. doi:10.1096/FJ.11-196915.

Kim, B., Arcos, S., Rothamel, K., Jian, J., Rose, K. L., McDonald, W. H., et al. (2020). Discovery of Widespread Host Protein Interactions with the Pre-replicated Genome of CHIKV Using VIR-CLASP. *Mol. Cell* 78, 624–640. doi:10.1016/J.MOLCEL.2020.04.013/.

Koch, R. (1882). The etiology of tuberculosis. *Berliner Klin. Wocbenschift* 15, 109–115. Available at: http://materiais.dbio.uevora.pt/Micro/Classicos.pdf [Accessed February 10, 2022].

Kollist, H., Zandalinas, S. I., Sengupta, S., Nuhkat, M., Kangasjärvi, J., and Mittler, R. (2019). Rapid Responses to Abiotic Stress: Priming the Landscape for the Signal Transduction Network. *Trends Plant Sci.* 24, 25–37. doi:10.1016/J.TPLANTS.2018.10.003.

Koper-Zwarthoff, E. C., Brederod, F. T., Walstra, P., and Bol, J. F. (1979). Nucleotide sequence of the 3′-noncoding region of alfalfa mosaic virus RNA 4 and its homology with the genomic RNAs. *Nucleic Acids Res.* 7, 1887–1900. doi:10.1093/nar/7.7.1887.

Krab, I. M., Caldwell, C., Gallie, D. R., and Bol, J. F. (2005). Coat protein enhances translational efficiency of Alfalfa mosaic virus RNAs and interacts with the elF4G component of initiation factor elF4F. *J. Gen. Virol.* 86, 1841–1849. doi:10.1099/VIR.0.80796-0.

Krapp, S., Greiner, E., Amin, B., Sonnewald, U., and Krenz, B. (2017). The stress granule component G3BP is a novel interaction partner for the nuclear shuttle proteins of the nanovirus pea necrotic yellow dwarf virus and geminivirus abutilon mosaic virus. *Virus Res.* 227, 6–14. doi:10.1016/J.VIRUSRES.2016.09.021.

Krug, R. M., Morgan, M. A., and Shatkin, A. J. (1976). Influenza viral mRNA contains internal N6-methyladenosine and 5'-terminal 7-methylguanosine in cap structures. *J. Virol.* 20, 45–53. doi:10.1128/JVI.20.1.45-53.1976.

Kumakura, N., Takeda, A., Fujioka, Y., Motose, H., Takano, R., and Watanabe, Y. (2009). SGS3 and RDR6 interact and colocalize in cytoplasmic SGS3/RDR6-bodies. *FEBS Lett.* 583, 1261–1266. doi:10.1016/J.FEBSLET.2009.03.055.

Kumar, S., and Mohapatra, T. (2021). Deciphering Epitranscriptome: Modification of mRNA Bases Provides a New Perspective for Post-transcriptional Regulation of Gene Expression. *Front. Cell Dev. Biol.* 9, 550. doi:10.3389/FCELL.2021.628415/BIBTEX.

Lang, F., Singh, R. K., Pei, Y., Zhang, S., Sun, K., and Robertson, E. S. (2019). EBV epitranscriptome reprogramming by METTL14 is critical for viral-associated tumorigenesis. *PLOS Pathog.* 15, e1007796. doi:10.1371/JOURNAL.PPAT.1007796.

Latham, L. J., Jones, R. A. C., and Coutts, B. A. (2004). Yield losses caused by virus infection in four combinations of non-persistently aphid-transmitted virus and cool-season crop legume. *Aust. J. Exp. Agric.* 44, 57–63. doi:10.1071/EA03060.

Lavi, S., and Shatkin, A. J. (1975). Methylated simian virus 40 specific RNA from nuclei and cytoplasm of infected BSC 1 cells. *Proc. Natl. Acad. Sci. U. S. A.* 72, 2012–2016. doi:10.1073/pnas.72.6.2012.

Lence, T., Akhtar, J., Bayer, M., Schmid, K., Spindler, L., Ho, C. H., et al. (2016). M6A modulates neuronal functions and sex determination in Drosophila. *Nature* 540, 242–247. doi:10.1038/NATURE20568.

Li, D., Zhang, H., Hong, Y., Huang, L., Li, X., Zhang, Y., et al. (2014). Genome-Wide Identification, Biochemical Characterization, and Expression Analyses of the YTH Domain-Containing RNA-Binding Protein Family in Arabidopsis and Rice. *Plant Mol. Biol. Report.* 32, 1169–1186. doi:10.1007/s11105-014-0724-2.

Li, F., and Wang, A. (2018). RNA decay is an antiviral defense in plants that is counteracted by viral RNA silencing suppressors. *PLOS Pathog.* 14, e1007228. doi:10.1371/JOURNAL.PPAT.1007228.

Li, Z., Shi, J., Yu, L., Zhao, X., Ran, L., Hu, D., et al. (2018). N 6 -methyl-adenosine level in Nicotiana tabacum is associated with tobacco mosaic virus. *Virol. J.* 15. doi:10.1186/S12985-018-0997-4.

Lichinchi, G., Gao, S., Saletore, Y., Gonzalez, G. M., Bansal, V., Wang, Y., et al. (2016a). Dynamics of the human and viral m(6)A RNA methylomes during HIV-1 infection of T cells. *Nat. Microbiol.* 1, 16011. doi:10.1038/nmicrobiol.2016.11.

Lichinchi, G., Zhao, B. S., Wu, Y., Lu, Z., Qin, Y., He, C., et al. (2016b). Dynamics of Human and Viral RNA Methylation during Zika Virus Infection. *Cell Host Microbe* 20, 666–673. doi:10.1016/j.chom.2016.10.002.

Linder, B., and Jaffrey, S. R. (2019a). Discovering and mapping the modified nucleotides that comprise the epitranscriptome of mrna. *Cold Spring Harb. Perspect. Biol.* 11. doi:10.1101/CSHPERSPECT.A032201.

Linder, B., and Jaffrey, S. R. (2019b). Discovering and Mapping the Modified Nucleotides That Comprise the Epitranscriptome of mRNA. *Cold Spring Harb. Perspect. Biol.* 11. doi:10.1101/CSHPERSPECT.A032201.

Liu, J., Xu, Y. P., Li, K., Ye, Q., Zhou, H. Y., Sun, H., et al. (2021). The m6A methylome of SARS-CoV-2 in host cells. *Cell Res.* 31, 404–414. doi:10.1038/S41422-020-00465-7.

Liu, J., Yue, Y., Han, D., Wang, X., Fu, Y., Zhang, L., et al. (2014). A METTL3-METTL14 complex mediates mammalian nuclear RNA N6-adenosine methylation. *Nat. Chem. Biol.* 10, 93–95. doi:10.1038/nchembio.1432.

Liu, J., Yue, Y., Liu, J., Cui, X., Cao, J., Luo, G., et al. (2018). VIRMA mediates preferential m6A mRNA methylation in 3′UTR and near stop codon and associates with alternative polyadenylation. *Cell Discov. 2018 41* 4, 1–17. doi:10.1038/s41421-018-0019-0.

Liu, N., Dai, Q., Zheng, G., He, C., Parisien, M., and Pan, T. (2015). N6 -methyladenosine-dependent RNA structural switches regulate RNA-protein interactions. *Nature* 518, 560–564. doi:10.1038/NATURE14234.

Liu, N., Zhou, K. I., Parisien, M., Dai, Q., Diatchenko, L., and Pan, T. (2017). N6-methyladenosine alters RNA structure to regulate binding of a low-complexity protein. *Nucleic Acids Res.* 45, 6051–6063. doi:10.1093/NAR/GKX141.

Liu, Y., You, Y., Lu, Z., Yang, J., Li, P., Liu, L., et al. (2019). N6-methyladenosine RNA modification–mediated cellular metabolism rewiring inhibits viral replication. *Science.).* 365, 1171–1176. doi:10.1126/science.aax4468.

Lu, M., Zhang, Z., Xue, M., Zhao, B. S., Harder, O., Li, A., et al. (2020). N6-methyladenosine modification enables viral RNA to escape recognition by RNA sensor RIG-I. *Nat. Microbiol. 2020 54* 5, 584–598. doi:10.1038/s41564-019-0653-9.

Luo, G.-Z., MacQueen, A., Zheng, G., Duan, H., Dore, L. C., Lu, Z., et al. (2014). Unique features of the m 6 A methylome in Arabidopsis thaliana. *Nat. Commun. 2014 51* 5, 1–8. doi:10.1038/ncomms6630.

Luo, S., and Tong, L. (2014). Molecular basis for the recognition of methylated adenines in RNA by the eukaryotic YTH domain. *Proc. Natl. Acad. Sci. U. S. A.* 111, 13834–13839. doi:10.1073/PNAS.1412742111.

Luo, Y., Na, Z., and Slavoff, S. A. (2018). P-Bodies: Composition, Properties, and Functions. *Biochemistry* 57, 2424–2431. doi:10.1021/ACS.BIOCHEM.7B01162.

Ma, H., Wang, X., Cai, J., Dai, Q., Natchiar, S. K., Lv, R., et al. (2019). N 6-Methyladenosine methyltransferase ZCCHC4 mediates ribosomal RNA methylation. *Nat. Chem. Biol.* 15, 88–94. doi:10.1038/S41589-018-0184-3.

Ma, X., Nicole, M. C., Meteignier, L. V., Hong, N., Wang, G., and Moffett, P. (2015). Different roles for RNA silencing and RNA processing components in virus recovery and virus-induced gene silencing in plants. *J. Exp. Bot.* 66, 919–932. doi:10.1093/JXB/ERU447.

Mäkinen, K., Lõhmus, A., and Pollari, M. (2017). Plant RNA regulatory network and RNA granules in virus infection. *Front. Plant Sci.* 8, 2093. doi:10.3389/FPLS.2017.02093/.

Makkouk, K., Pappu, H., and Kumari, S. G. (2012). Virus Diseases of Peas, Beans, and Faba Bean in the Mediterranean Region. *Adv. Virus Res.* 84, 367–402. doi:10.1016/B978-0-12-394314-9.00011-7.

Manners, O., Baquero-Perez, B., and Whitehouse, A. (2019). m 6 A: Widespread regulatory control in virus replication. *Biochim. Biophys. Acta - Gene Regul. Mech.* 1862, 370–381. doi:10.1016/J.BBAGRM.2018.10.015.

Marsh, L. E., Pogue, G. P., and Hall, T. C. (1989). Similarities among plant virus (+) and (−) RNA termini imply a common ancestry with promoters of eukaryotic tRNAs. *Virology* 172, 415–427. doi:10.1016/0042-6822(89)90184-0.

Martínez-Pérez, M. (2016). Una proteína de Arabidopsis thaliana perteneciente a la familia AlkB de dioxigenasas dependientes de hierro (II) y 2-oxoglutarato interfiere en el ciclo infeccioso del virus del

mosaico de la alfalfa. Trabajo Fin de Master. UPV.
Martínez-Pérez, M. (2020). Involvement of the host RNA N 6-adenosine methylation (m6A) pathway in the infection cycle of Alfalfa mosaic virus. Doctoral Thesis.
Martínez-Pérez, M., Aparicio, F., López-Gresa, M. P., Bellés, J. M., Sánchez-Navarro, J. A., and Pallás, V. (2017). Arabidopsis m6A demethylase activity modulates viral infection of a plant virus and the m6A abundance in its genomic RNAs. *Proc. Natl. Acad. Sci. U. S. A.* 114, 10755–10760. doi:10.1073/pnas.1703139114.
Martínez-Pérez, M., Gómez-Mena, C., Alvarado-Marchena, L., Nadi, R., Micol, J. L., Pallas, V., et al. (2021). The m6A RNA Demethylase ALKBH9B Plays a Critical Role for Vascular Movement of Alfalfa Mosaic Virus in Arabidopsis. *Front. Microbiol.* 12. doi:10.3389/FMICB.2021.745576.
Martínez De Alba, A. E., Moreno, A. B., Gabriel, M., Mallory, A. C., Christ, A., Bounon, R., et al. (2015). In plants, decapping prevents RDR6-dependent production of small interfering RNAs from endogenous mRNAs. *Nucleic Acids Res.* 43, 2902–2913. doi:10.1093/nar/gkv119.
Maruri-López, I., Figueroa, N. E., Hernández-Sánchez, I. E., and Chodasiewicz, M. (2021). Plant Stress Granules: Trends and Beyond. *Front. Plant Sci.* 12, 1538. doi:10.3389/FPLS.2021.722643/BIBTEX.
McFadden, M. J., Gokhale, N. S., and Horner, S. M. (2017). Protect this house: cytosolic sensing of viruses. *Curr. Opin. Virol.* 22, 36–43. doi:10.1016/J.COVIRO.2016.11.012.
McFadden, M. J., and Horner, S. M. (2021). N6-Methyladenosine Regulates Host Responses to Viral Infection. *Trends Biochem. Sci.* 46, 366–377. doi:10.1016/J.TIBS.2020.11.008.
Mendel, M., Chen, K. M., Homolka, D., Gos, P., Pandey, R. R., McCarthy, A. A., et al. (2018). Methylation of Structured RNA by the m6A Writer METTL16 Is Essential for Mouse Embryonic Development. *Mol. Cell* 71, 986-1000.e11. doi:10.1016/j.molcel.2018.08.004.
Meteignier, L. V., Zhou, J., Cohen, M., Bhattacharjee, S., Brosseau, C., Caamal Chan, M. G., et al. (2016). NB-LRR signaling induces translational repression of viral transcripts and the formation of RNA processing bodies through mechanisms differing from those activated by UV stress and RNAi. *J. Exp. Bot.* 67, 2353–2366. doi:10.1093/JXB/ERW042.
Meyer, K. D., and Jaffrey, S. R. (2017). Rethinking m 6 A Readers, Writers, and Erasers. *Annu. Rev. Cell Dev. Biol.* doi:10.1146/annurev-cellbio-100616.
Meyer, K. D., Saletore, Y., Zumbo, P., Elemento, O., Mason, C. E., and Jaffrey, S. R. (2012). Comprehensive analysis of mRNA methylation reveals enrichment in 3′ UTRs and near stop codons. *Cell* 149, 1635–1646. doi:10.1016/j.cell.2012.05.003.
Miao, Z., Zhang, T., Qi, Y., Song, J., Han, Z., and Ma, C. (2020). Evolution of the RNA N6-methyladenosine methylome mediated by genomic duplication. *Plant Physiol.* 182, 345–360. doi:10.1104/PP.19.00323.
Mielecki, D., Zugaj, D. Ł., Muszewska, A., Piwowarski, J., Chojnacka, A., Mielecki, M., et al. (2012). Novel AlkB Dioxygenases—Alternative Models for In Silico and In Vivo Studies. *PLoS One* 7, e30588. doi:10.1371/journal.pone.0030588.
Mishima, Y., and Tomari, Y. (2016). Codon Usage and 3' UTR Length Determine Maternal mRNA Stability in Zebrafish. *Mol. Cell* 61, 874–885. doi:10.1016/J.MOLCEL.2016.02.027.
Molinie, B., Wang, J., Lim, K. S., Hillebrand, R., Lu, Z. X., Van Wittenberghe, N., et al. (2016). m6A-LAIC-seq reveals the census and complexity of the m6A epitranscriptome. *Nat. Methods 2016 138* 13, 692–698. doi:10.1038/nmeth.3898.
Moreno, A., and Fereres, A. (2012). Virus Diseases in Lettuce in the Mediterranean Basin. *Adv. Virus Res.* 84, 247–288. doi:10.1016/B978-0-12-394314-9.00007-5.
Moreno, P., Medina, V., and Romero, J. (2016). "Virus: aspectos generales," in *Enfermedades de plantas causadas por virus y viroides*, eds. M. A. Ayllón, M. Cambra, C. Llave, and E. Moriones, 25–48.
Moss, B., Gershowitz, A., Stringer, J. R., Holland, L. E., and Wagner, E. K. (1977). 5'-Terminal and internal methylated nucleosides in herpes simplex virus type 1 mRNA. *J. Virol.* 23, 234–239. doi:10.1128/JVI.23.2.234-239.1977.
Moury, B., and Verdin, E. (2012). Viruses of Pepper Crops in the Mediterranean Basin: A Remarkable Stasis. *Adv. Virus Res.* 84, 127–162. doi:10.1016/B978-0-12-394314-9.00004-X.
Navarro, J. A., Sanchez-Navarro, J. A., and Pallas, V. (2019). Key checkpoints in the movement of plant

viruses through the host. *Adv. Virus Res.* 104, 1–64. doi:10.1016/BS.AIVIR.2019.05.001.

Nechushtai, R., Conlan, A. R., Harir, Y., song, L., yogev, ohad, Eisenberg-Domovich, Y., et al. (2012). Characterization of Arabidopsis NEET Reveals an Ancient Role for NEET Proteins in Iron Metabolism. *Plant Cell* 24, 2139–2154. doi:10.1105/TPC.112.097634.

Oerum, S., Meynier, V., Catala, M., and Tisne, C. (2021). A comprehensive review of m6A/m6Am RNA methyltransferase structures. *Nucleic Acids Res.* 49, 7239–7255. doi:10.1093/NAR/GKAB378.

Ok, S. H., Jeong, H. J., Bae, J. M., Shin, J. S., Luan, S., and Kim, K. N. (2005). Novel CIPK1-associated proteins in Arabidopsis contain an evolutionarily conserved C-terminal region that mediates nuclear localization. *Plant Physiol.* 139, 138–150. doi:10.1104/PP.105.065649.

Olsthoorn, R., and Bol, J. (2002). Role of an essential triloop hairpin and flanking structures in the 3' untranslated region of Alfalfa mosaic virus RNA in in vitro transcription. *J. Virol.* 76, 8747–8756. doi:10.1128/JVI.76.17.8747-8756.2002.

Olsthoorn, R. C. L., Haasnoot, P. C. J., and Bol, J. F. (2004). Similarities and Differences between the Subgenomic and Minus-Strand Promoters of an RNA Plant Virus. *J. Virol.* 78, 4048–4053. doi:10.1128/JVI.78.8.4048-4053.2004.

Olsthoorn, R. C. L., Mertens, S., Brederode, F. T., and Bol, J. F. (1999). A conformational switch at the 3' end of a plant virus RNA regulates viral replication. *EMBO J.* 18, 4856–4864. doi:10.1093/emboj/18.17.4856.

Pallas, V., Aparicio, F., Herranz, M. C., Sanchez-Navarro, J. A., and Scott, S. W. (2013). "The Molecular Biology of Ilarviruses," in *Advances in Virus Research* (Academic Press Inc.), 139–181. doi:10.1016/B978-0-12-407698-3.00005-3.

Pallas, V., and García, J. A. (2011). How do plant viruses induce disease? Interactions and interference with host components. *J. Gen. Virol.* 92, 2691–2705. doi:10.1099/VIR.0.034603-0/CITE/REFWORKS.

Pandey, N., Niranjan, B., Williams, A., Sun, J., Brown, V., Bond, U., et al. (1994). Point Mutations in the Stem-Loop at the 3' End of Mouse Histone mRNA Reduce Expression by Reducing the Efficiency of 3' End Formation. *Mol. Cell. Biol.* 14, 1709–1720.

Parrella, G., Lanave, C., Marchoux, G., Finetti Sialer, M. M., Di Franco, A., and Gallitelli, D. (2000). Evidence for two distinct subgroups of Alfalfa mosaic virus (AMV) from France and Italy and their relationships with other AMV strains. *Arch. Virol. 2000 14512* 145, 2659–2667. doi:10.1007/S007050070014.

Pathipanowat, W., Jones, R. A. C., and Sivasithamparam, K. (1995). Studies on seed and pollen transmission of Alfalfa Mosaic, Cucumber Mosaic and Bean Yellow Mosaic Viruses in cultivars and accesions of annual Medicago species. *Aust. J. Agric. Res.* 46, 153–165. doi:10.1071/AR9950153.

Peiro, A., Izquierdo-Garcia, A. C., Sanchez-Navarro, J. A., Pallas, V., Mulet, J. M., and Aparicio, F. (2014). Patellins 3 and 6, two members of the Plant Patellin family, interact with the movement protein of Alfalfa mosaic virus and interfere with viral movement. *Mol. Plant Pathol.* 15, 881–891. doi:10.1111/MPP.12146.

Pendleton, K. E., Chen, B., Liu, K., Hunter, O. V., Xie, Y., Tu, B. P., et al. (2017). The U6 snRNA m6A Methyltransferase METTL16 Regulates SAM Synthetase Intron Retention. *Cell* 169, 824-835.e14. doi:10.1016/J.CELL.2017.05.003.

Pinto, R., Vågbø, C. B., Jakobsson, M. E., Kim, Y., Baltissen, M. P., O'Donohue, M. F., et al. (2020). The human methyltransferase ZCCHC4 catalyses N6-methyladenosine modification of 28S ribosomal RNA. *Nucleic Acids Res.* 48, 830–846. doi:10.1093/NAR/GKZ1147.

Pontier, D., Picart, C., El Baidouri, M., Roudier, F., Xu, T., Lahmy, S., et al. (2019). The m6A pathway protects the transcriptome integrity by restricting RNA chimera formation in plants. *Life Sci. Alliance* 2. doi:10.26508/lsa.201900393.

Price, A. M., Hayer, K. E., McIntyre, A. B. R., Gokhale, N. S., Abebe, J. S., Della Fera, A. N., et al. (2020). Direct RNA sequencing reveals m6A modifications on adenovirus RNA are necessary for efficient splicing. *Nat. Commun.* 11. doi:10.1038/S41467-020-19787-6.

Protter, D. S. W., and Parker, R. (2016). Principles and Properties of Stress Granules. *Trends Cell Biol.* 26, 668–679. doi:10.1016/j.tcb.2016.05.004.

Qiu, W., Zhang, Q., Zhang, R., Lu, Y., Wang, X., Tian, H., et al. (2021). N 6-methyladenosine RNA modification suppresses antiviral innate sensing pathways via reshaping double-stranded RNA. *Nat. Commun.* 12. doi:10.1038/S41467-021-21904-Y.

Reineke, L. C., and Lloyd, R. E. (2013). Diversion of stress granules and P-bodies during viral infection. *Virology* 436, 255–267. doi:10.1016/J.VIROL.2012.11.017.

Ren, W., Lu, J., Huang, M., Gao, L., Li, D., Greg Wang, G., et al. (2019). Structure and regulation of ZCCHC4 in m6A-methylation of 28S rRNA. *Nat. Commun.* 10. doi:10.1038/S41467-019-12923-X.

Reusken, C. B. E. M., and Bol, J. F. (1996). Structural elements of the 3'-terminal coat protein binding site in alfalfa mosaic virus RNAs. *Nucleic Acids Res.* 24, 2660. doi:10.1093/NAR/24.14.2660.

Ries, R. J., Zaccara, S., Klein, P., Olarerin-George, A., Namkoong, S., Pickering, B. F., et al. (2019). m6A enhances the phase separation potential of mRNA. *Nature* 571, 424–428. doi:10.1038/s41586-019-1374-1.

Rodríguez Úbeda, J. (2020). Estudios sobre la implicación de la metilación m6A en la regulación del ciclo infectivo del Virus del Mosaico de la Alfalfa (AMV). Trabajo Fin de Master. UPV.

Roundtree, I. A., Luo, G. Z., Zhang, Z., Wang, X., Zhou, T., Cui, Y., et al. (2017). YTHDC1 mediates nuclear export of N6-methyladenosine methylated mRNAs. *Elife* 6. doi:10.7554/ELIFE.31311.

Rubio-Costa, P. (2021). Identificación y análisis filogenético de los dominios alkb de las replicasas de virus de plantas. Trabajo Fin de Grado UPV.

Rubio, R. M., Depledge, D. P., Bianco, C., Thompson, L., and Mohr, I. (2018). RNA m 6 A modification enzymes shape innate responses to DNA by regulating interferon β. *Genes Dev.* 32, 1472–1484. doi:10.1101/GAD.319475.118/-/DC1.

Růžička, K., Zhang, M., Campilho, A., Bodi, Z., Kashif, M., Saleh, M., et al. (2017). Identification of factors required for m6A mRNA methylation in Arabidopsis reveals a role for the conserved E3 ubiquitin ligase HAKAI. *New Phytol.* 215, 157–172. doi:10.1111/nph.14586.

Saletore, Y., Meyer, K., Korlach, J., Vilfan, I. D., Jaffrey, S., and Mason, C. E. (2012). The birth of the Epitranscriptome: deciphering the function of RNA modifications. *Genome Biol.* 13, 175. doi:10.1186/GB-2012-13-10-175/FIGURES/5.

Samira, R., Li, B., Kliebenstein, D., Li, C., Davis, E., Gillikin, J. W., et al. (2018). The bHLH transcription factor ILR3 modulates multiple stress responses in Arabidopsis. *Plant Mol. Biol.* 97, 297–309. doi:10.1007/S11103-018-0735-8/FIGURES/8.

Samson, L., and Cairns, J. (1977). A new pathway for DNA repair in Escherichia coli [36]. *Nature*. doi:10.1038/267281a0.

Sánchez-Navarro, J. A., and Bol, J. F. (2001). Role of the alfalfa mosaic virus movement protein and coat protein in virus transport. *Mol. Plant. Microbe. Interact.* 14, 1051–1062. doi:10.1094/MPMI.2001.14.9.1051.

Sánchez-Navarro, J. A., Carmen Herranz, M., and Pallás, V. (2006). Cell-to-cell movement of Alfalfa mosaic virus can be mediated by the movement proteins of Ilar-, bromo-, cucumo-, tobamo- and comoviruses and does not require virion formation. *Virology* 346, 66–73. doi:10.1016/J.VIROL.2005.10.024.

Schwartz, S., Mumbach, M. R., Jovanovic, M., Wang, T., Maciag, K., Bushkin, G. G., et al. (2014). Perturbation of m6A writers reveals two distinct classes of mRNA methylation at internal and 5' sites. *Cell Rep.* 8, 284–296. doi:10.1016/J.CELREP.2014.05.048.

Scutenaire, J., Deragon, J. M., Jean, V., Benhamed, M., Raynaud, C., Favory, J. J., et al. (2018). The YTH domain protein ECT2 is an m6A reader required for normal trichome branching in arabidopsis. *Plant Cell* 30, 986–1005. doi:10.1105/TPC.17.00854.

Seo, J.-K., Kim, K.-H., Seo, J.-K., and Kim, K.-H. (2016). Long-Distance Movement of Viruses in Plants. *Curr. Res. Top. Plant Virol.*, 153–172. doi:10.1007/978-3-319-32919-2_6.

Sereno, E. (2020). España se consolida como el segundo exportador de alfalfa deshidratada en el mundo. Available at: https://www.eleconomista.es/aragon/noticias/10308827/01/20/Espana-se-consolida-como-el-segundo-exportador-de-alfalfa-deshidratada-en-el-mundo.html [Accessed February 11, 2022].

Shen, L., Liang, Z., Gu, X., Chen, Y., Teo, Z. W. N., Hou, X., et al. (2016). N6-Methyladenosine RNA Modification Regulates Shoot Stem Cell Fate in Arabidopsis. *Dev. Cell* 38, 186–200.

doi:10.1016/J.DEVCEL.2016.06.008.
Shi, H., Wang, X., Lu, Z., Zhao, B. S., Ma, H., Hsu, P. J., et al. (2017). YTHDF3 facilitates translation and decay of N 6-methyladenosine-modified RNA. *Cell Res.* 27, 315–328. doi:10.1038/CR.2017.15.
Shima, H., Matsumoto, M., Ishigami, Y., Ebina, M., Muto, A., Sato, Y., et al. (2017). S-Adenosylmethionine Synthesis Is Regulated by Selective N6-Adenosine Methylation and mRNA Degradation Involving METTL16 and YTHDC1. *Cell Rep.* 21, 3354–3363. doi:10.1016/J.CELREP.2017.11.092.
Shoaib, Y., Usman, B., Kang, H., and Jung, K.-H. (2022). Epitranscriptomics: An Additional Regulatory Layer in Plants' Development and Stress Response. *Plants* 11, 1033. doi:10.3390/PLANTS11081033.
Smith, I. (1991). *Manual de enfermedades de las plantas*. Mundi-Pren.
Tan, B., and Gao, S. J. (2018). RNA epitranscriptomics: Regulation of infection of RNA and DNA viruses by N6-methyladenosine (m6A). *Rev. Med. Virol.* 28, e1983. doi:10.1002/RMV.1983.
Tan, B., Liu, H., Zhang, S., Da Silva, S. R., Zhang, L., Meng, J., et al. (2018). Viral and cellular N 6-methyladenosine and N 6,2'-O-dimethyladenosine epitranscriptomes in the KSHV life cycle. *Nat. Microbiol.* 3, 108–120. doi:10.1038/S41564-017-0056-8.
Taylor, M. W. (2014). Introduction: A Short History of Virology. *Viruses Man A Hist. Interact.*, 1. doi:10.1007/978-3-319-07758-1_1.
Tenllado, F., and Bol, J. F. (2000). Genetic dissection of the multiple functions of alfalfa mosaic virus coat protein in viral RNA replication, encapsidation, and movement. *Virology* 268, 29–40. doi:10.1006/VIRO.1999.0170.
Theler, D., Dominguez, C., Blatter, M., Boudet, J., and Allain, F. H. T. (2014). Solution structure of the YTH domain in complex with N6-methyladenosine RNA: A reader of methylated RNA. *Nucleic Acids Res.* 42, 13911–13919. doi:10.1093/NAR/GKU1116.
Thomas, P. E., Wu, X., Liu, M., Gaffney, B., Ji, G., Li, Q. Q., et al. (2012). Genome-wide control of polyadenylation site choice by CPSF30 in arabidopsisC W OA. *Plant Cell* 24, 4376–4388. doi:10.1105/TPC.112.096107.
Tian, S., Wu, N., Zhang, L., and Wang, X. (2021). RNA N6-methyladenosine modification suppresses replication of rice black streaked dwarf virus and is associated with virus persistence in its insect vector. *Mol. Plant Pathol.* 22, 1070–1081. doi:10.1111/MPP.13097.
Tirumuru, N., Zhao, B. S., Lu, W., Lu, Z., He, C., and Wu, L. (2016). N6-methyladenosine of HIV-1 RNA regulates viral infection and HIV-1 Gag protein expression. *Elife* 5. doi:10.7554/eLife.15528.
Tsai, K., Courtney, D. G., and Cullen, B. R. (2018). Addition of m6A to SV40 late mRNAs enhances viral structural gene expression and replication. *PLOS Pathog.* 14, e1006919. doi:10.1371/JOURNAL.PPAT.1006919.
van den Born, E., Omelchenko, M. V., Bekkelund, A., Leihne, V., Koonin, E. V., Dolja, V. V., et al. (2008). Viral AlkB proteins repair RNA damage by oxidative demethylation. *Nucleic Acids Res.* 36, 5451–5461. doi:10.1093/nar/gkn519.
Van der Vossen, E., and Bol, J. (1996). Analysis of Cis-Acting Elements in the 5' Leader Sequence of Alfalfa Mosaic Virus RNA 3. *Virology* 220, 539–543.
Van Pelt-Heerschap, H., Verbeek, H., Willem, J., and Van Vloten-Doting, L. (1988). The location of coat protein and viral RNAs of alfalfa mosaic virus in infected tobacco leaves and protoplasts. *Virology* 160, 297–300.
Van Tran, N., Muller, L., Ross, R. L., Lestini, R., Létoquart, J., Ulryck, N., et al. (2018). Evolutionary insights into Trm112-methyltransferase holoenzymes involved in translation between archaea and eukaryotes. *Nucleic Acids Res.* 46, 8483–8499. doi:10.1093/NAR/GKY638.
Varadi, M., Zsolyomi, F., Guharoy, M., Tompa, P., and Levy, Y. K. (2015). Functional advantages of conserved intrinsic disorder in RNA-binding proteins. *PLoS One* 10. doi:10.1371/journal.pone.0139731.
Vespa, L., Vachon, G., Berger, F., Perazza, D., Faure, J. D., and Herzog, M. (2004). The Immunophilin-Interacting Protein AtFIP37 from Arabidopsis Is Essential for Plant Development and Is Involved in Trichome Endoreduplication. *Plant Physiol.* 134, 1283. doi:10.1104/PP.103.028050.
Wan, Y., Tang, K., Zhang, D., Xie, S., Zhu, X., Wang, Z., et al. (2015). Transcriptome-wide high-throughput

deep m6A-seq reveals unique differential m6A methylation patterns between three organs in Arabidopsis thaliana. *Genome Biol.* 16. doi:10.1186/S13059-015-0839-2.

Wang, C., Yang, J., Song, P., Zhang, W., Lu, Q., Yu, Q., et al. (2022). FIONA1 is an RNA N6-methyladenosine methyltransferase affecting Arabidopsis photomorphogenesis and flowering. *Genome Biol. 2022 231* 23, 1–29. doi:10.1186/S13059-022-02612-2.

Wang, T., Kong, S., Tao, M., and Ju, S. (2020). The potential role of RNA N6-methyladenosine in Cancer progression. *Mol. Cancer 2020 191* 19, 1–18. doi:10.1186/S12943-020-01204-7.

Wang, X., Lu, Z., Gomez, A., Hon, G. C., Yue, Y., Han, D., et al. (2014). N 6-methyladenosine-dependent regulation of messenger RNA stability. *Nature* 505, 117–120. doi:10.1038/nature12730.

Wang, X., Zhao, B. S., Roundtree, I. A., Lu, Z., Han, D., Ma, H., et al. (2015). N6-methyladenosine modulates messenger RNA translation efficiency. *Cell* 161, 1388–1399. doi:10.1016/J.CELL.2015.05.014/.

Ward, A. M., Bidet, K., Yinglin, A., Ler, S. G., Hogue, K., Blackstock, W., et al. (2011). Quantitative mass spectrometry of DENV-2 RNA-interacting proteins reveals that the DEAD-box RNA helicase DDX6 binds the DB1 and DB2 3' UTR structures. *RNA Biol.* 8, 1173–1186. doi:10.4161/RNA.8.6.17836/SUPPL_FILE/KRNB_A_10917836_SM0001.ZIP.

Warda, A. S., Kretschmer, J., Hackert, P., Lenz, C., Urlaub, H., Höbartner, C., et al. (2017). Human METTL16 is a N 6 -methyladenosine (m 6 A) methyltransferase that targets pre-mRNAs and various non-coding RNAs . *EMBO Rep.* 18, 2004–2014. doi:10.15252/EMBR.201744940.

Wei, L. H., Song, P., Wang, Y., Lu, Z., Tang, Q., Yu, Q., et al. (2018). The m6A reader ECT2 controls trichome morphology by affecting mRNA stability in arabidopsis. *Plant Cell* 30, 968–985. doi:10.1105/tpc.17.00934.

Weimer, J. L. (1931). Alfalfa mosaic. *Phytopathology* 21, 122–123.

White, J. P., Cardenas, A. M., Marissen, W. E., and Lloyd, R. E. (2007). Inhibition of Cytoplasmic mRNA Stress Granule Formation by a Viral Proteinase. *Cell Host Microbe* 2, 295–305. doi:10.1016/J.CHOM.2007.08.006.

Williams, G. D., Gokhale, N. S., and Horner, S. M. (2019). Regulation of Viral Infection by the RNA Modification *N6* -Methyladenosine. *Annu. Rev. Virol.* 6, 235–253. doi:10.1146/annurev-virology-092818-015559.

Winkler, R., Gillis, E., Lasman, L., Safra, M., Geula, S., Soyris, C., et al. (2018). m6A modification controls the innate immune response to infection by targeting type I interferons. *Nat. Immunol. 2018 202* 20, 173–182. doi:10.1038/s41590-018-0275-z.

Wu, F., Cheng, W., Zhao, F., Tang, M., Diao, Y., and Xu, R. (2019). Association of N6-methyladenosine with viruses and related diseases. *Virol. J.* 16, 1–10. doi:10.1186/S12985-019-1236-3/TABLES/1.

Xia, T.-L., Li, X., Wang, X., Zhu, Y.-J., Zhang, H., Cheng, W., et al. (2021). N(6)-methyladenosine-binding protein YTHDF1 suppresses EBV replication and promotes EBV RNA decay. *EMBO Rep.* 22, e50128. doi:10.15252/EMBR.202050128.

Xiao, W., Adhikari, S., Dahal, U., Chen, Y. S., Hao, Y. J., Sun, B. F., et al. (2016). Nuclear m6A Reader YTHDC1 Regulates mRNA Splicing. *Mol. Cell* 61, 507–519. doi:10.1016/J.MOLCEL.2016.01.012.

Xu, C., Wang, X., Liu, K., Roundtree, I. A., Tempel, W., Li, Y., et al. (2014). Structural basis for selective binding of m6A RNA by the YTHDC1 YTH domain. *Nat. Chem. Biol.* 10, 927–929. doi:10.1038/NCHEMBIO.1654.

Xu, K., Yang, Y., Feng, G. H., Sun, B. F., Chen, J. Q., Li, Y. F., et al. (2017). Mettl3-mediated m 6 A regulates spermatogonial differentiation and meiosis initiation. *Cell Res.* 27, 1100–1114. doi:10.1038/CR.2017.100.

Xu, M., Mazur, M. J., Tao, X., and Kormelink, R. (2020). Cellular RNA hubs: Friends and foes of plant viruses. *Mol. Plant-Microbe Interact.* 33, 40–54. doi:10.1094/MPMI-06-19-0161-FI/.

Xue, M., Zhao, B. S., Zhang, Z., Lu, M., Harder, O., Chen, P., et al. (2019). Viral N 6-methyladenosine upregulates replication and pathogenesis of human respiratory syncytial virus. *Nat. Commun.* 10. doi:10.1038/S41467-019-12504-Y.

Yardımcı, N., Eryiğit, H., and Erdal, I. (2006). EFFECT OF ALFALFA MOSAIC VIRUS (AMV) ON THE

CONTENT OF SOME MACRO- AND MICRONUTRIENTS IN ALFALFA. *J. Cult. Collect.* 5, 90–93. Available at: http://www.bioline.org.br/request?cc06013 [Accessed February 11, 2022].

Ye, F., Chen, E. R., and Nilsen, T. W. (2017). Kaposi's Sarcoma-Associated Herpesvirus Utilizes and Manipulates RNA N6-Adenosine Methylation To Promote Lytic Replication. *J. Virol.* 91. doi:10.1128/JVI.00466-17/.

Yoon, K., Ringeling, F. R., Vissers, C., Jacob, F., Jimenez-cyrus, D., Su, Y., et al. (2018). HHS Public Access. 171, 877–889. doi:10.1016/j.cell.2017.09.003.Temporal.

Youn, J. Y., Dyakov, B. J. A., Zhang, J., Knight, J. D. R., Vernon, R. M., Forman-Kay, J. D., et al. (2019). Properties of Stress Granule and P-Body Proteomes. *Mol. Cell* 76, 286–294. doi:10.1016/J.MOLCEL.2019.09.014.

Yu, Q., Liu, S., Yu, L., Xiao, Y., Zhang, S., Wang, X., et al. (2021). RNA demethylation increases the yield and biomass of rice and potato plants in field trials. *Nat. Biotechnol. 2021 3912* 39, 1581–1588. doi:10.1038/s41587-021-00982-9.

Yue, H., Nie, X., Yan, Z., and Weining, S. (2019). N6-methyladenosine regulatory machinery in plants: composition, function and evolution. *Plant Biotechnol. J.* 17, 1194–1208. doi:10.1111/pbi.13149.

Yue, J. ;, Wei, Y. ;, and Zhao, M. (2022). The Reversible Methylation of m6A Is Involved in Plant Virus Infection. *Biology (Basel).* 11, 271. doi:10.3390/BIOLOGY11020271.

Zhang, F., Zhang, Y. C., Liao, J. Y., Yu, Y., Zhou, Y. F., Feng, Y. Z., et al. (2019a). The subunit of RNA n6-methyladenosine methyltransferase OsFIP regulates early degeneration of microspores in rice. *PLoS Genet.* 15. doi:10.1371/JOURNAL.PGEN.1008120.

Zhang, G., Lv, Z., Diao, S., Liu, H., Duan, A., He, C., et al. (2021a). Unique features of the m6A methylome and its response to drought stress in sea buckthorn (Hippophae rhamnoides Linn.). *RNA Biol.* 18, 794–803. doi:10.1080/15476286.2021.1992996.

Zhang, K., Zhuang, X., Dong, Z., Xu, K., Chen, X., Liu, F., et al. (2021b). The dynamics of N 6-methyladenine RNA modification in interactions between rice and plant viruses. *Genome Biol.* 22. doi:10.1186/S13059-021-02410-2.

Zhang, Q., Sharma, N. R., Zheng, Z. M., and Chen, M. (2019b). Viral Regulation of RNA Granules in Infected Cells. *Virol. Sin. 2019 342* 34, 175–191. doi:10.1007/S12250-019-00122-3.

Zhang, T. Y., Wang, Z. Q., Hu, H. C., Chen, Z. Q., Liu, P., Gao, S. Q., et al. (2021c). Transcriptome-Wide N6-Methyladenosine (m6A) Profiling of Susceptible and Resistant Wheat Varieties Reveals the Involvement of Variety-Specific m6A Modification Involved in Virus-Host Interaction Pathways. *Front. Microbiol.* 12. doi:10.3389/FMICB.2021.656302/FULL.

Zhang, Y., Geng, X., Li, Q., Xu, J., Tan, Y., Xiao, M., et al. (2020). m6A modification in RNA: biogenesis, functions and roles in gliomas. *J. Exp. Clin. Cancer Res.* 39, 1–16. doi:10.1186/S13046-020-01706-8.

Zhang, Y., Wang, X., Zhang, X., Wang, J., Ma, Y., Zhang, L., et al. (2019c). RNA-binding protein YTHDF3 suppresses interferon-dependent antiviral responses by promoting FOXO3 translation. *Proc. Natl. Acad. Sci. U. S. A.* 116, 976–981. doi:10.1073/PNAS.1812536116.

Zhao, B. S., Roundtree, I. A., and He, C. (2016). Post-transcriptional gene regulation by mRNA modifications. *Nat. Rev. Mol. Cell Biol.* 18, 31–42. doi:10.1038/NRM.2016.132.

Zhao, X., Yang, Y., Sun, B. F., Shi, Y., Yang, X., Xiao, W., et al. (2014). FTO-dependent demethylation of N6-methyladenosine regulates mRNA splicing and is required for adipogenesis. *Cell Res.* 24, 1403–1419. doi:10.1038/CR.2014.151.

Zheng, G., Dahl, J. A., Niu, Y., Fedorcsak, P., Huang, C. M., Li, C. J., et al. (2013). ALKBH5 Is a Mammalian RNA Demethylase that Impacts RNA Metabolism and Mouse Fertility. *Mol. Cell* 49, 18–29. doi:10.1016/J.MOLCEL.2012.10.015.

Zheng, H., Li, S., Zhang, X., and Sui, N. (2020a). Functional Implications of Active N6-Methyladenosine in Plants. *Front. Cell Dev. Biol.* 8, 291. doi:10.3389/FCELL.2020.00291/BIBTEX.

Zheng, H., Wang, G., and Zhang, L. (1997). Alfalfa Mosaic Virus Movement Protein Induces Tubules in Plant Protoplasts. *Mol. Plant-Microbe Interact. MPMI* 10, 1010–1014.

Zheng, H. xiang, Sun, X., Zhang, X. sheng, and Sui, N. (2020b). m6A Editing: New Tool to Improve Crop Quality? *Trends Plant Sci.* 25, 859–867. doi:10.1016/J.TPLANTS.2020.04.005.

Zheng, Q., Hou, J., Zhou, Y., Li, Z., and Cao, X. (2017). The RNA helicase DDX46 inhibits innate immunity by entrapping m 6 A-demethylated antiviral transcripts in the nucleus. *Nat. Immunol.* 18, 1094–1103. doi:10.1038/NI.3830.

Zhong, S., Li, H., Bodi, Z., Button, J., Vespa, L., Herzog, M., et al. (2008). MTA is an Arabidopsis messenger RNA adenosine methylase and interacts with a homolog of a sex-specific splicing factor. *Plant Cell* 20, 1278–1288. doi:10.1105/TPC.108.058883.

Zhou, J., Wan, J., Gao, X., Zhang, X., Jaffrey, S. R., and Qian, S. B. (2015). Dynamic m6A mRNA methylation directs translational control of heat shock response. *Nat. 2015 5267574* 526, 591–594. doi:10.1038/nature15377.

Zhou, L., Tian, S., and Qin, G. (2019). RNA methylomes reveal the m6A-mediated regulation of DNA demethylase gene SlDML2 in tomato fruit ripening. *Genome Biol.* 20. doi:10.1186/S13059-019-1771-7.

Zhou, Z., Lv, J., Yu, H., Han, J., Yang, X., Feng, D., et al. (2020). Mechanism of RNA modification N6-methyladenosine in human cancer. *Mol. Cancer* 19, 1–20. doi:10.1186/s12943-020-01216-3.